USBM H0232062

DEVELOPMENT OF A SAFER, MORE EFFICIENT HYDRAULIC-BASED TECHNIQUE FOR RAPID EXCAVATION OF COAL, ROCK, AND OTHER MINERALS

TELEDYNE BROWN ENGINEERING
HUNTSVILLE, ALABAMA

FINAL REPORT

April 1975

Prepared for the

U.S. DEPARTMENT OF THE INTERIOR
BUREAU OF MINES
WASHINGTON, D.C.

Bureau of Mines Open File Report 75-75

NOTICE

GENERAL DISCLAIMER

This document may be affected by one or more of the following statements

- **This document has been reproduced from the best copy furnished by the sponsoring agency. It is being released in the interest of making available as much information as possible.**
- **This document may contain data which exceeds the sheet parameters. It was furnished in this condition by the sponsoring agency and is the best copy available.**
- **This document may contain tone-on-tone or color graphs, charts and/or pictures which have been reproduced in black and white.**
- **This document is paginated as submitted by the original source.**
- **Portions of this document are not fully legible due to the historical nature of some of the material. However, it is the best reproduction available from the original submission.**

FOREWORD

This report was prepared by Brown Engineering Company, Inc., Electronics and Engineering, Huntsville, Alabama, under USBM Contract Number H0232062. The contract was initiated under the Coal Mine Health and Safety Program. It was administered under the technical directive of the Twin Cities Mining Research Center with Mr. Jacob N. Frank acting as the Technical Project Officer. Mr. Frank Pavlich was the contract administrator for the Bureau of Mines.

This report is a summary of the work recently completed as part of this contract during the period June 26, 1973 to March 31, 1975. This report was submitted by the authors on April 14, 1975.

ABSTRACT

This report discusses the results of the development and in situ testing of a prototype hydraulic mining machine which uses a water jet with solid particles added. Of the 124 tests performed with the excavator, 89 were carried out to evaluate the ability of the excavator to cut in situ rock. Several different particle materials, which ranged from coal to steel shot, were injected; target material consisted of limestone and concrete. Two different water/particle nozzle systems were developed and tested. One system combined axial particle feed with an annular water nozzle; the other system was the inverse, having particles peripherally fed into an axial water nozzle.

The following conclusions were drawn from the test results. Solid particles can be injected into a high-velocity stream without great difficulty at reasonable feed rates and without significant deterioration in the downstream jet. The addition of particles does appear to improve the cutting ability of the jet as compared to the use of water alone. The cutting ability appears to increase as the mass of the particle is increased. At the pressures tested (i.e., $P \leq 15{,}000$ psi), and even with the addition of particles, hydraulic jets do not appear to be as energy-efficient in excavating hard rock as other techniques. However, hydraulic methods appear to improve as the pressure is increased or as hardness (i.e., more easily excavated material) is decreased.

Approved:

N. E. Chatterton, Ph.D.
Manager
Research Department

TABLE OF CONTENTS

LIST OF ILLUSTRATIONS

LIST OF ILLUSTRATIONS (Concluded)

LIST OF TABLES

1. INTRODUCTION

The mechanical cutting of rock-like material is a controlled or semi-controlled process of exceeding the strength of the material. By applying sufficient energy to a confined area, the maximum stress is exceeded, causing fracture planes to develop and propagate through the material. Overstressing the material can be induced in many basic ways such as: applying a force with a sharp instrument, setting off an explosive charge, heating a localized area to produce thermal stress, and applying a high energy jet, to mention just a few. Fracturing occurs whenever the force acting per unit area exceeds the maximum stress of the local material.

Characteristically, rocky materials being commonly excavated have compressive strengths about 1/10 to 1/3 that of carbon steel and tensile strengths significantly less than the compressive strength. Relative to a carbon steel, rock-like material is soft and brittle.

Probably the oldest technique for cutting rock-like material is the application of force with a sharp instrument. This produces a stress in the material which is proportional to the applied force and inversely proportional the area of contact. A significant mechanical advantage can be obtained using this technique by reducing the contact area and thereby increasing the stress for a given applied force. However, this same stress is applied to the instrument doing the cutting, which eventually leads to damage or dulling of the instrument.

For a high-energy incompressible fluid jet impacting normal to the surface, the stress produced is proportional to the impact pressure of the jet, which is one-half of the product of the density times the square of the velocity. The velocity is proportional to the pressure applied to the fluid in accelerating it to the given velocity. Therefore, the resulting stress is directly proportional to the pressure used in pumping the fluid. As a result, increasing the direct stress can only be achieved by increasing the pressure used to pump the fluid. Since pressure

is related to energy expenditure, this means that increased stress requires increased energy expenditure.

In comparing the two previous methods, it is obvious that the ability to reduce the contact area to a size sufficient to induce destructive stresses offers significant advantages; whereas the use of an expendable fluid offers some advantages in not having to periodically repair, refurbish, and/or replace the cutting mechanism.

This report discusses the development of a machine in which attempts were made to combine the better aspects of both techniques. The method used was the following. Solid particles of material were injected into a high-velocity water stream. The advantage of the addition of solid particles was to have been twofold. First, assuming the particle would be accelerated to the normal velocity of the undisturbed jet, the higher density of the particles would produce a greater impact pressure. Secondly, the shape of the particles would automatically cause the impact force to be applied over a smaller area than that ordinarily associated with the displaced water jet. This would produce a proportional increase in the stress. From the above, it was reasoned that the cutting action of a fluid jet could be improved by the addition of solid particles.

To verify this hypothesis, a prototype test unit was designed, fabricated, and tested. The results of these tests indicated the following:

- Using water alone, the test unit did not appear to cut rock as efficiently as reported in tests of some of the other laboratory units (see References 1-1 and 1-2 for example).

- The cutting action of a water jet was increased by the addition of solid particles. The increase was not as great as would appear to be indicated by theoretical considerations.

- The major problem addressed was developing a method of injecting particles into the jet without causing serious degradation of the water jet. The objective of this development effort was fully met.

REFERENCES - SECTION 1

1-1. McClain, W. C. and G. A. Cristy, "Examination of High Pressure Water Jets for Use in Rock Tunnel Excavation", Report ORNL-HUD-1, Oak Ridge National Laboratory, January 1970

1-2. Harris, H. D., "Rock Cutting with Water Jets", National Research Council of Canada, Ottawa, Presentation at 75th Annual General Meeting of the Canadian Institute of Mining and Metallurgy, April 15 - 18, 1973

2. THEORETICAL BACKGROUND

2.1 IMPACT PRESSURE

Some typical rock properties are listed in Table 2-1. In order to cause rock fragmentation, the impact force applied to the material must exceed the maximum compressive strength.

According to the weak shock relation, the impact pressure of a solid projectile can be expressed by

$$P = \rho\left(\frac{CV}{2}\right) \tag{2-1}$$

and

$$C = \left(\frac{E}{\rho}\right)^{1/2} \tag{2-2}$$

where

ρ - density

C - sound speed

V - impact velocity

E - elastic modulus.

The equations are valid only for similar materials impacting.

Early estimates of the impact pressure are shown in Figures 2-1 and 2-2. (Note: These estimates were made using rock properties slightly different from those shown in Table 2-1.) For the proposed design concept ($V \approx 1{,}200$ ft/sec), the impact pressure was estimated to be approximately one order of magnitude higher than the compression strength of the rock and was predicted to cause rock fragmentation.

2.2 PENETRATION DEPTH

Since there was no rock-rock impact (similar impact) data available in the velocity range of interest, a scaling law was used to convert

TABLE 2-1. TYPICAL ROCK PROPERTIES

MATERIAL	DENSITY (lb/ft^3)	COMPRESIVE STRENGTH (kpsi)	TENSILE STRENGTH (kpsi)	ELASTIC CONSTANT (Mpsi)
Granite	165	14.22 to 35.6	1.0 to 3.6	2.8 to 8.5
Diorite		25.6 to 42.7	2.1 to 4.3	10 to 14.2
Dolerite	187	28.4 to 49.8	2.1 to 5.0	11.4 to 15.6
Gabbro	190	25.6 to 42.7	2.1 to 4.3	10 to 15.6
Basalt	178	21.3 to 42.7	1.4 to 4.3	8.5 to 14.2
Sandstone	159	2.8 to 24.2	0.6 to 3.6	0.7 to 11.4
Shale	144	1.4 to 14.2	0.3 to 1.4	1.4 to 5
Limestone	156	4.3 to 35.6	0.7 to 3.6	1.4 to 11.4
Dolomite	159	11.4 to 35.6	2.1 to 3.6	5.7 to 12.0
Coal	78 to 124	0.7 to 7.1	0.3 to 0.7	1.4 to 2.8
Quartzite	165	7.1 to 28.4	0.7 to 2.8	
Gneiss	184	7.1 to 28.4	0.7 to 2.8	
Marble	165	14.2 to 35.6	1.0 to 2.8	
Slate	165	14.2 to 28.4	1.0 to 2.8	

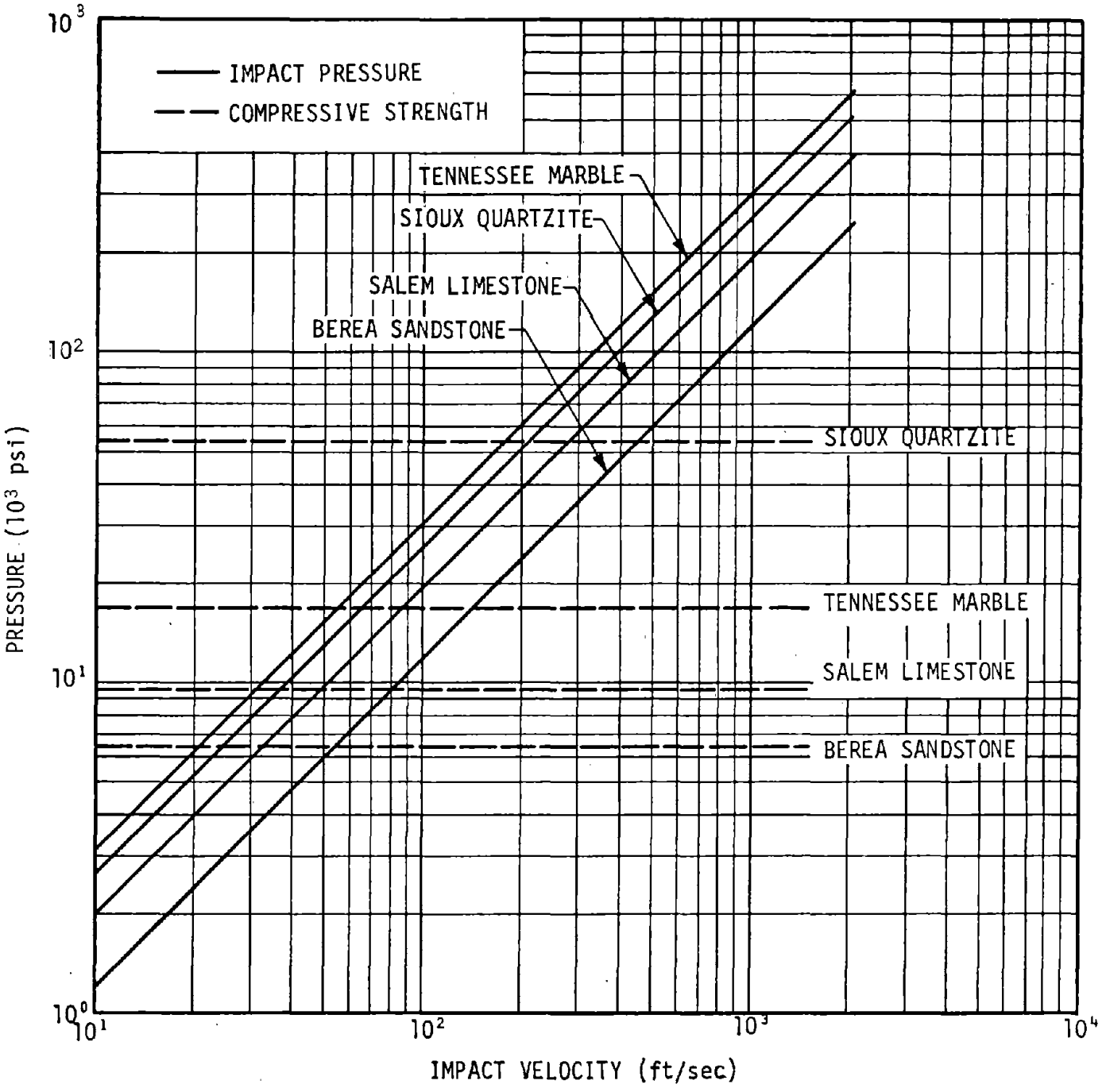

FIGURE 2-1. COMPARISON OF IMPACT PRESSURE AS A FUNCTION OF COMPRESSION STRENGTH OF ROCK SAMPLES

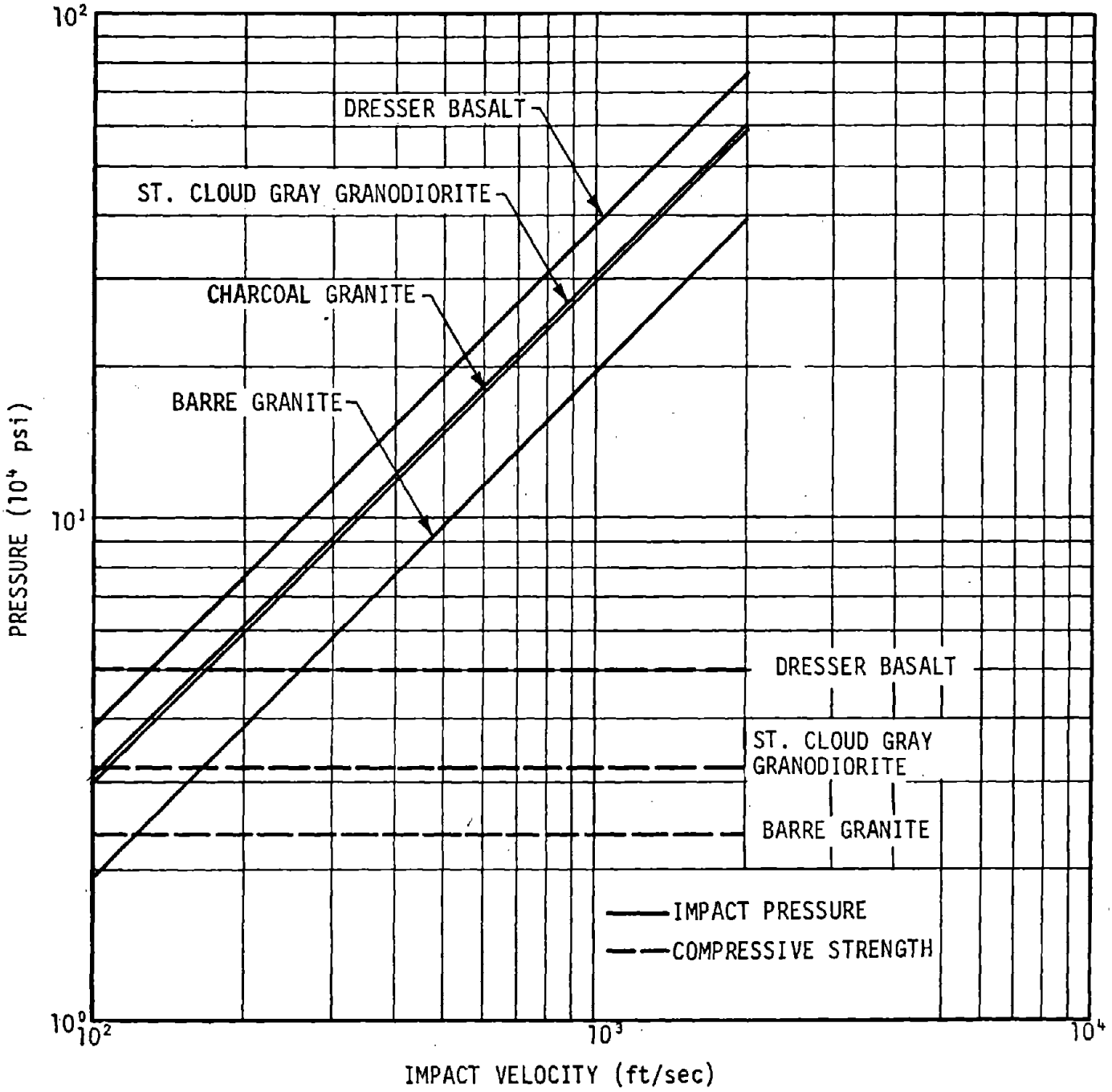

FIGURE 2-2. COMPARISON OF IMPACT PRESSURE AS A FUNCTION OF COMPRESSION STRENGTH OF ROCK SAMPLES

steel-rock impact data in Reference 2-1 to rock-rock impact. In Reference 2-2, a scaling law for dissimilar material impact (i.e., the projectile material differs from target material) was proposed:

$$\left(\frac{\ell}{d}\right)_{B-A} = F\left(\frac{\ell}{d}\right)_{A-A} \tag{2-3}$$

where

B-A - indicates a projectile of material B impacting on a target of material A

ℓ - depth of penetration

d - diameter of the projectile

F - scaling factor given by the equation

and

$$F = \frac{2U}{V}\left(\frac{\rho_B}{\rho_A}\right)^{1/3} \tag{2-4}$$

where U is the particle velocity in the target immediately after impact, and is defined in the following equation:

$$U = \frac{V}{1 + \left(\frac{\rho_A\ C_A}{\rho_B\ C_B}\right)} \tag{2-5}$$

where

C_A - sound speed of material A

C_B - sound speed of material B.

Equations 2-4 and 2-5 are derived by the shock wave theory and can be applied to a weak shock or an elastic wave regime.

It is easily verified that when materials A and B are the same, Equations 2-4 and 2-5 reduce to

$F = 1$

and

$$U = \frac{V}{2}$$

which are the similar impact solutions.

From Reference 2-1, the data of steel projectiles impacting on Berea sandstone is fit by a straight line:

$$\left(\frac{\ell}{d}\right)_{\text{steel-rock}} = 0.0833\ (-1.0 + 0.01\ V)$$

where the impact velocity, V, is in ft/sec.

A combination of Equations 2-4 and 2-5 gives

$$\left(\frac{\ell}{d}\right)_{\text{rock-rock}} = \frac{1 + \frac{(\rho_C)_{\text{rock}}}{(\rho_C)_{\text{steel}}}}{2\left(\frac{\rho_{\text{steel}}}{\rho_{\text{rock}}}\right)^{1/3}} \left(\frac{\ell}{d}\right)_{\text{steel-rock}} \qquad (2\text{-}6)$$

With the properties $\rho_{\text{rock}} = 131.7$ lb/ft^3 (Berea sandstone), $C_{\text{rock}} = 8.56 \times 10^3$ ft/sec, $\rho_{\text{steel}} = 492.96$ lb/ft^3, and $C_{\text{steel}} = 1.692 \times 10^4$ ft/sec, the above equation reduces to

$$\left(\frac{\ell}{d}\right)_{\text{rock-rock}} = 0.366 \left(\frac{\ell}{d}\right)_{\text{steel-rock}}$$

or

$$\left(\frac{\ell}{d}\right)_{\text{rock-rock}} = 0.0305\ (-1.0 + 0.01\ V)\ . \qquad (2\text{-}7)$$

Equation 2-7 is plotted in Figure 2-3 for comparison with that of a steel projectile.

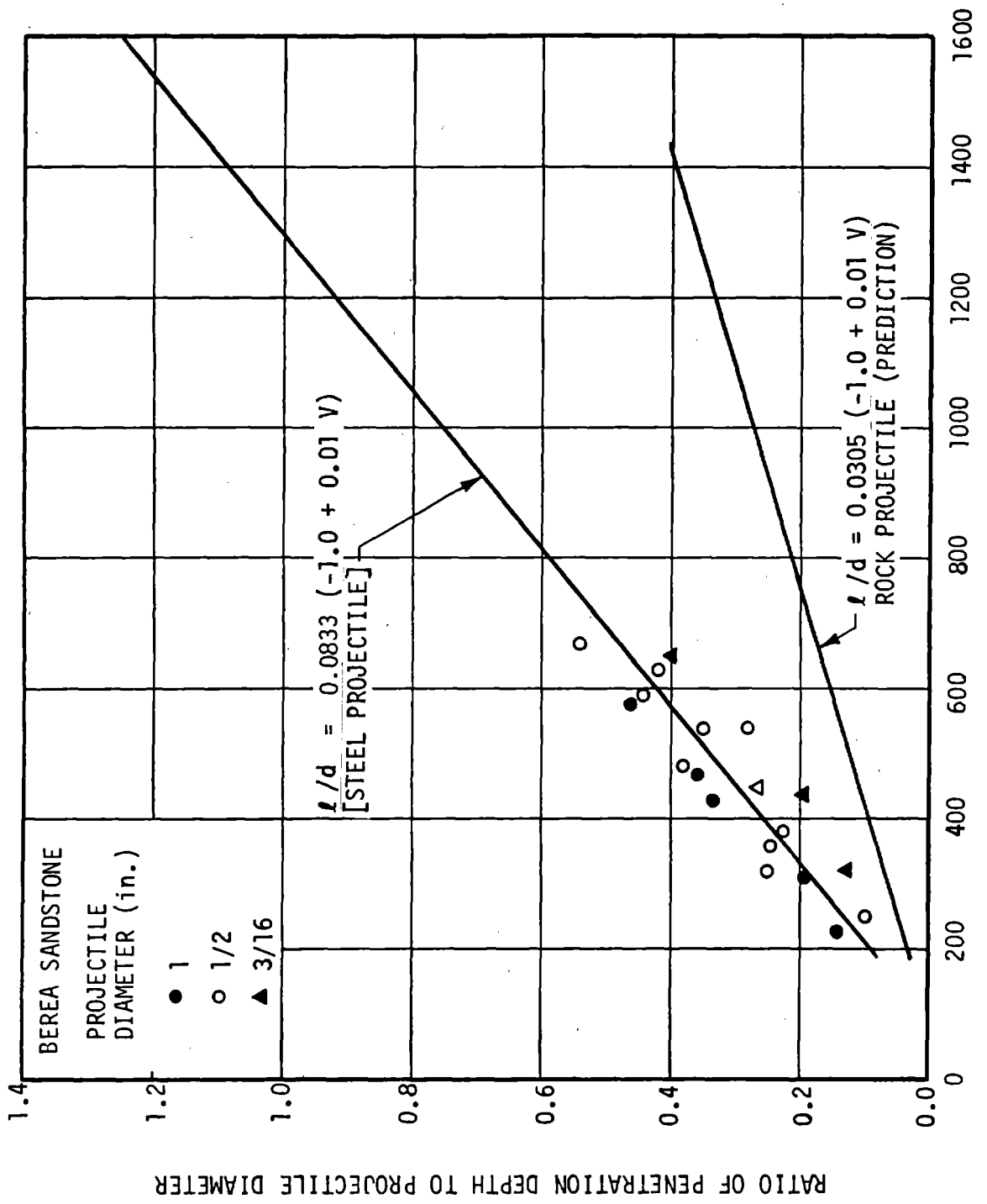

FIGURE 2-3. PENETRATION RATIO AS A FUNCTION OF IMPACT VELOCITY

2.3 SPECIFIC ENERGY

The specific energy is defined as the energy required to cut a unit volume of rock. Assuming that the shape of the crater is a paraboloid, the crater diameter, D, and the penetration depth, ℓ, of a spherical projectile for "similar impact" may be expressed as (Ref. 2-3).

$$\frac{D}{\ell} = 17.34\ (V)^{-1/6} \tag{2-8}$$

Since the volume removed from impact is

$$\gamma = \frac{1}{8}\ \pi\ D^2\ \ell\ , \tag{2-9}$$

the specific energy is

$$S.E. = \frac{\text{Kinetic Energy}}{\gamma} = \frac{\frac{1}{2}\ m\ V^2}{\gamma} \tag{2-10}$$

where m is the projectile mass, as defined in the following equation:

$$m = \rho_{rock}\left(\frac{\pi}{6}\ d^3\right) \tag{2-11}$$

Substituting Equations 2-8, 2-9, and 2-11 into Equation 2-10 gives

$$S.E. = \frac{\frac{1}{2}\ \rho_{rock}\left(\frac{\pi}{6}\ d^3\right) V^2}{\frac{1}{8}\ \pi\ D^2\ \ell} = \frac{2}{3}\ \rho_{rock}\left(\frac{d}{D}\right)^2\left(\frac{d}{\ell}\right) V^2$$

$$= 0.2217 \times 10^{-2} \times \rho_{rock}\left(\frac{\ell}{d}\right)^{-3}\ V^{7/3}\ . \tag{2-12}$$

For Berea sandstone, from Equation 2-7

$$S.E. = 0.781 \times 10^2\ \frac{\rho\ V^{7/3}}{(-1 + 0.01\ V)^3}\ . \tag{2-13}$$

At the impact velocity of 1,200 ft/sec, Equation 2-13 yields

$$S.E. = 2{,}122 \text{ ft-lb/in}^3 \quad .$$

As expected, this result is higher than that for steel projectiles (approximately 700 ft-lb/in^3) but much lower than that for a water jet (14,686 ft-lb/in^3).

The results of rock-rock impact at various velocities are plotted in Figure 2-4.

Even if the above qualitative analysis applied only for a single rock projectile impinging on a rock target, it was reasoned that it demonstrated the superiority of the proposed design over the water jet because it lowered the specific energy and would cut at a much faster rate (deeper penetration and higher impact pressure) than a water jet.

REFERENCES - SECTION 2

2-1. Ripkin, J. F. and J. M. Wetzel, "A Study of the Framentation of Rock by Impingement With Water and Solid Impactors", ARPA Contract No. H0210021, Report No. 131, University of Minnesota, February 1972

2-2. Bjork, R. L. "Review of Physical Processes in Hypervelocity Impact and Penetration", Sixth Symposium on Hypervelocity Impact, August 1963

2-3. Demardo, B. P., "Projectile Shape Effects on Hypervelocity Impact Craters in Aluminum", NASA TND-4953, December 1968

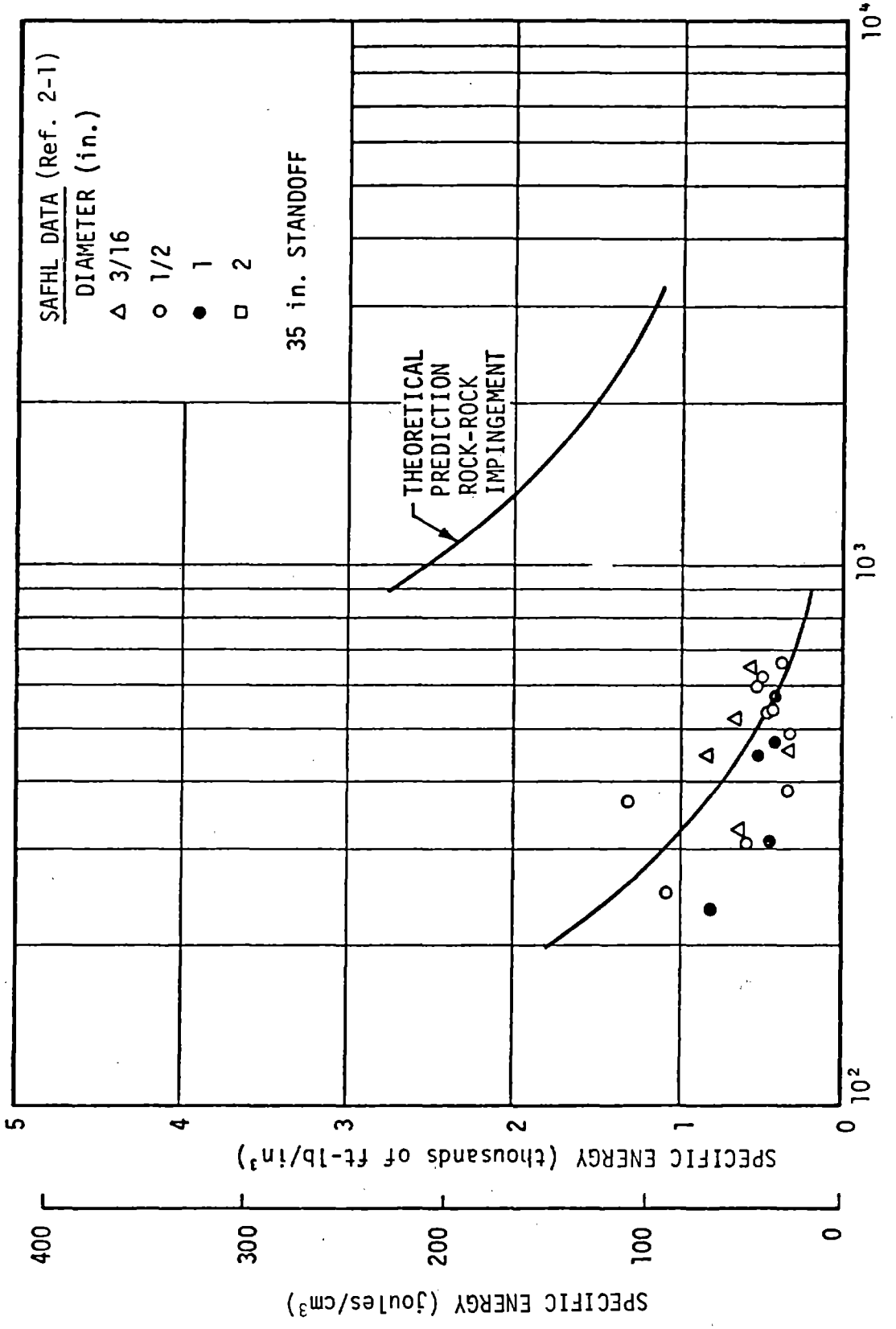

FIGURE 2-4. COMPARISON OF SPECIFIC ENERGY OF ROCK EXCAVATION (from Ref. 2-1)

3. EQUIPMENT DESIGN

The hydraulic excavator consisted of: 1) a high-pressure water supply system; 2) a water/particle nozzle system; and 3) a control system. Figure 3-1 is a schematic showing the main components of the system.

High-pressure water was supplied to the nozzle from a 1.5 ft^3 capacity transfer barrier (TB-1 in Figure 3-1). Pressure to drive the water from the transfer barrier was supplied by a 6-ft^3-capacity high-pressure bottle (PV-1 in Figure 3-1) filled with nitrogen. Nitrogen was pumped into the bottle at pressures as high as 15,000 psi using a pressure intensifier (PI-1) operated by a 100 psi air compressor. Before each test shot, the nozzle side of the transfer barrier was charged with water by a high-pressure hydraulic pump (PM-1).

The water/particle nozzle system consisted of a particle hopper, a water/particle injection chamber, and a secondary nozzle.

The first of two nozzles designed for the tests consisted of an axially located particle-feed nozzle as shown in Figure 3-2. The water emerged from an annular orifice, converged on the particles, and exited from a secondary nozzle as shown in Figure 3-2.

The second nozzle consisted of an axially located water nozzle. Particles were fed peripherally by the ejector action of the water jet. The particle-laden water jet exited through a secondary nozzle as shown in Figure 3-3.

The nozzle could be traversed in the horizontal plane by a chain drive at rates selected by drive gear ratios. Movement in the vertical plane was not possible during a test; however, static adjustments could be made with jack screws and by loosening the hydraulic fittings.

The control system included a remote electrical operating station connected to the system by 25 feet of wire. Three on-off switches on this panel controlled the screw feed motor for the first nozzle design, the traversing motor, and the remote-actuated high-pressure hydraulic valve. A schematic diagram of the electrical system is shown in Figure 3-4.

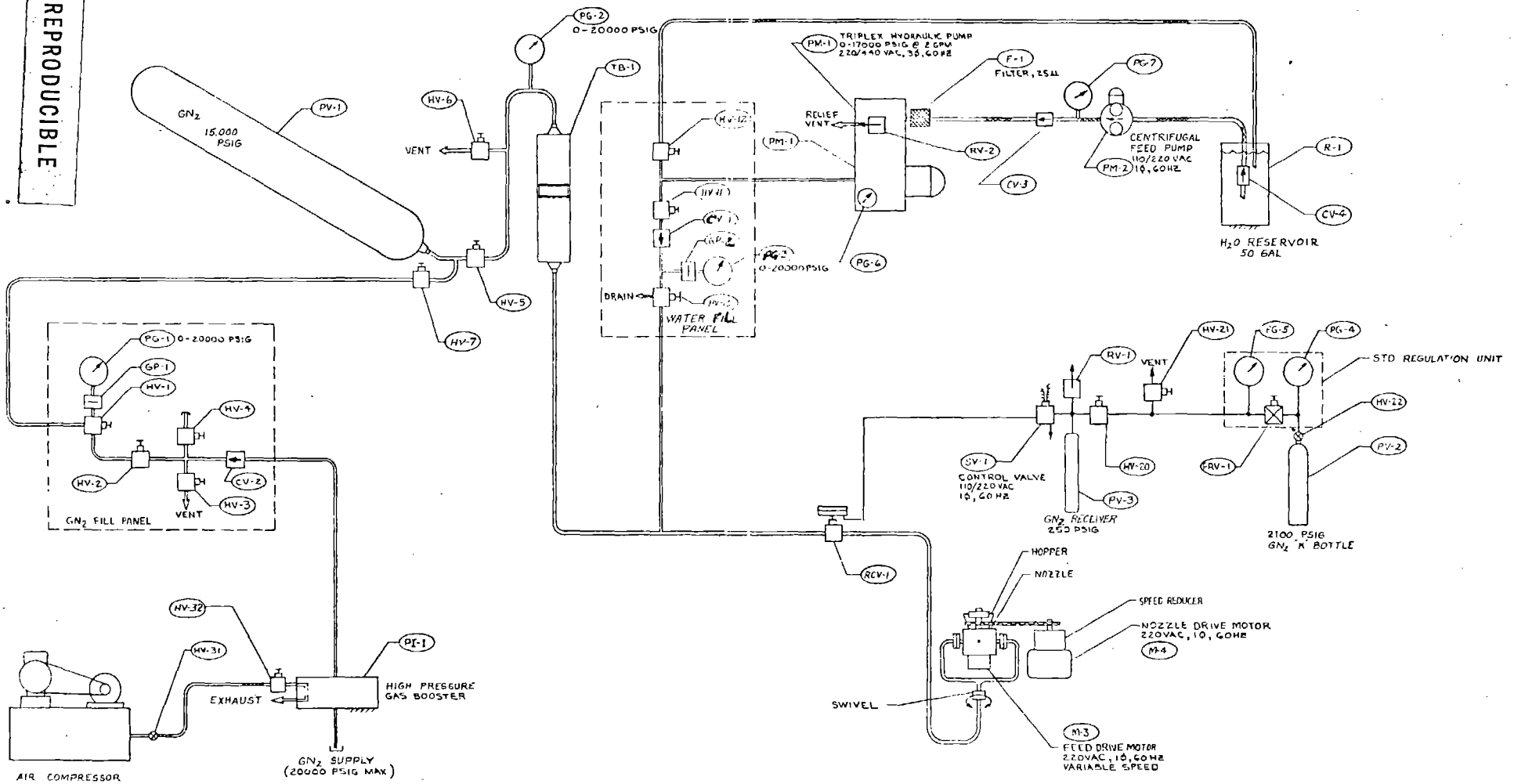

FIGURE 3-1. HYDRAULIC EXCAVATION SYSTEM MECHANICAL SCHEMATIC

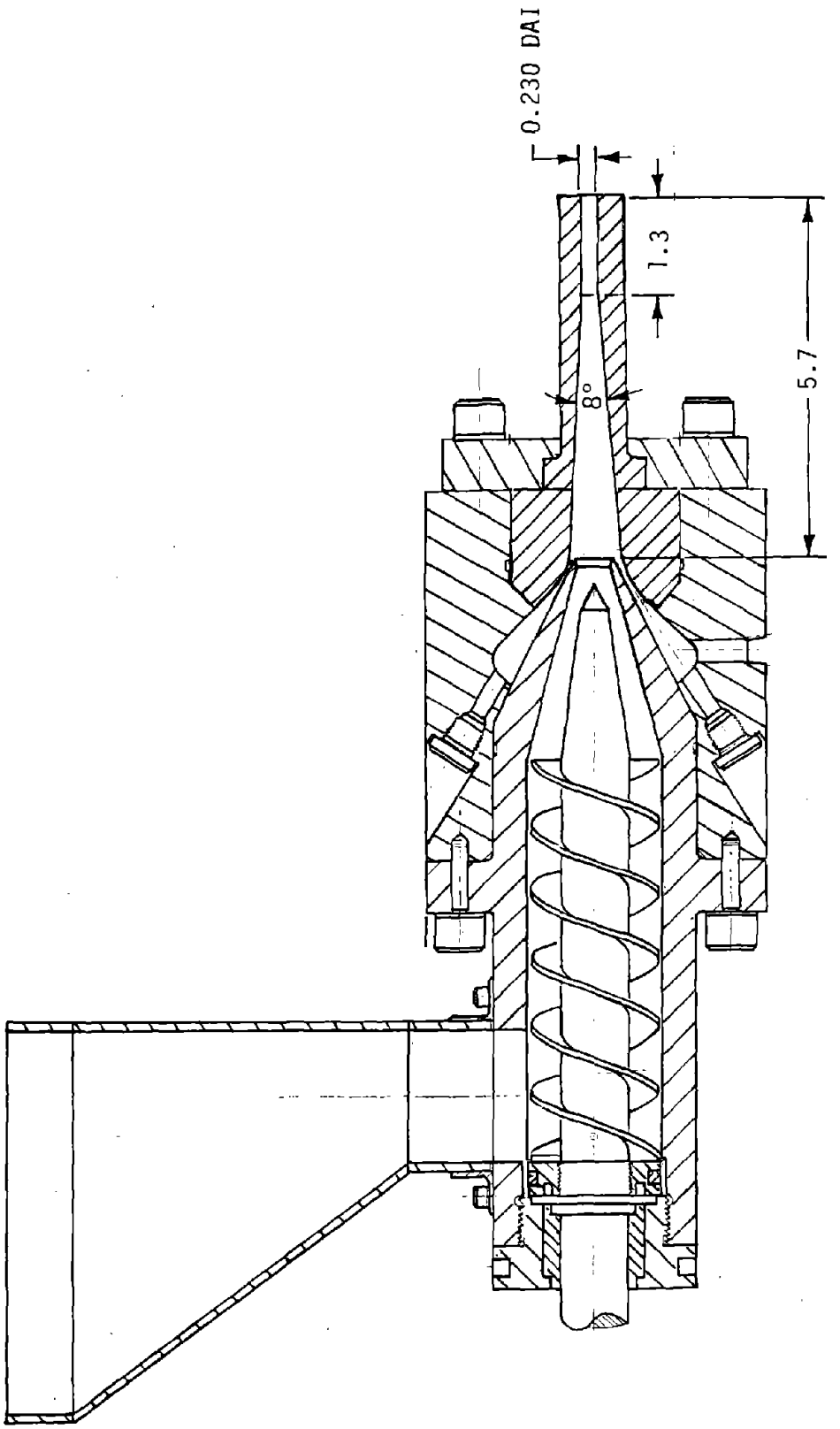

FIGURE 3-2. AXIAL FED PERIPHERAL JET NOZZLE

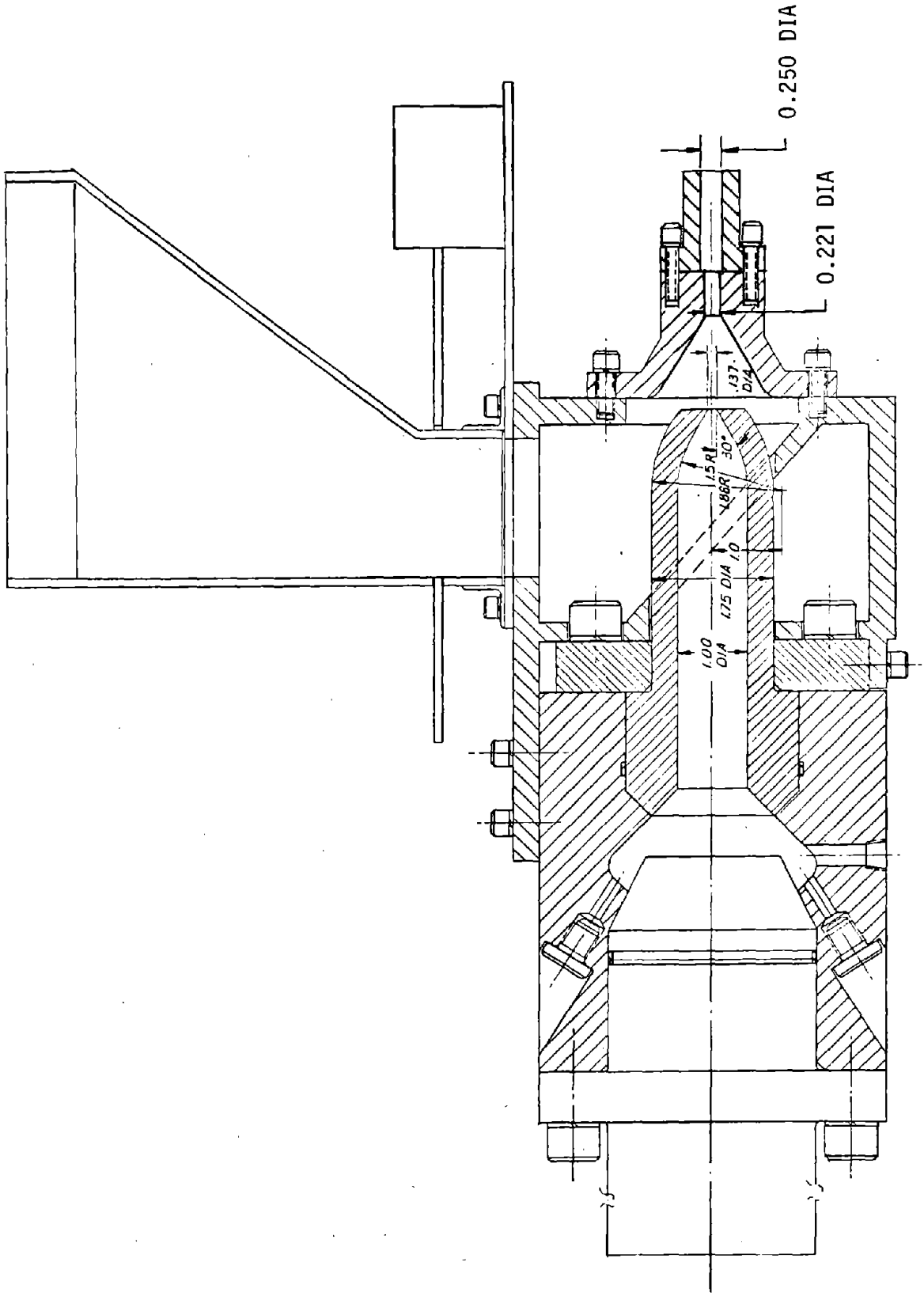

FIGURE 3-3. PERIPHERAL FED AXIAL JET NOZZLE

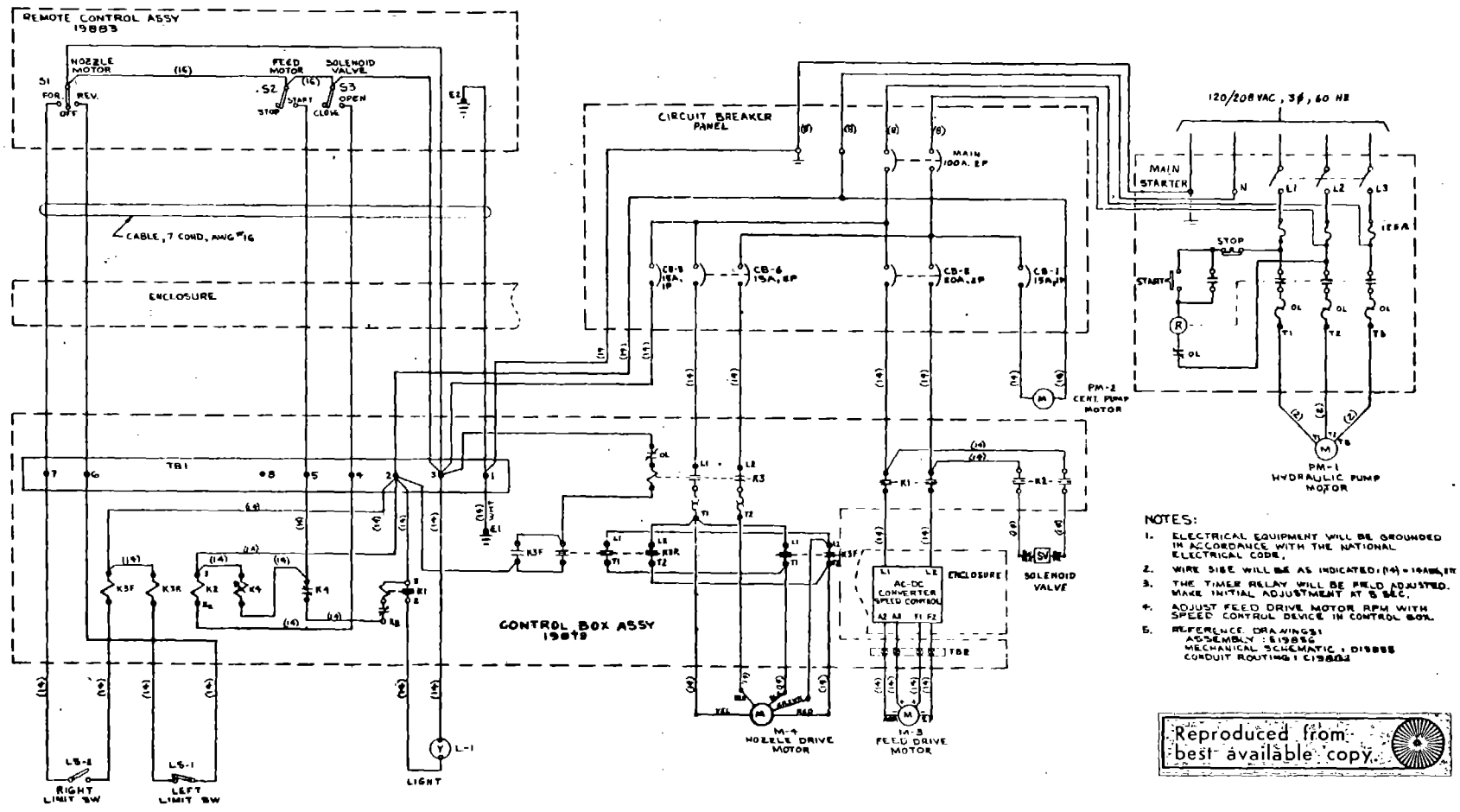

FIGURE 3-4. HYDRAULIC EXCAVATION SYSTEM ELECTRICAL SCHEMATIC

Some system specifications are:

- Pneumatic system

  Volume: 6 cubic feet
  Working gas: nitrogen
  Working pressure: 15,000 psi

- Hydraulic system

  Transfer barrier volume: 1.5 cubic feet

  Working fluid: water with 2 percent water soluble oil

  Remote valve operating time: Open - 2 to 3 seconds maximum
  Closed - not applicable

  Remote valve control pressure: 250 psi maximum

  Remote valve operating supply: K bottle, N_2

  High-pressure hydraulic pump: Output pressure - 15,000 psi
  Rate - 2.6 gpm
  Input - 60 psi

  Water quality: filter to 25 micron

- Nozzle assembly (nominal specifications)

  Stream velocity: 1,200 ft/sec
  Particle size: 1/8 inch
  Flow rate: 60 gpm
  Particle flow rate: 1,600/sec maximum
  Screw feed rate: 3 to 60 rpm (Nozzle One)

- Traversing assembly

  Traverse rate: 6 deg/sec, 4.5 deg/sec, 3 deg/sec, 1.8 deg/sec
  Traverse angle: 30 deg
  Vertical angle set: $\pm$10 deg

- Electrical requirements

  Hydraulic pump: 25 kW, 240 V, 3 phase
  Feed Pump: 0.5 kW, 110 V, 1 phase
  Compressor: 25 kW, 240 V, 3 phase
  Screw feed: 1 kW, 230 V, 1 phase
  Remote operation valve: 110/220 V, 60 cycle, 1 kW

- Mechanical

  System weight: 13,000 lb (est.)
  Nozzle height above ground: 60 inches
  System length: 26 feet

4. EQUIPMENT FABRICATION

With the exception of the water/particle nozzle system and necessary plumbing, the excavator was assembled from off-the-shelf hardware and components. The transfer barrier was made-to-order by the manufacturer, but is considered standard equipment. The two water/particle nozzle system were fabricated in the Teledyne Brown Engineering machine shop facilities.

The excavator was mounted on a road-haulable trailer 24 feet long. The nozzle assembly was mounted at the rear end of the trailer directed rearward.

Photographs of the excavator system are shown in Figures 4-1 through 4-10.

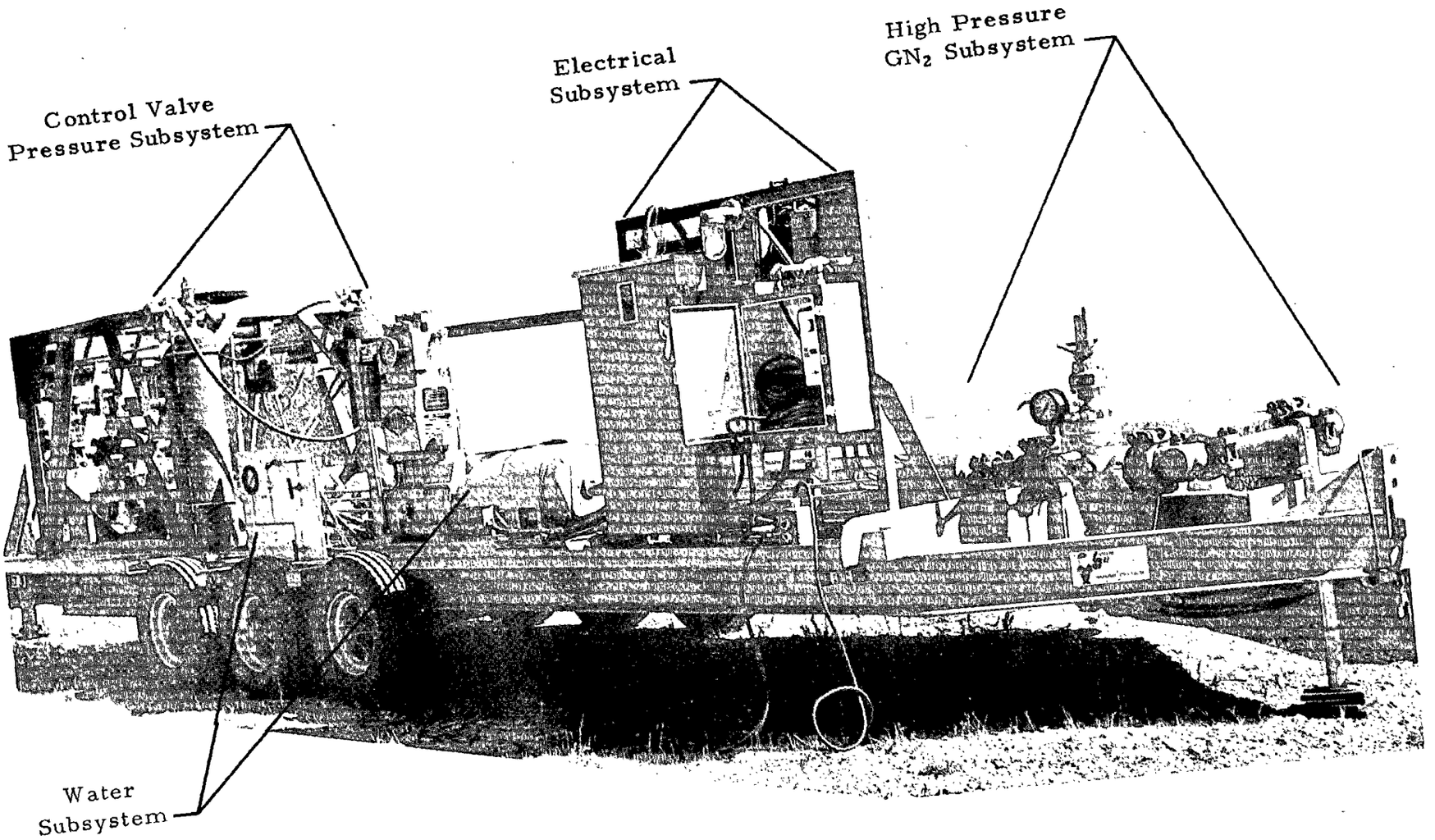

FIGURE 4-1. HYDRAULIC EXCAVATION SYSTEM SUBSYSTEM IDENTIFICATION

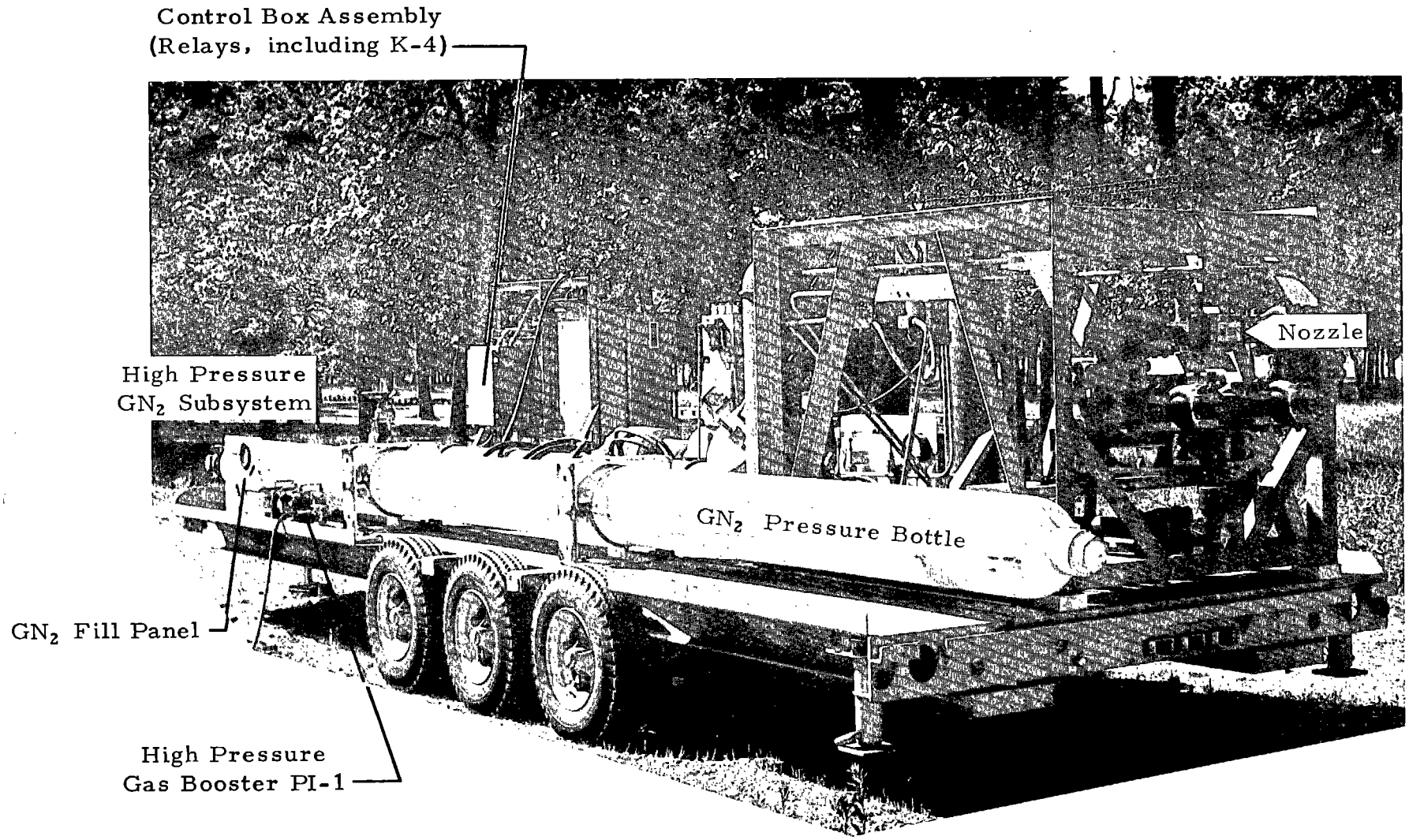

FIGURE 4-2. HYDRAULIC EXCAVATION SYSTEM - GN_2 SUBSYSTEM IDENTIFICATION

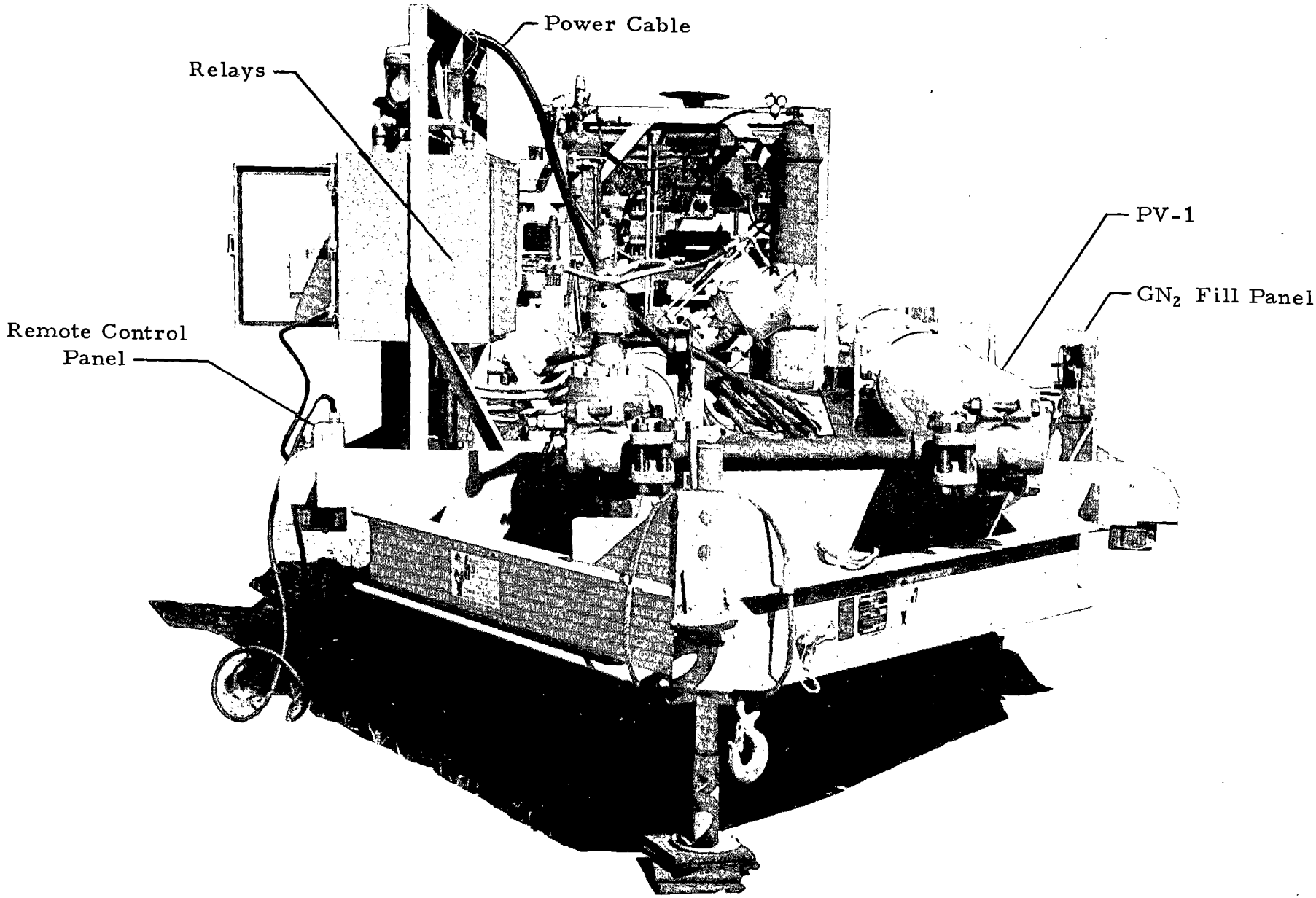

FIGURE 4-3. HYDRAULIC EXCAVATION SYSTEM

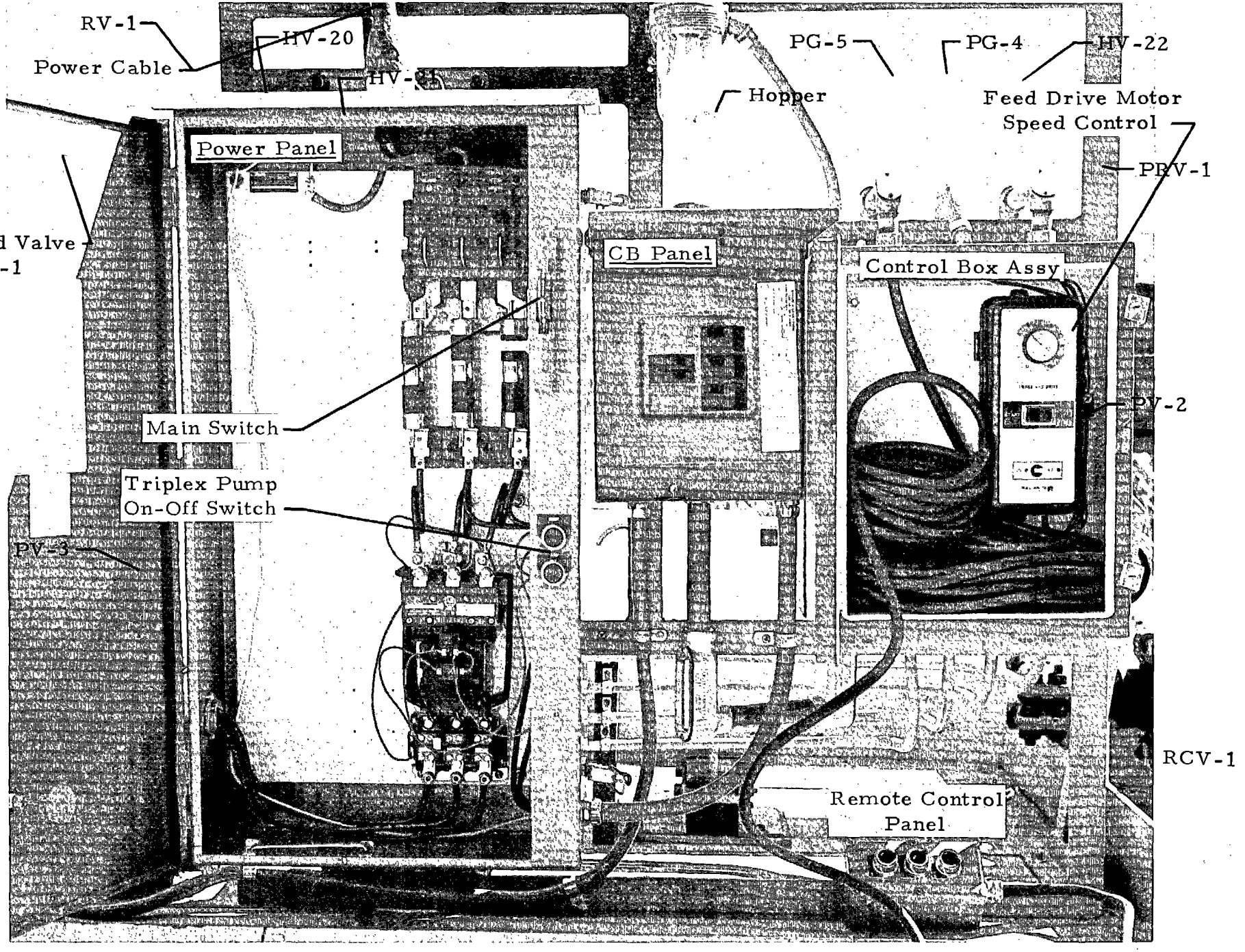

FIGURE 4-4. HYDRAULIC EXCAVATION SYSTEM - ELECTRICAL SUBSYSTEM

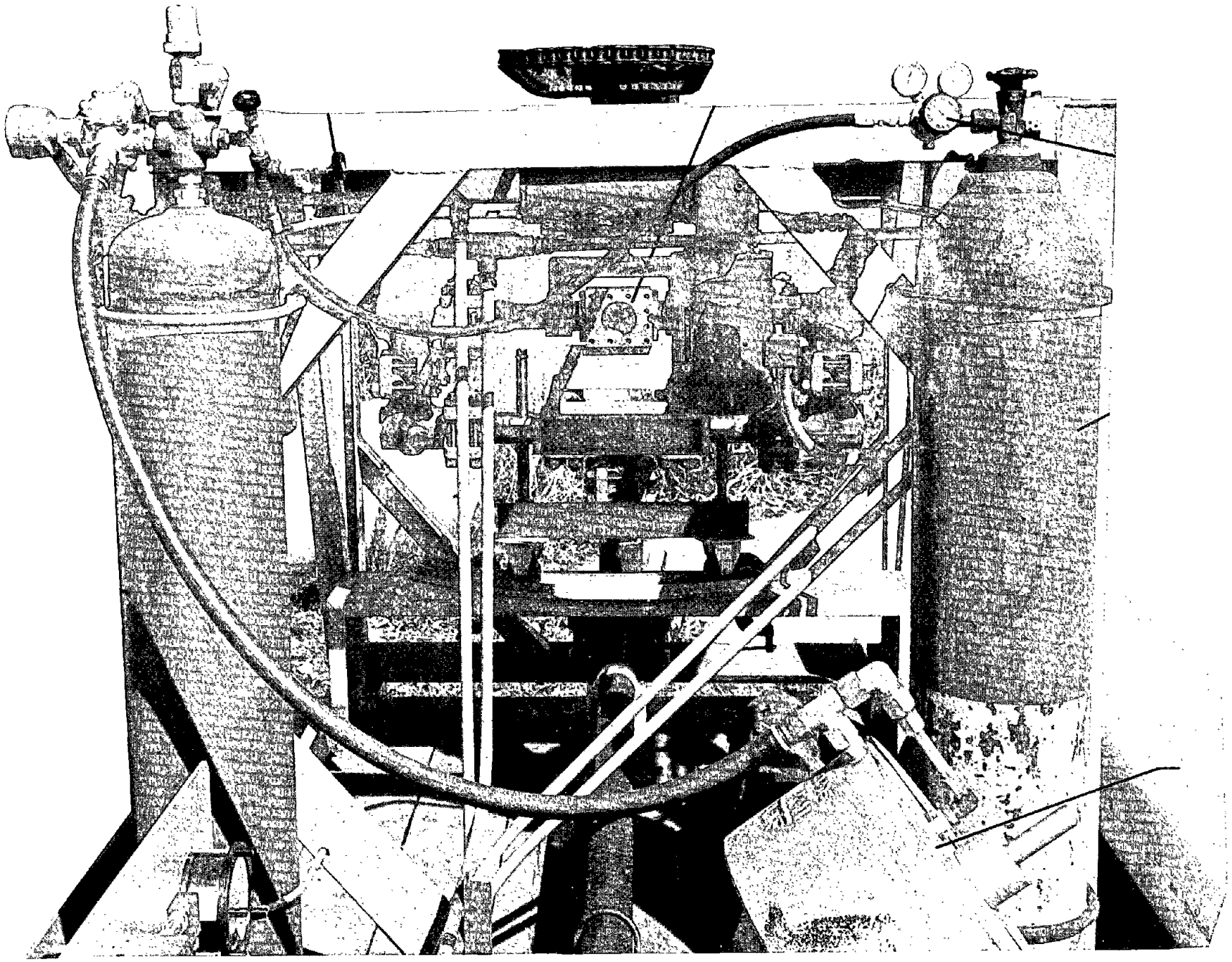

FIGURE 4-5. CONTROL VALVE PRESSURE AND HOPPER FILL SUBSYSTEM

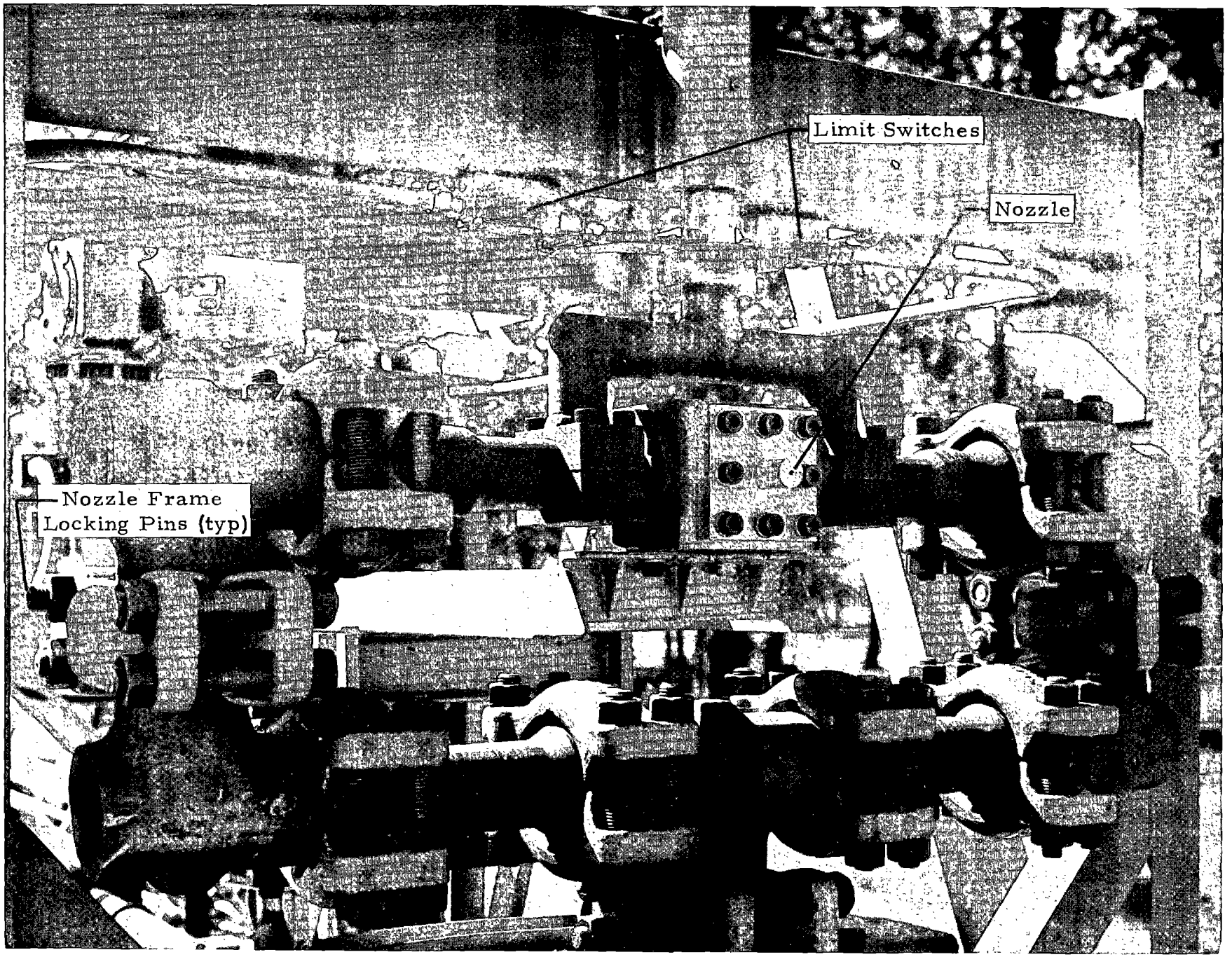

FIGURE 4-6. WATER SUBSYSTEM NOZZLE

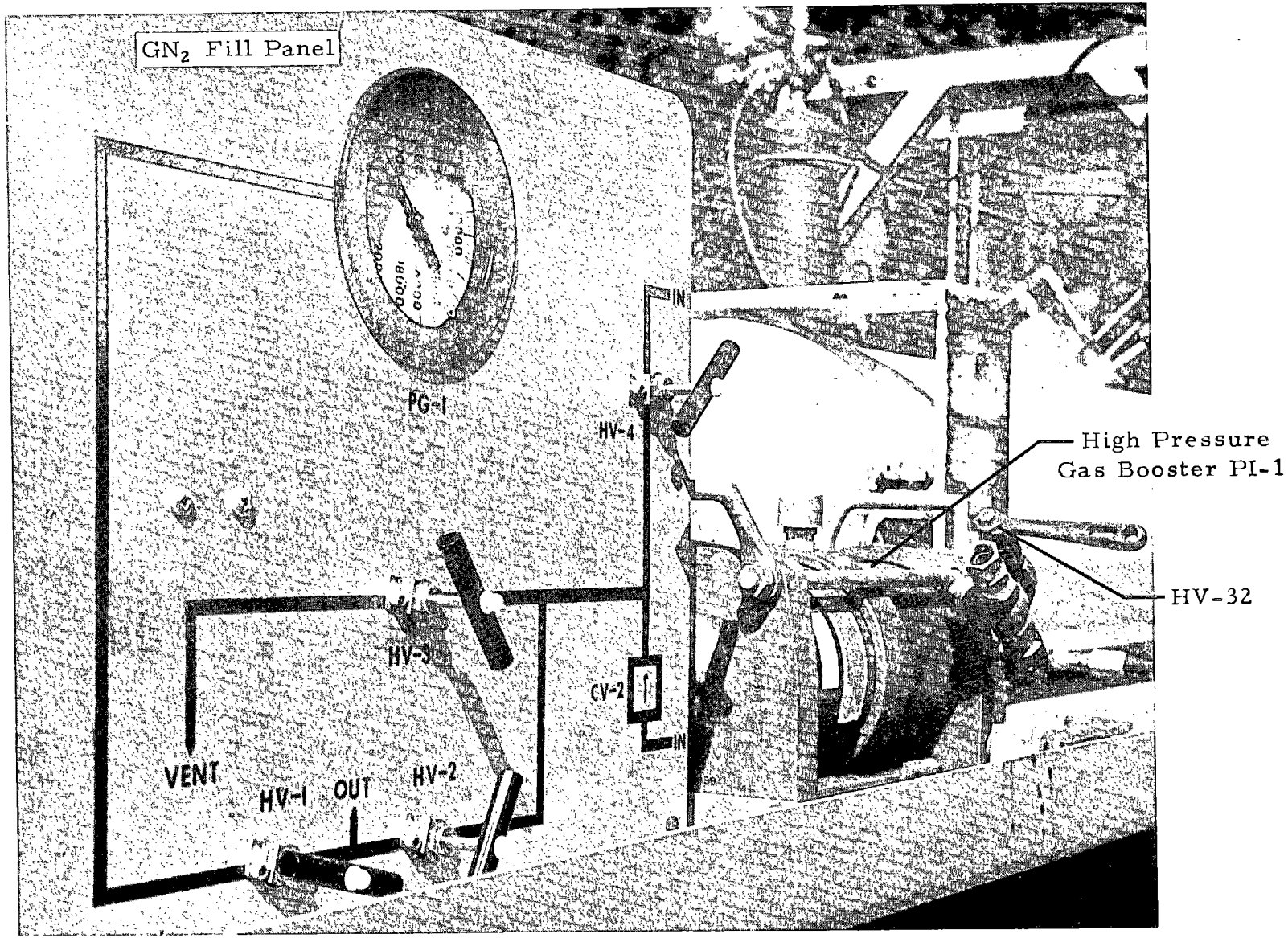

FIGURE 4-7. HIGH PRESSURE GN_2 SUBSYSTEM - VIEW 1

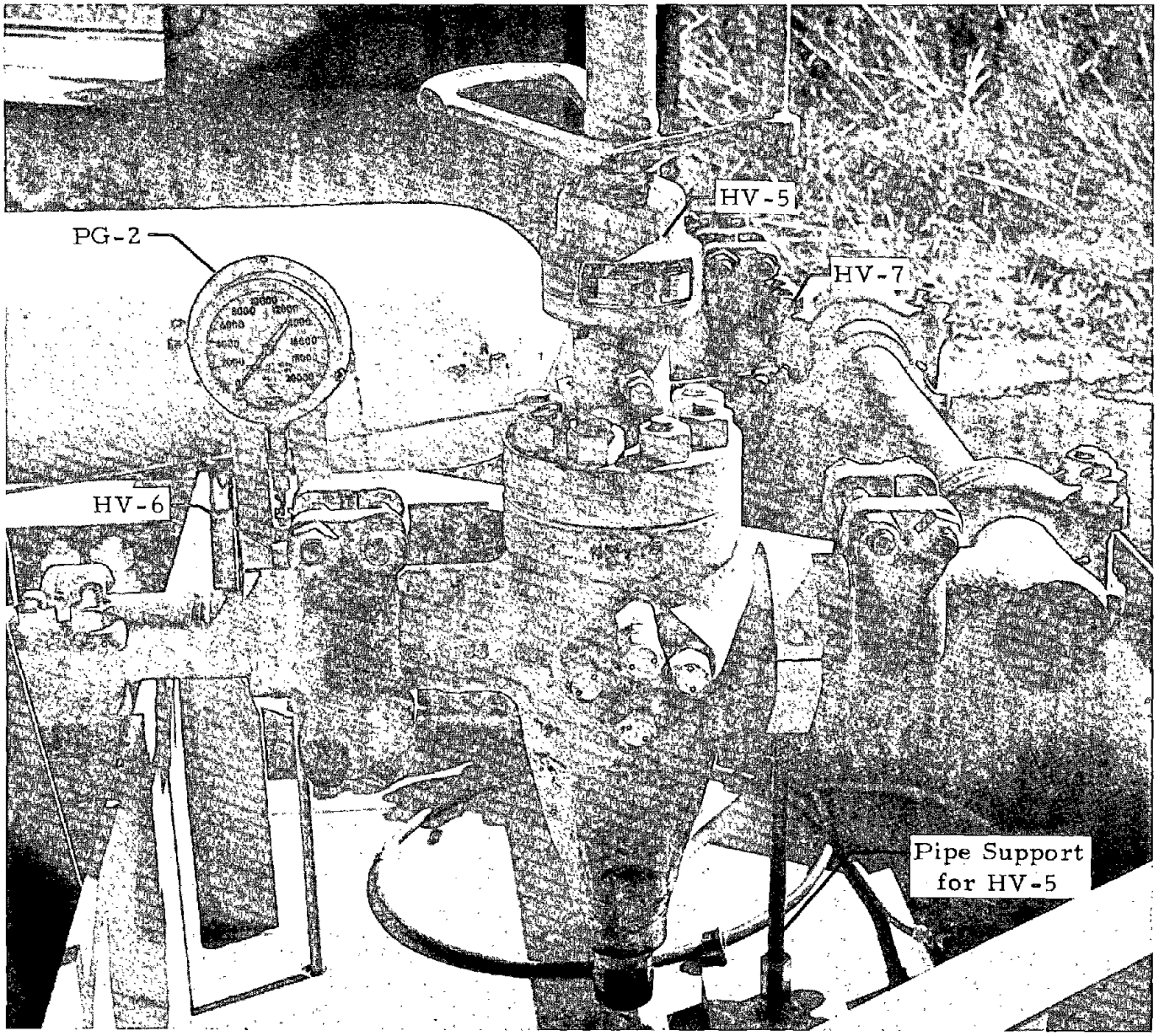

FIGURE 4-8. HIGH PRESSURE GN_2 SUBSYSTEM - VIEW 2

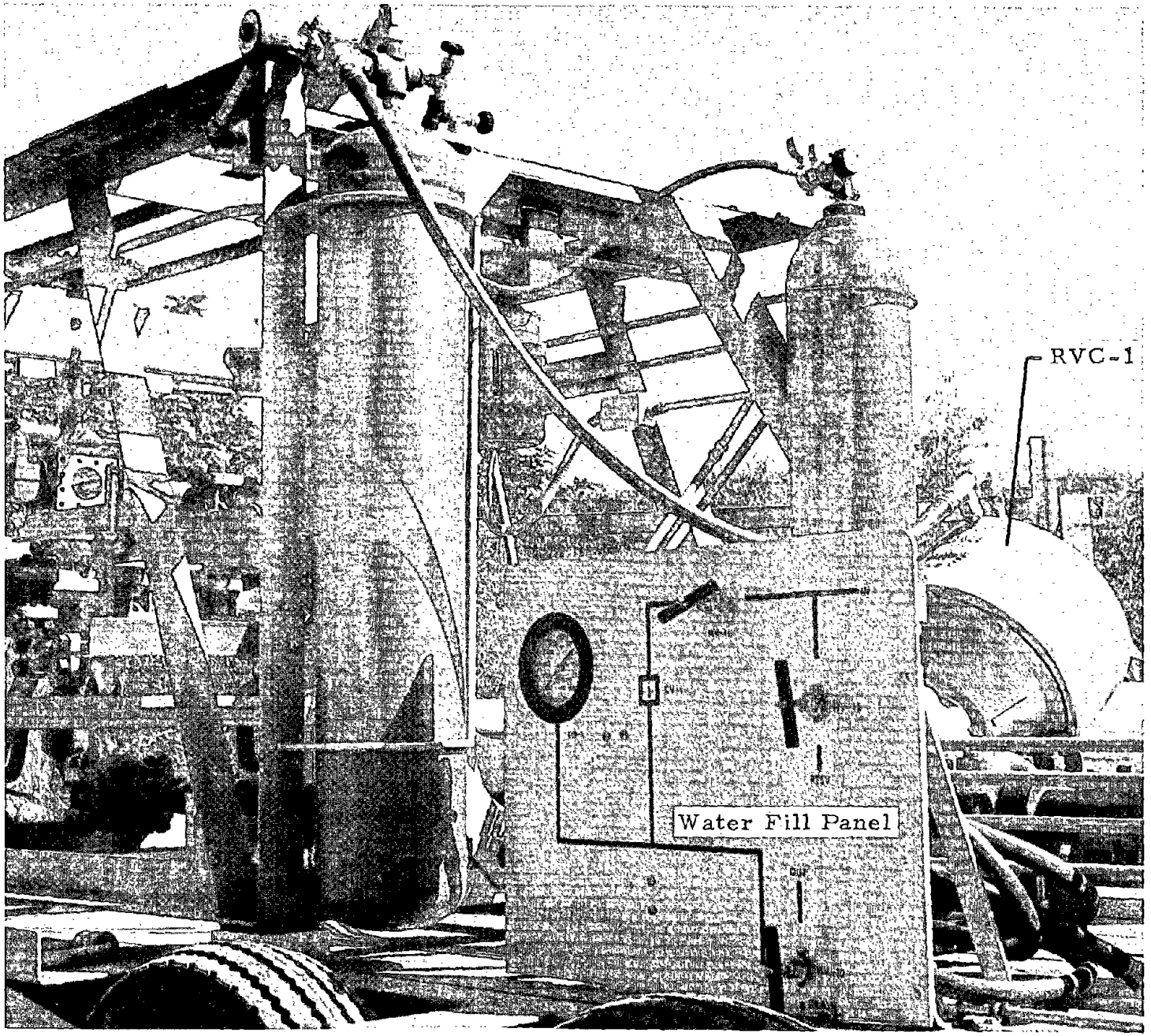

FIGURE 4-9. WATER SUBSYSTEM PANEL

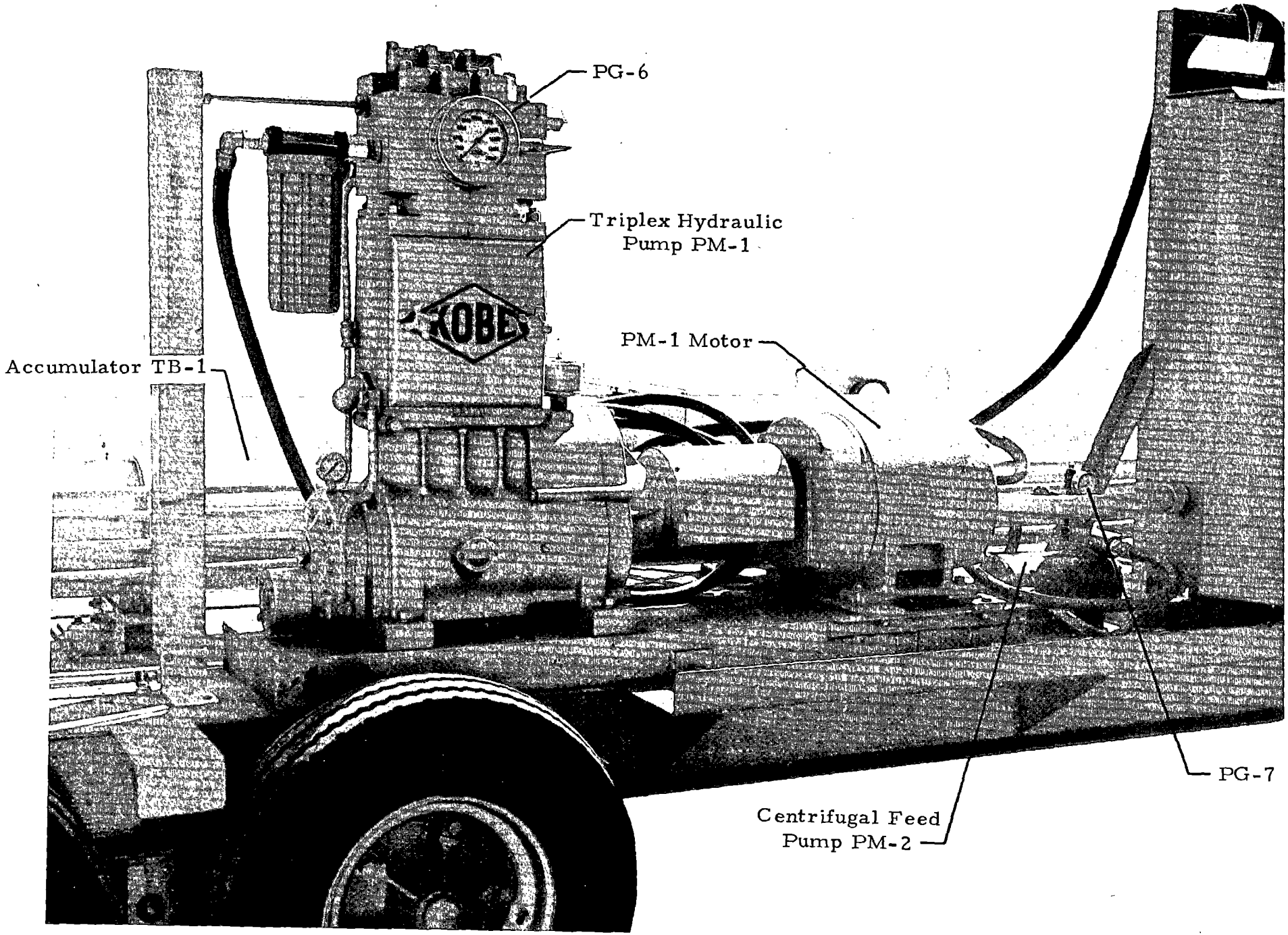

FIGURE 4-10. WATER SUBSYSTEM PUMPS

5. INITIAL TESTS

The purpose of the initial testing was to verify the operating procedures and perfect the water/particle nozzle portion of the excavator. The configuration of the axial-fed peripheral jet nozzle was fired with the screw feed in place but without particle feed. The jet atomized badly, and high back pressure pumped large quantities of water back through the particle feed chamber.

From the first test results, it was concluded that the annular opening which formed the water nozzle entered at too great an angle relative to the axis of symmetry. To determine the proper contour, a dummy rock nozzle was constructed with a pressure measurement opening along the axis as shown in Figure 5-1. Proper functioning of the particle feed and water jet required a contour which would produce an aspiration effect (i.e., a pressure less than ambient) on the rock nozzle exit. Aspiration was finally achieved using the configuration shown in Figure 5-1 without the secondary nozzle in place.

Sizing of the exit diameter of the secondary nozzle was also a critical factor. Referring to Figure 5-1, the jet leaving the annular opening "X" diverges inward because of the action of the orifice and the wall being treated two-dimensionally and also because the net volume available within a shell of constant incremental radius decreases as the radius decreases. At the axis, as the annular streams converge, backflow can occur if the central portion of the jet does not possess sufficient axial momentum forward to emerge. The forces tending to cause backflow can be reduced by increasing the exit diameter of the secondary nozzle. Sizing of the exit diameter of the secondary nozzle, shown in Figure 5-1, was achieved by starting with an exit diameter which was known to be too small and increasing the diameter by 0.050 inch until aspiration was achieved. The final exit diameter was 0.250 inch.

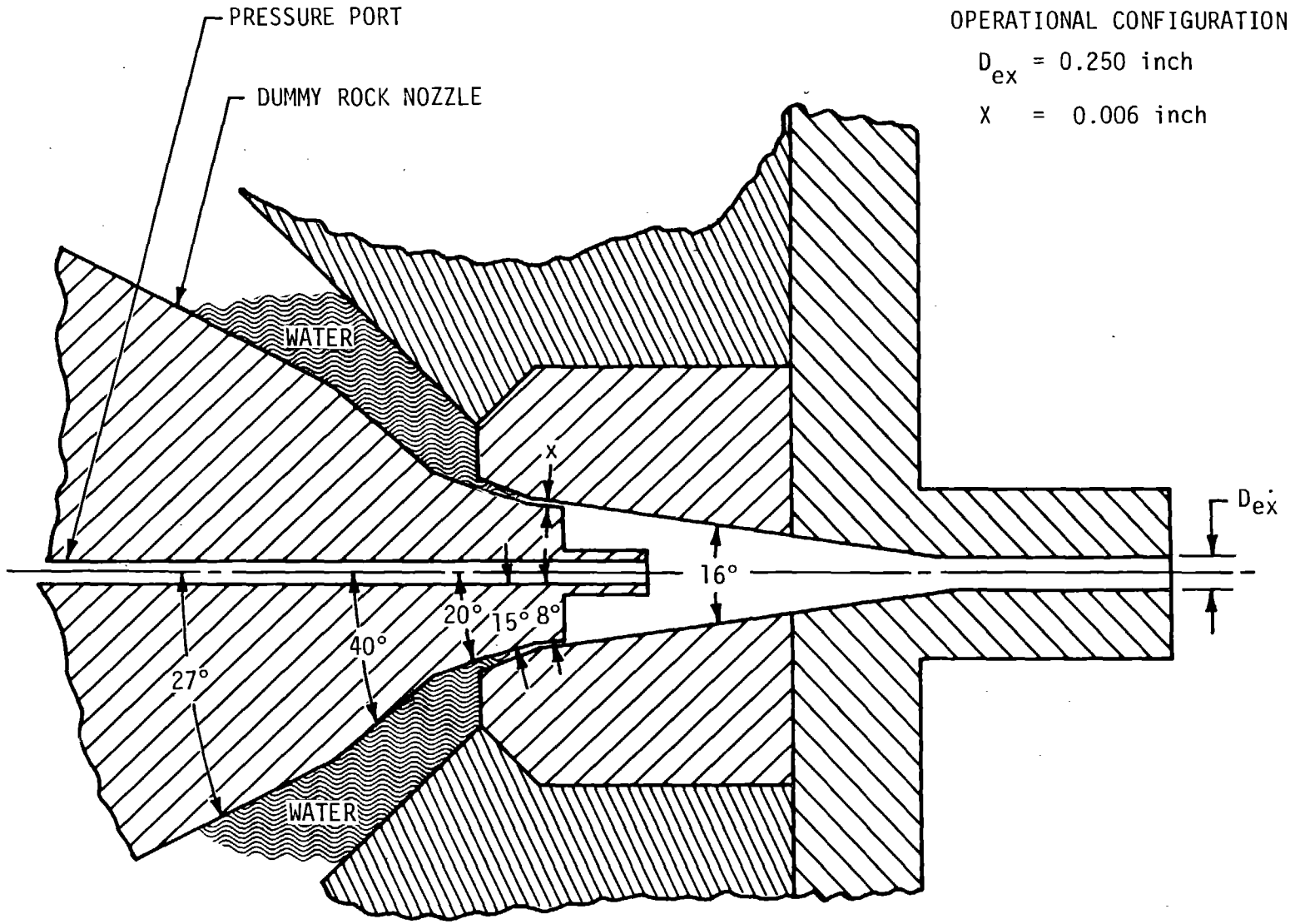

FIGURE 5-1. NOZZLE CONFIGURATION NO. 1

The latter technique produced the basic approaches used in the development of the nozzle. By using this approach, the two water/particle nozzle configurations shown in Figures 5-2 and 5-3 were developed with the latter appearing to give the best performance.

Some typical performance figures for the nozzle configurations are listed in Tables 5-1 and 5-2. The mass flow rate and test time could be varied by changing the width of the annular orifice. For Configuration 4, the gap was set statically at 0.006 inch and resulted in a mass flow rate of 5.74×10^3 gm/sec and a test time of 7.4 second. For Configuration 5, the gap was reduced to approximately 0.004 inch and produced a mass flow rate of 4.33×10^3 gm/sec and a time of approximately 10 seconds, which was nearer the desired specifications.

The flow rate through the annular orifice was found to be greater than that which could be accounted for theoretically. The effective gap is the width of the orifice which would have produced the mass flow rate corresponding to the operating pressures. A calculation of the strain produced in the nozzle could not explain the indicated increase in the gap.

The maximum theoretical velocity was computed on the basis of the average velocity produced by the initial and final operating pressure. The minimum theoretical velocity was computed on the basis of the mass flow of water flowing uniformly through the exit of the secondary nozzle. During testing, it was concluded that the effective jet velocity was probably closer to the minimum velocity.

During tests with particle feed, it was concluded that the aspiration created by the water jet was the factor controlling particle feed. The rotation rate of the mechanical feed screw appeared to have minimal effect on the particle feed rate. The only exception was that, during some tests when the rotation rate was zero, a noticable reduction in particle feed was experienced. From these results, it was concluded that the feed screw acted more to prevent clogging of the particle feed passages than as a means of force-feeding the nozzle. Overall, the

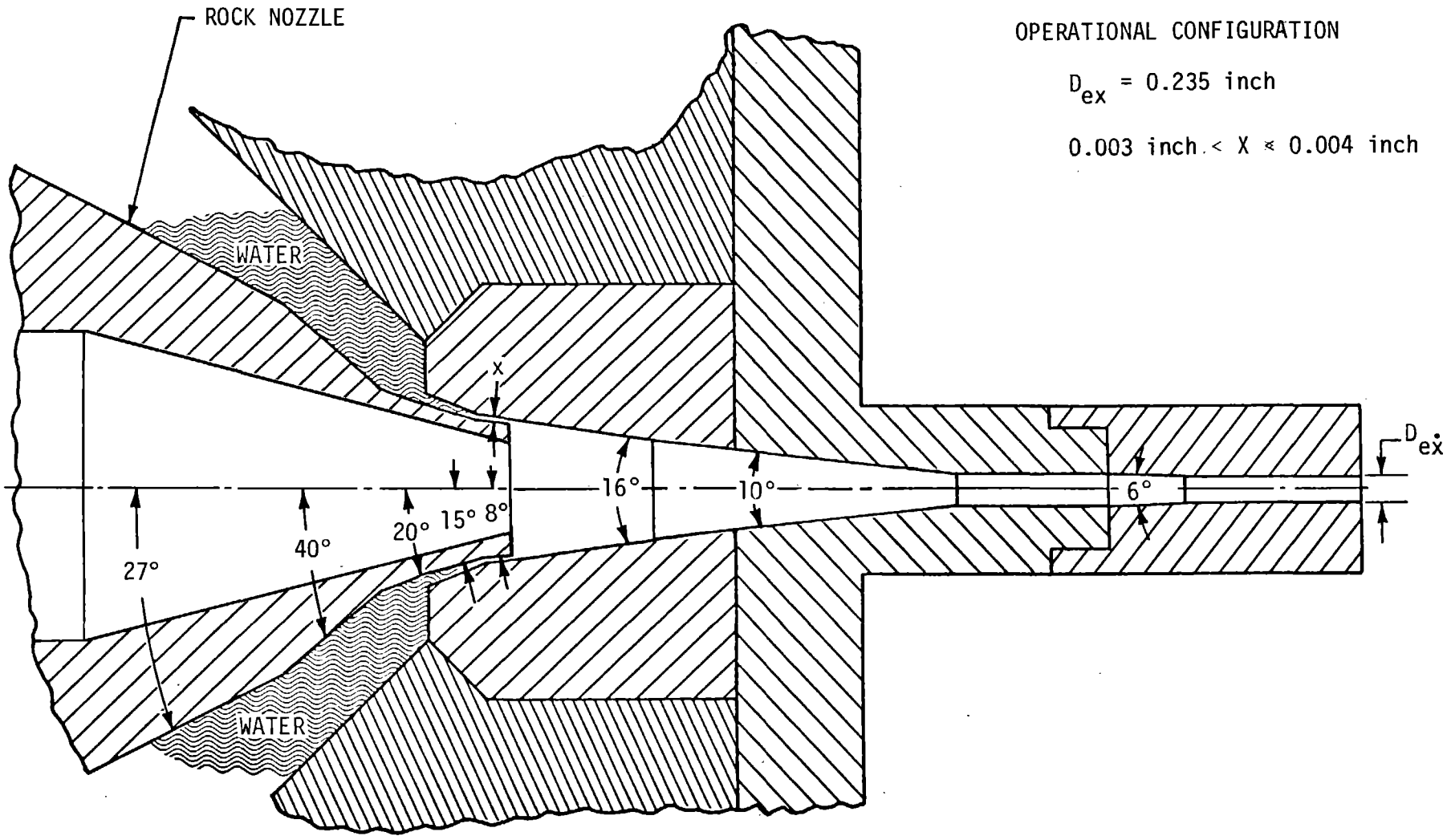

FIGURE 5-2. NOZZLE CONFIGURATION NO. 4

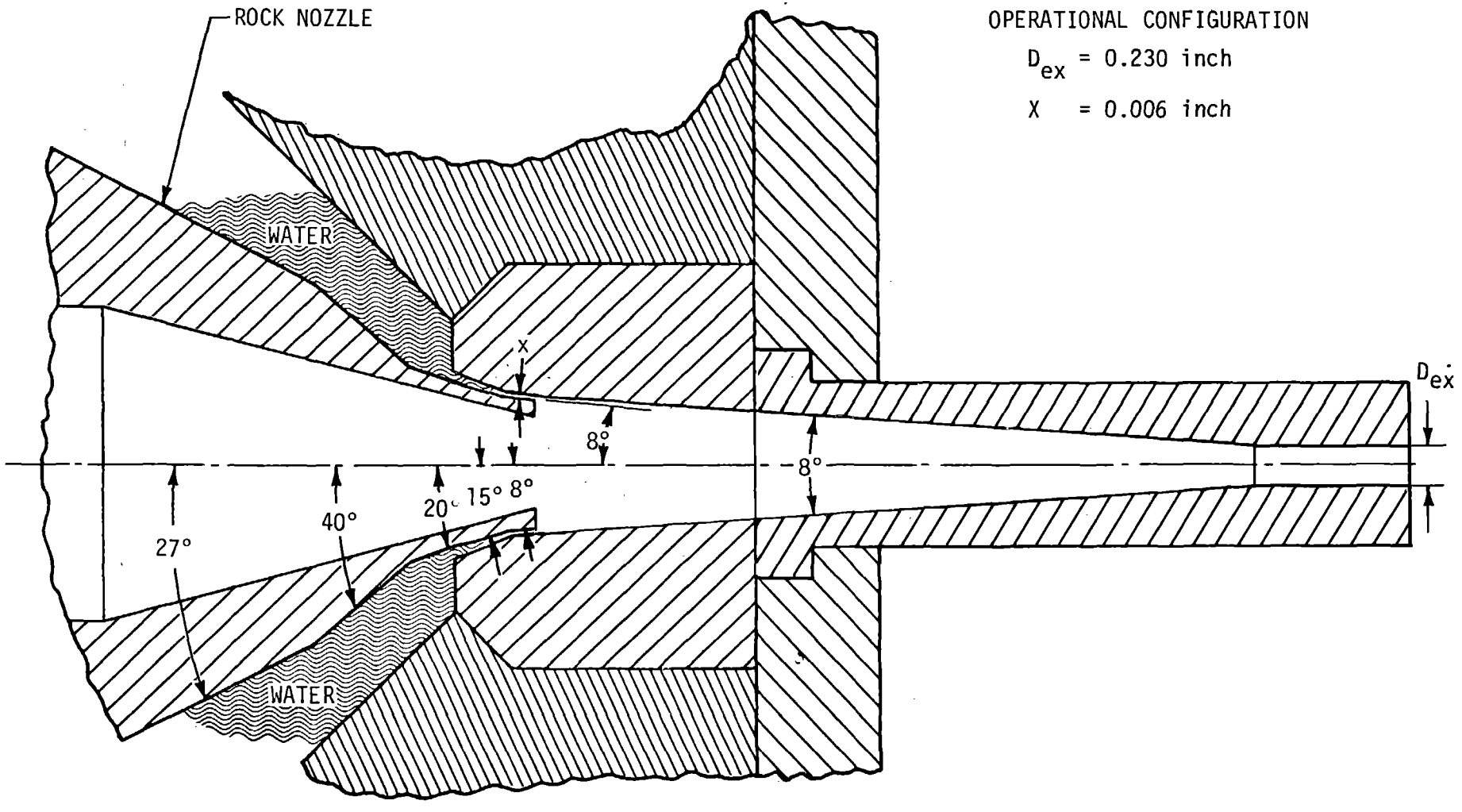

FIGURE 5-3. NOZZLE CONFIGURATION NO. 5

TABLE 5-1. NOZZLE CONFIGURATION NO. 4 PERFORMANCE

Water Mass Flow Rate	5.74×10^3 gm/sec
Initial Pressure	9.8×10^7 N/m^2
Final Pressure	7.24×10^7 N/m^2
Test Time	7.4 second
Static Gap "X"	0.006 inch
Effective Gap "X"	0.085 inch
Minimum Theoretical Velocity (Water Plus Particles)	2.14×10^4 cm/sec
Maximum Theoretical Velocity	4.12×10^4 cm/sec
Approximate Particle Injection Rate (Shop Polishing Balls)	~ 1700/sec

TABLE 5-2. NOZZLE CONFIGURATION NO. 5 PERFORMANCE

Water Mass Flow Rate	4.33×10^3 gm/sec
Initial Pressure	9.8×10^7 N/m^2
Final Pressure	7.24×10^7 N/m^2
Test Time	9.8 second
Static Gap "X"	0.004 inch
Effective Gap "X"	0.0064 inch
Minimum Theoretical Velocity (Water Plus Particles)	1.55×10^4 cm/sec
Maximum Theoretical Velocity	4.126×10^4 cm/sec
Approximate Particle Rate	
Crushed Limestone 1/16 < size < 1/8	10,000/sec
Crushed Limestone 1/8 < size < 3/16	3,350/sec

particle feed rates demonstrated by Nozzle Configuration No. 4 and No. 5 were considerably better than had been anticipated.

By using "shop deburring balls" having diameters approximately 0.150 inch and consisting of hard ceramic-like material, a maximum feed rate of 1,700 particles/sec was achieved by Nozzle Configuration No. 4. By using crushed limestone particles in sizes ranging from 1/16 to 1/8 inch, a particle feed rate of approximately 10,000 particles/sec was obtained with Configuration No. 5.

Based on the specific energy and the apparent spread of the jet, it was concluded that Nozzle Configuration No. 5 gave better performance than Configuration No. 4. Therefore, Nozzle Configuration No. 5 was used during the in situ testing.

As previously described, the development of Nozzle Configuration No. 4 and No. 5 was carried out by boring out the diameter of the secondary nozzle until aspiration was obtained. If the mass flow were passing through the secondary nozzle at the theoretical velocity, the corresponding exit diameters would have been 0.166 inch and 0.144 inch for Configuration No. 4 and No. 5, respectively. Comparing these diameters to the actual diameters (i.e., D_{ex} = 0.230 inch and D_{ex} = 0.235 inch) necessary to produce aspiration suggests a significant degree of turbulence and/or frictional loss within the nozzle.

As an attempt to reduce the loss in velocity head of the jet, a nozzle configuration having peripheral feed was tested. Figure 5-4 shows the configuration tested. The nozzle design follows that recommended by McCarthy and Molley (Ref. 5-1). Some typical performance characteristics are shown in Table 5-3. The mass flow rate and test time for Configuration No. 6 was 3.4×10^3 gm/sec and 12.5 seconds, respectively. As before, the secondary nozzle diameter was bored out in a stepwise fashion to a diameter of 0.221 inch. The secondary nozzle had no tendency to produce backflow and the 0.221-inch exit diameter was arrived at only because it produced sufficient aspiration for particle feed. The maximum particle feed rate of 1,600/sec obtained with this configuration using limestone particles in sizes ranging from 1/8 to 3/16 inch was approximately half that obtained with Configuration No. 5. However, the jet velocity of this nozzle appeared to be significantly higher than that predicted for Configurations 4 and 5.

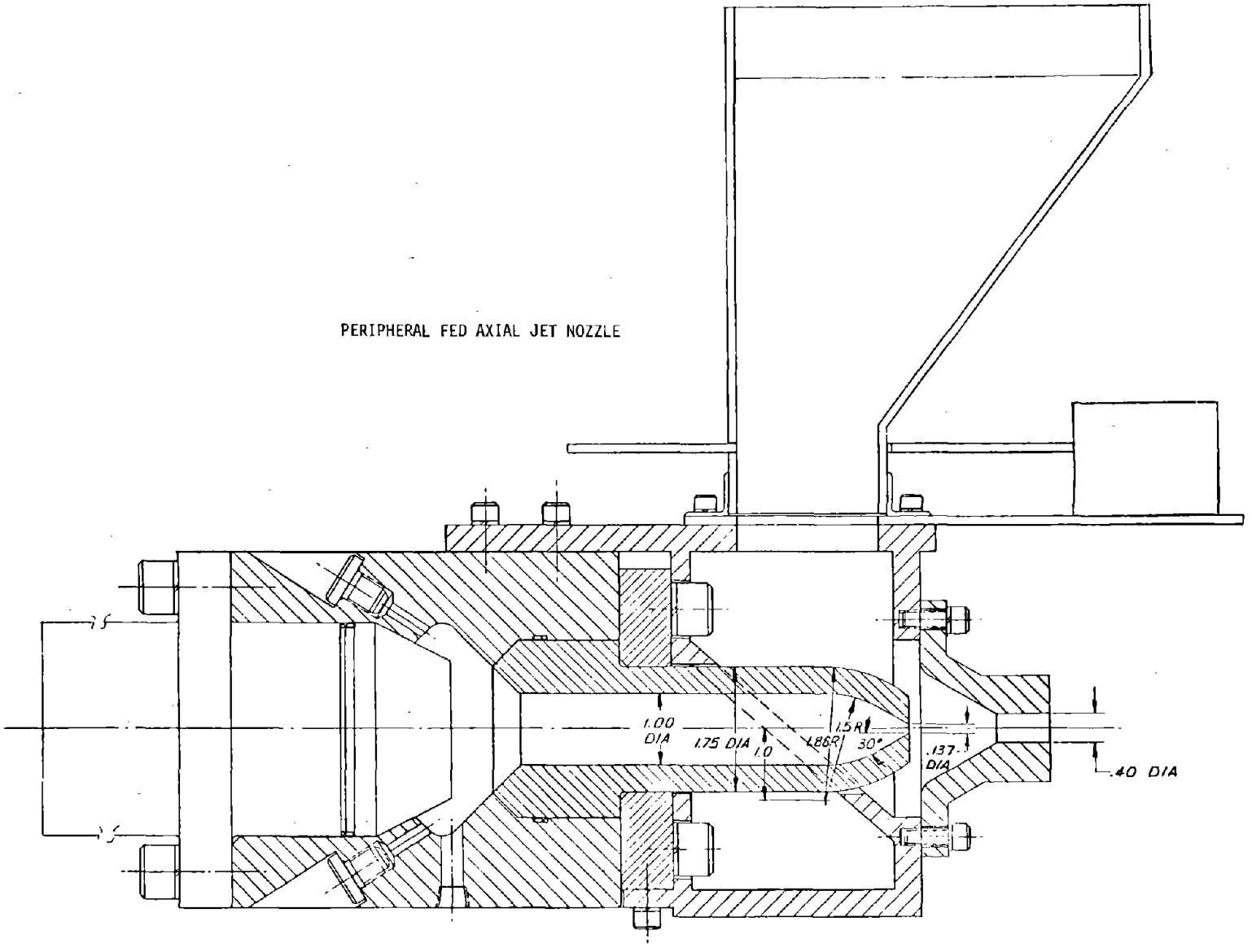

FIGURE 5-4. NOZZLE CONFIGURATION NO. 6

TABLE 5-3. NOZZLE CONFIGURATION NO. 6 PERFORMANCE

Water Mass Flow Rate	3.4×10^3 gm/sec
Initial Pressure	10×10^7 N/m^2
Final Pressure	7.24×10^7 N/m^2
Test Time	12.5 second
Theoretical Velocity	4.159×10^4 cm/sec
Approximate Particle Injection Rate (Crushed Limestone 1/8 < size < 3/16)	1,600/sec

Figures 5-5 and 5-6 are photographs of the jets of Configurations 5 and 6, respectively. As can seen in the photographs, the jet issuing from the Configuration No. 6 nozzle has less tendency to spread. This implies a greater downstream momentum flux and specific energy.

Figure 5-7 shows the approximate jet spread for Nozzle Configurations 5 and 6. In generating these dimensionless results, the radius of the secondary nozzle r_{ex} = 0.1175 inch was used as the parameter for Configuration No. 5 and the primary nozzle radius r_{ex} = 0.0685 inch was used for Configuration No. 6. The basic data for Nozzle Configuration No. 6 was obtained by analyzing photographs and examining the crater sizes produced during in situ testing. Both techniques were considered because it is suspected that the peripheral jet flow of configuration No. 6 produced an excessive degree of atomization along the outer periphery of the jet which the films show as significant jet spread. On the other hand, considering the cavity size versus stand-off distance indicates only the size of the high energy portion of the jet. Included in Figure 5-7 is cavity size data taken during tests with particle flow, with water only and with the nozzle extension removed (see Figure 5-3).

Because of the sharp definition of the outer periphery of the Configuration No. 6 jet (see Figure 5-6) only film analysis was used in determining the jet spread.

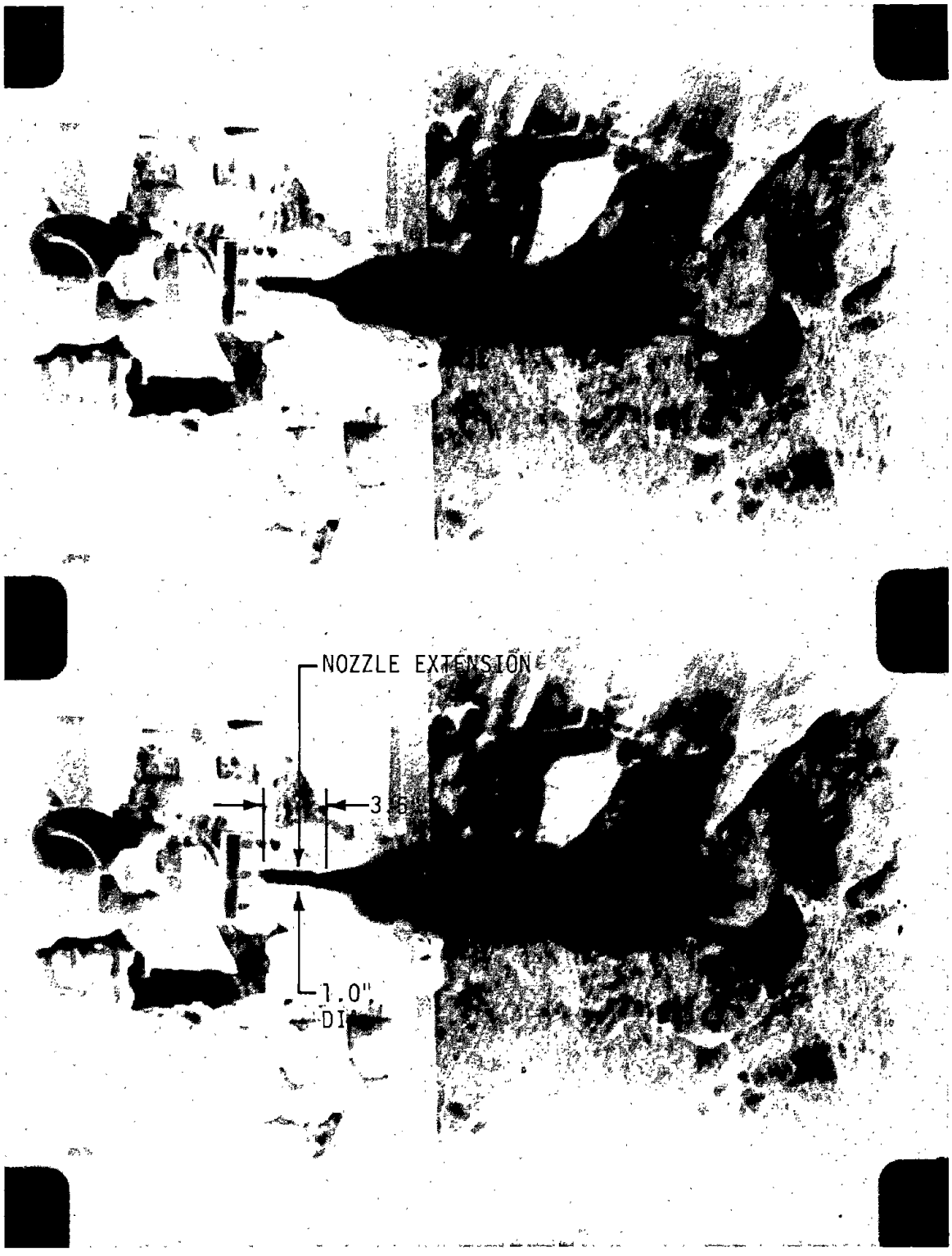

FIGURE 5-5. CONFIGURATION NO. 5 JET PLUME

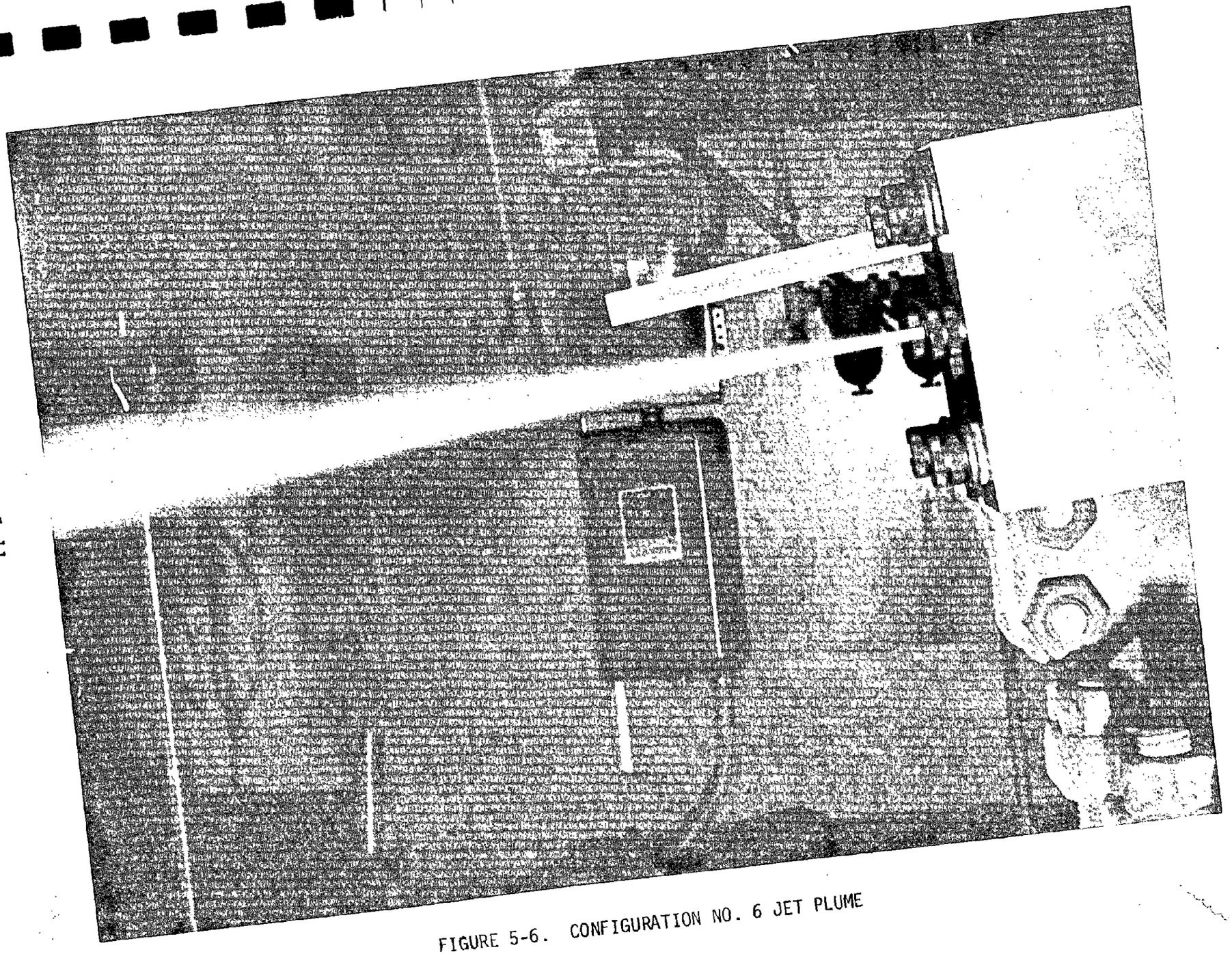

FIGURE 5-6. CONFIGURATION NO. 6 JET PLUME

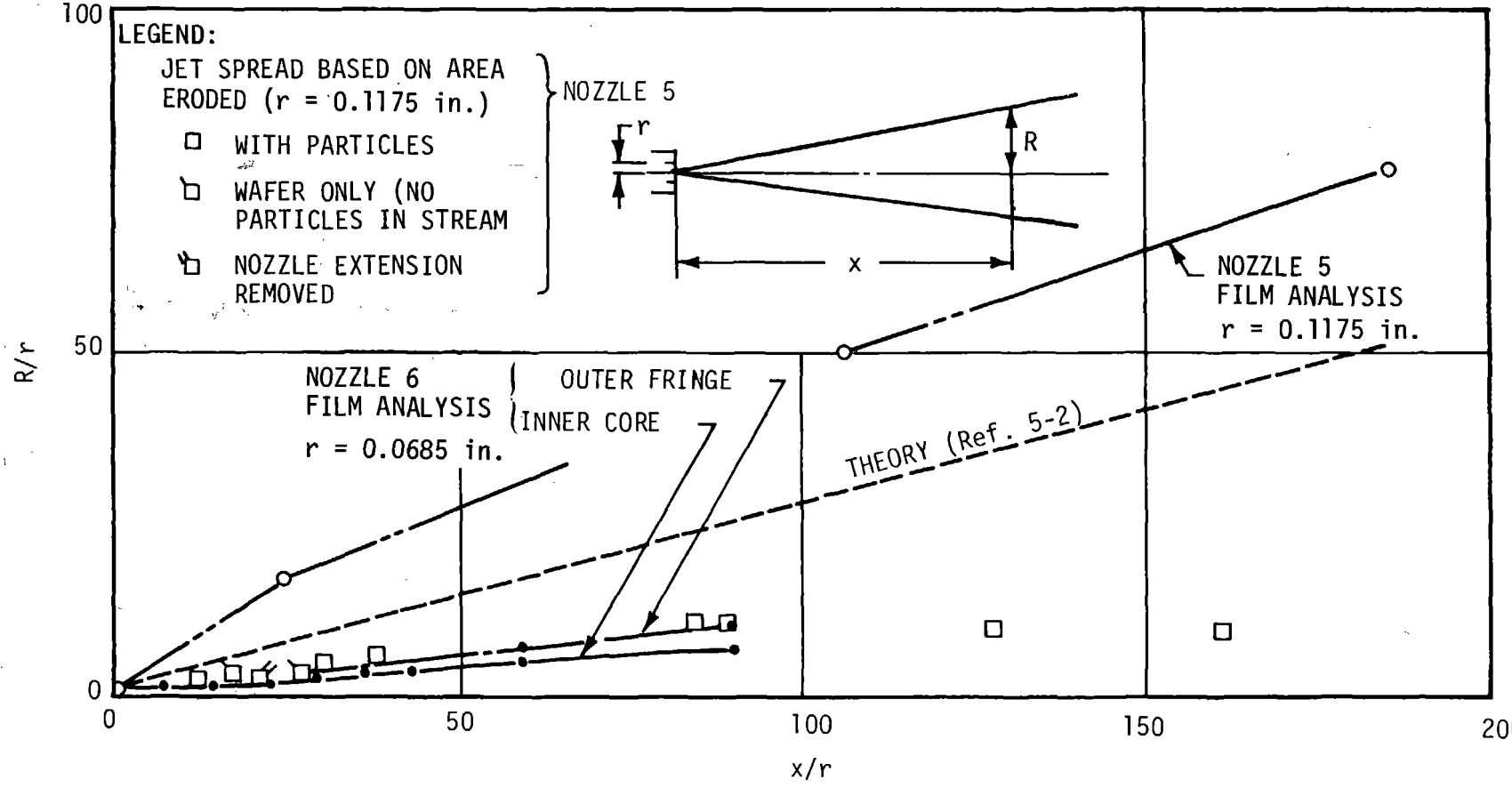

FIGURE 5-7. WATER-ROCK NOZZLE JET SPREAD

As can be seen in the figure, the spread of the jet produced by Configuration No. 6 jet is much less than that indicated by Configuration No. 5, film analysis. Jet spread as indicated by Configuration No. 5, crater size, is approximately the same as that indicated by Configuration No. 6. The latter suggests that, at the point of impact, the energy delivered to the wall per unit area was approximately the same for both configurations. This conclusion is also supported by the excavation test results (i.e., both nozzles indicated the same excavation ability).

A theoretical indication of the jet spread as given by Abromovich (Ref. 5-2) is also shown in Figure 5-7.

One series of tests were carried out using both nozzle configurations to determine if the particles were arriving at the target intact. From observation of the target area when particles were fired at hard rock, no particles were found which were the size of the original particles. Therefore, a test of each nozzle was conducted using wood as the target material. Observation of the target after the firing showed many particles embedded in the wood, and from this it was concluded that the particles did arrive at the target intact.

A complete list of tests and results are contained in Appendix A of this report.

REFERENCES - SECTION 5

5-1. McCarthy, M. J. and N. A. Molley, "Review of Stability of Liquid Jets and the Influence of Nozzle Design", The Chemical Engineering Journal, Number 7, Printed in the Netherlands, p. 1-20, 1974

5-2. Abromovich, G. N., "The Theory of Turbulent Jets", The MIT Press, Cambridge, Massachusetts, 1963

6. IN SITU TESTS

6.1 SUMMARY

A list of all tests conducted with the excavator is contained in Appendix A. Table 6-1 is a summary of the test matrix.

TABLE 6-1. TEST SUMMARY

Total Number of Tests	124
Number of Development Tests	35
Number of Excavation Tests	89
Concrete Target	26
Limestone Target	63
Traverse Tests	32
Static Tests	57
Limestone Particles	59
Water Only	14
Shop Balls	10
Steel Shot	4
Coal Particles	2
Maximum Standoff Distance	120 in.
Minimum Standoff Distance	0.5 in.

Of the total 124 tests conducted, 35 were development tests and 89 were excavation tests. The development tests were discussed in Section 5 and were used to perfect and evaluate the various hydraulic systems and operating procedures of the excavator. The excavation tests were conducted to evaluate the cutting capabilities of the machine.

During the excavation testing, both concrete (26 tests) and limestone (63 tests) were used as target excavation material. Particle feed consisted of limestone (59 tests), shop polishing balls (10 tests), steel shot (4 tests) and coal particles (2 tests). A total of 14 tests was conducted using water without particles. The nozzle was traversed

across the target during 32 tests and held fixed during 57 tests. Distances from the nozzle to the target was varied from a maximum of 120 inch to a minimum of 0.5 inch. Most of the tests with concrete as the target material were conducted with the nozzle approximately 15 inches from the target. Most of the tests with limestone as the target material were conducted with a standoff distance of approximately 10 inches.

6.2 SPECIFIC ENERGY EVALUATION FROM TEST RESULTS

The specific energy is one measure of the cutting ability of a hydraulic jet. Equation 2-10 gave the specific energy, which for the purpose of evaluation, was written as

$$S.E. = 0.0214 \frac{G\ V^2}{\gamma} \quad \left(\frac{\text{joules}}{\text{cm}^3}\right) \tag{6-1}$$

where

G - gallons of water pumped in the test time interval

V - jet velocity (ft/sec)

γ - volume of material removed (in^3).

Because the mass of the particles (on the order of 4 to 6 pounds) was negligible compared to the mass of the water, it was ignored in computing the specific energy.

For Nozzle Configuration No. 5, a velocity of 2.1×10^4 cm/sec (680 ft/sec) was used. This value is nearly the same as the minimum velocity given in Table 5-2 and was arrived at by studying high-speed film taken during development tests.

During most of the tests, the transfer barrier was pumped to capacity, which corresponded to 11 gallons of water.

By using 11 gallons and 680 ft/sec, Equation 6-1 can be written as,

$$S.E. = \frac{1.09 \times 10^5}{\gamma} \quad \left(\frac{\text{joules}}{\text{cm}^3}\right) \tag{6-2}$$

For Nozzle Configuration No. 6, the velocity was computed by determining the average velocity required for the 11 gallons of water to flow through the 0.137-inch-diameter primary nozzle. For conditions where the initial pressure was 9,800 psi, the test time was approximately 15 seconds giving an average velocity of 29.77×10^3 cm/sec (976.9 ft/sec). When the pressure was nearly 14,000 psi, the test time was approximately 12.5 seconds resulting in a velocity of 35.73×10^3 cm/sec (1,172.2 ft/sec).

Again using 11 gallons, Equation 6-1 gives,

$$\text{S.E.})_{p \approx 9,800} = \frac{2.25 \times 10^5}{\gamma} \left(\frac{\text{joules}}{\text{cm}^3}\right) \qquad (6\text{-}3)$$

and

$$\text{S.E.})_{p \approx 14,000} = \frac{3.24 \times 10^5}{\gamma} \left(\frac{\text{joules}}{\text{cm}^3}\right) \qquad (6\text{-}4)$$

Equations 6-2, 6-3, and 6-4 were used in evaluating the specific energies for most of the tests where an estimate of the volume removed could be made.

6.3 IN SITU CONCRETE TEST RESULTS

Table 6-2 lists some of the specific energies obtained using Nozzle No. 5 with concrete as the target. As can be seen in the figure, the tests using shop polishing balls gave the lowest specific energies. The shop polishing balls consisted of a carborundum particle matrix filled with fiberglass resin. Table 6-3 shows the approximate mass of the particles used in the tests. As seen in Table 6-3, the shop polishing balls had a mass approximately 7 times as great as the limestone particles used in the concrete tests (i.e., $1/16 < \text{size} < 1/8$). The limestone particles indicated the next highest specific energy. The highest specific energy was obtained using water without particles. Generally, it appeared that the specific energy was reduced as the mass of the particle increased.

TABLE 6-2. SPECIFIC ENERGY RESULTS FOR CONCRETE

TEST	FEED MATERIAL	MATERIAL REMOVED (in^3)	STANDOFF DISTANCE (in)	SPECIFIC ENERGY (joules/cm^3)
R-18	Shop Polishing Balls	52.5 (860 cm^3)	49	2,076
R-38	Limestone 1/16 < size < 1/8 in.	11.0 (180 cm^3)	23.5	9,913
R-39	Water Only	1.2 (19.7 cm^3)	23.5	92,600
R-42	Limestone 1/16 < size < 1/8 in.	24.74 (405.4 cm^3)	25	4,406
R-43	Shop Polishing Balls	29.3 (480 cm^3)	30	3,722
R-44*	Shop Polishing Balls	73.2 (1,200 cm^3)	16.5	1,489
R-46*	Limestone 1/16 < size < 1/8 in.	21.0 (344 cm^3)	16.5	5,190

*R-44 and R-46 had traverse rates of approximately 1.9 in/sec and 1.6 in/sec, respectively.

TABLE 6-3. PARTICLE MASS

PARTICLE TYPE	APPROXIMATE MASS (kg/particle)
Steel Shot size Approximately 0.160	3.5×10^{-4}
Shop Polishing Balls 0.155 in. < size < 0.175 in.	1.4×10^{-4}
Limestone Particles 0.125 in. < size < 0.1875 in.	0.66×10^{-4}
Limestone Particles 0.625 in. < six < 0.125 in.	0.20×10^{-4}

Testing the rock nozzle using concrete as the target material could yield somewhat misleading results because of the aggregate and nonhomogeneous nature of the concrete. However, these results did indicate the excavator was producing specific energies in the range of interest. Results of previous work, for instance, as discussed in Reference 6-1, have indicated that specific energies less than 2,000 joules/cm^3 in limestone are promising. Test results with the concrete also indicated a potential order of magnitude decrease in specific energy could be obtained with particle injection (see specific energies for tests R-38 and R-39).

During most of the concrete tests, the jet would "scour" what appeared to be a paraboloid-shaped crater during static operation and an oblong crater with a parabolic cross-section during traverse operation. Photographs of single shot damage are shown in Figures 6-1 and 6-2. Figure 6-1 shows the single-shot damage resulting from stationary test R-43. Figure 6-2 shows the single-shot damage resulting from test R-44 with a traverse rate of approximately 1.9 in/sec.

6.4 IN SITU LIMESTONE TEST RESULTS

A total of 63 tests were conducted using limestone as the target material. The target material was either the quarried face of an abandoned limestone quarry or large limestone bolders.

During the test series, two different types of rock cutting were observed. During some tests, the jet would "scour" what appeared to be a paraboloid-shaped crater in the target area. At other times, the jet would break varying sized fragments from the rock surface. Approximately half of the 63 tests resulted in varying degrees of fragmentation. Figure 6-3 shows photographs of some of the fragmentation encountered. Figure 6-3a shows typically the size fragment which was chipped from the quarry face. Figure 6-3b and Figures 6-3c and 6-3d show a large bolder before and after test LS-70. The actual target area was approximately the center of the bolder face as seen in Figure 6-3d. The size of the fragment resulting from test LS-70 measured approximately 2,770 in^3 and produced the largest degree of fragmentation encountered in the entire

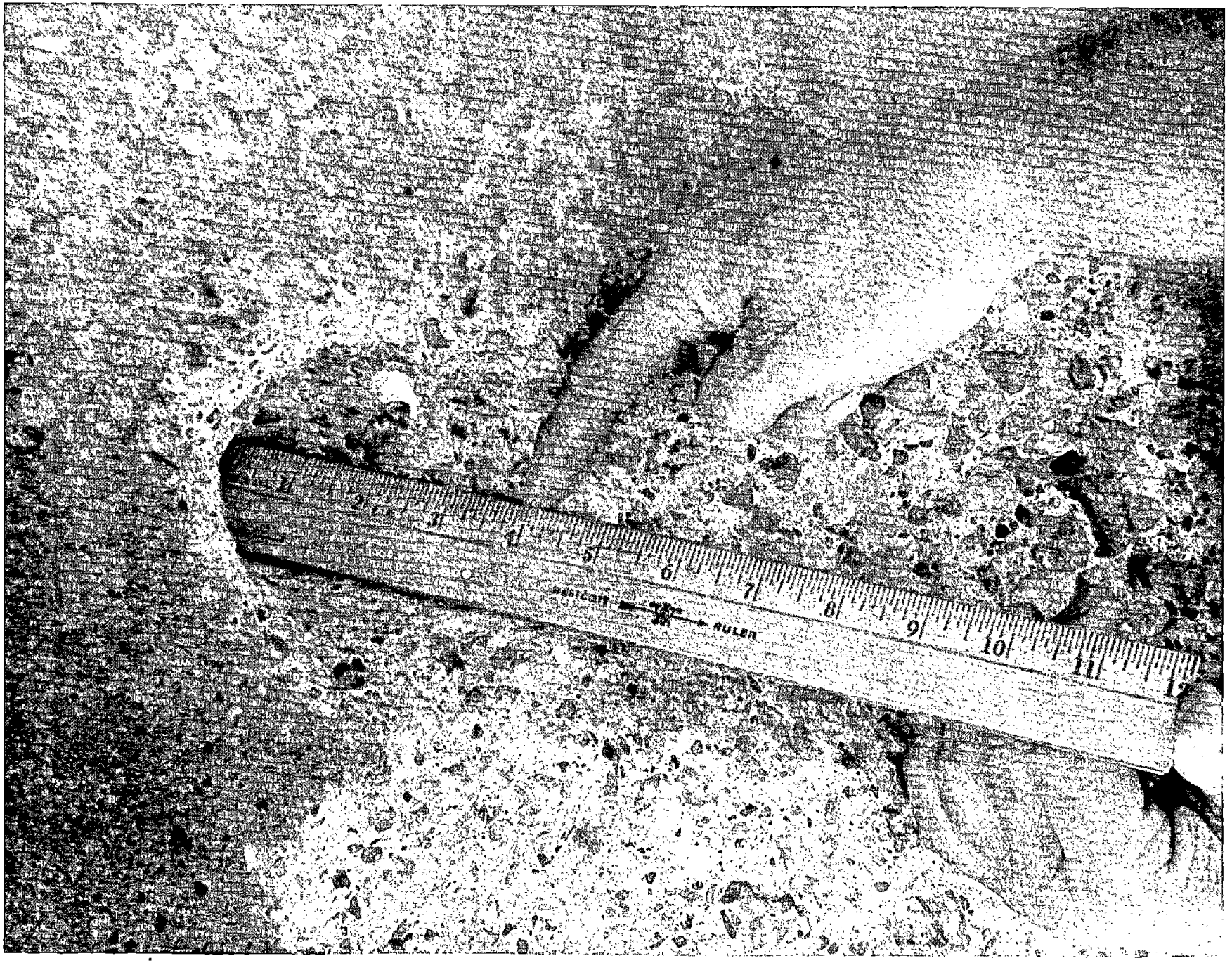

FIGURE 6-1. SINGLE-SHOT DAMAGE TO CONCRETE WITH NOZZLE STATIONARY; TEST R-43

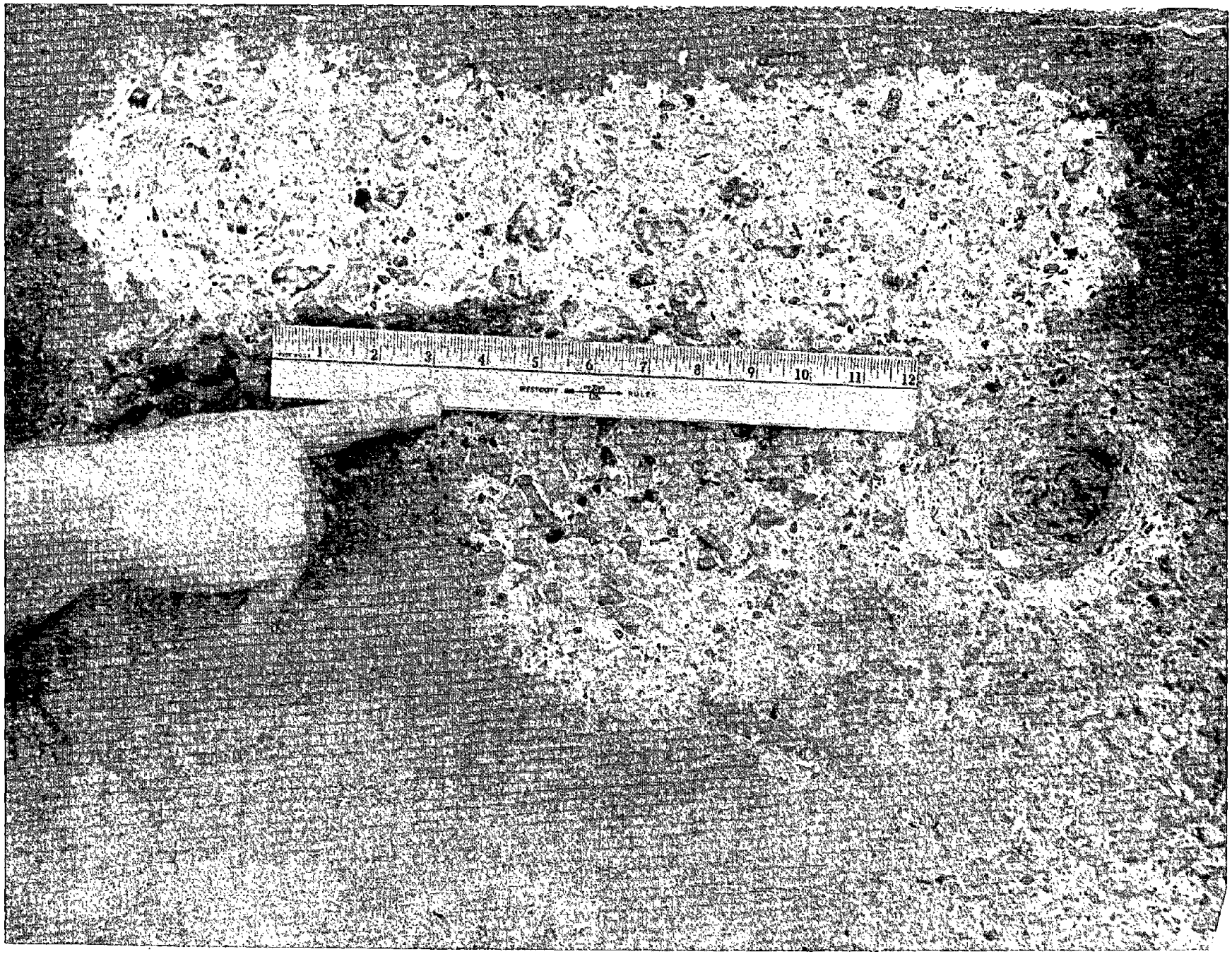

FIGURE 6-2. SINGLE-SHOT DAMAGE TO CONCRETE WITH NOZZLE TRAVERSED; TEST R-44

a. AFTER TEST LS-57

b. BEFORE TEST LS-70

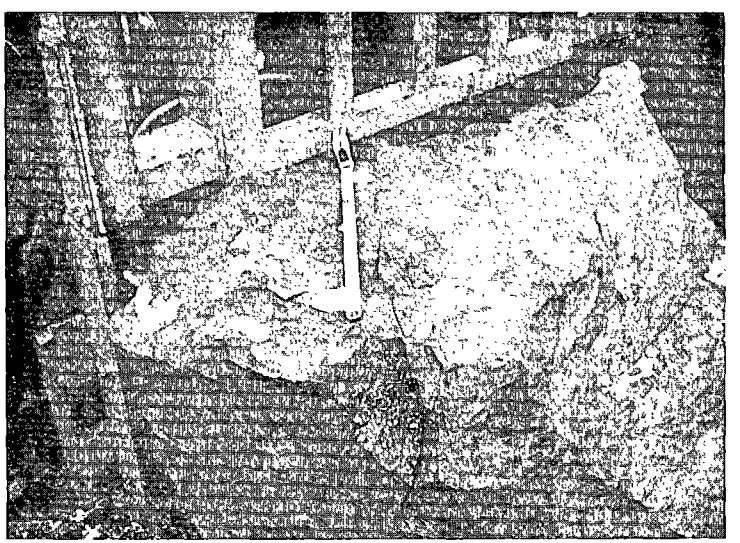

c. AFTER TEST LS-70

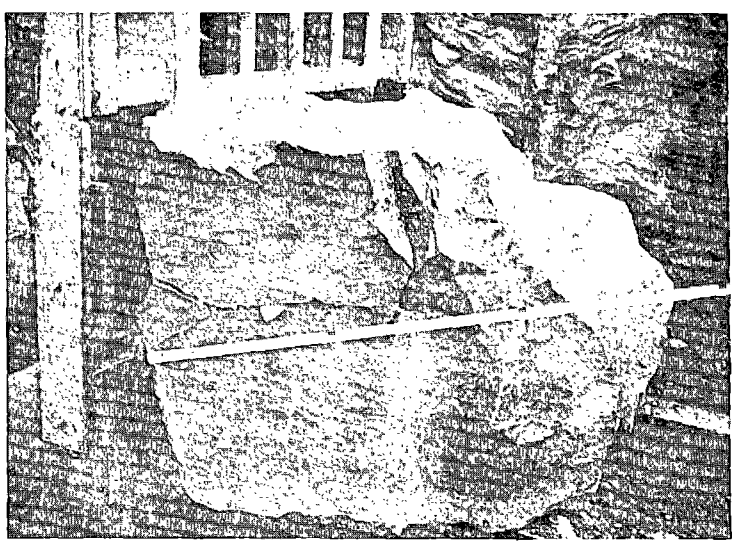

d. AFTER TEST LS-70

FIGURE 6-3. EXAMPLES OF FRAGMENTATION

test series. Including the entire fragmented volume in the computations resulted in a specific energy of approximately 39 joules/cm^3.

Various techniques were used to estimate the volume of material removed. When the jet produced a clean crater, modeling clay was used. This technique, when it could be used, produced the best estimate of the volume. Another technique consisted of spreading a plastic sheet below the test area and collecting fragments after each test. This technique gave rough estimates of the volume when significant fragmentation occurred. Overall the estimate of the volume was reasonably accurate when the result was a clean crater and somewhat rough when serious fragmentation occurred.

Generally, the in situ limestone test results tended to be somewhat erratic and difficult to evaluate. As one example, Figure 6-4 is a photograph of the target area taken before and after test LS-59. During this test, the standoff distance was approximately 6 inches and the nozzle was traversed at a rate of approximately 1.2 in/sec. As seen in the figure, only slight erosion of the surface occurred over an area approximately 10 inches long and 3 inches wide. After 6 additional tests of this same location, a significant amount of material eventually cracked from the target, resulting in what is seen in Figure 6-5. The three small craters on the right in Figure 6-5 resulted from stationary Tests LS-60, LS-61, and LS-62. Test LS-62 produced a larger volume removal and lower specific energy than either LS-60 or LS-61 even though no particles were injected during Test LS-62. The latter, i.e., lower specific energy without particles, appeared to be the exception rather than the rule.

Figure 6-6 shows results of a series of tests where the type of material entrained in the jet was varied. The standoff distance for these tests was approximately 10 inches, and the traverse rate was equivalent to approximately 1.5 in/sec. The uppermost kerf was produced as a result of Tests LS-100 and LS-101 where only water was used. The second and third

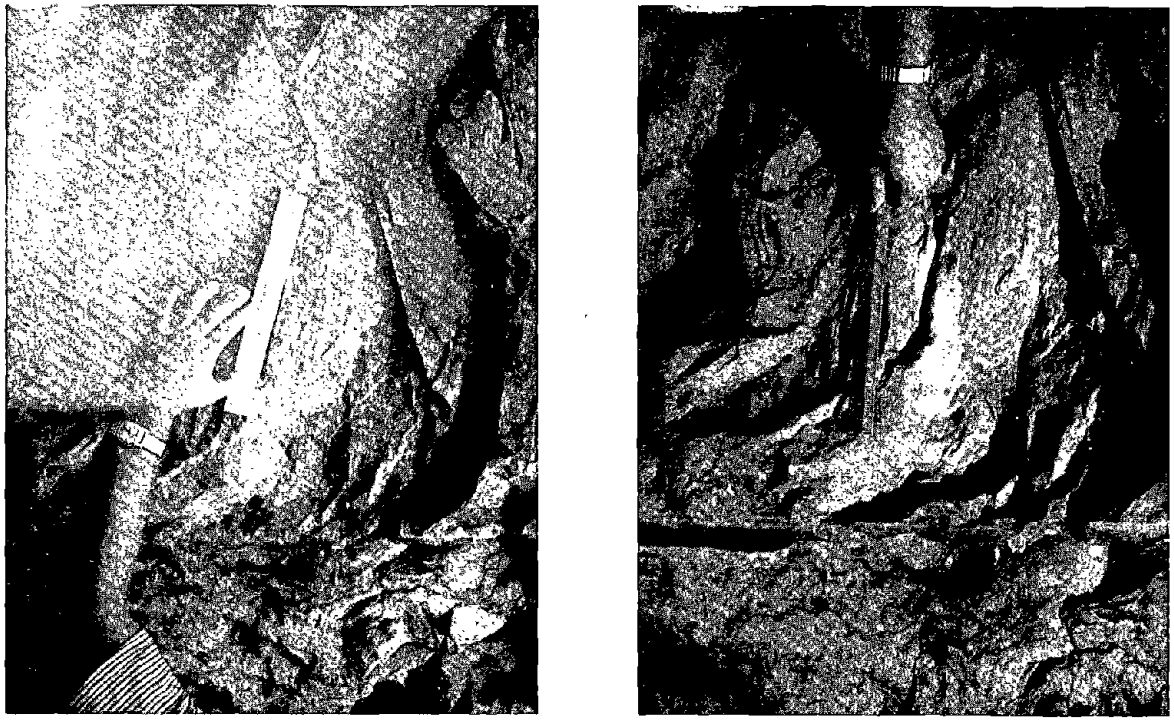

BEFORE LS-59

AFTER LS-59

FIGURE 6-4. PHOTOGRAPH OF LIMESTONE TARGET BEFORE AND AFTER TEST LS-59

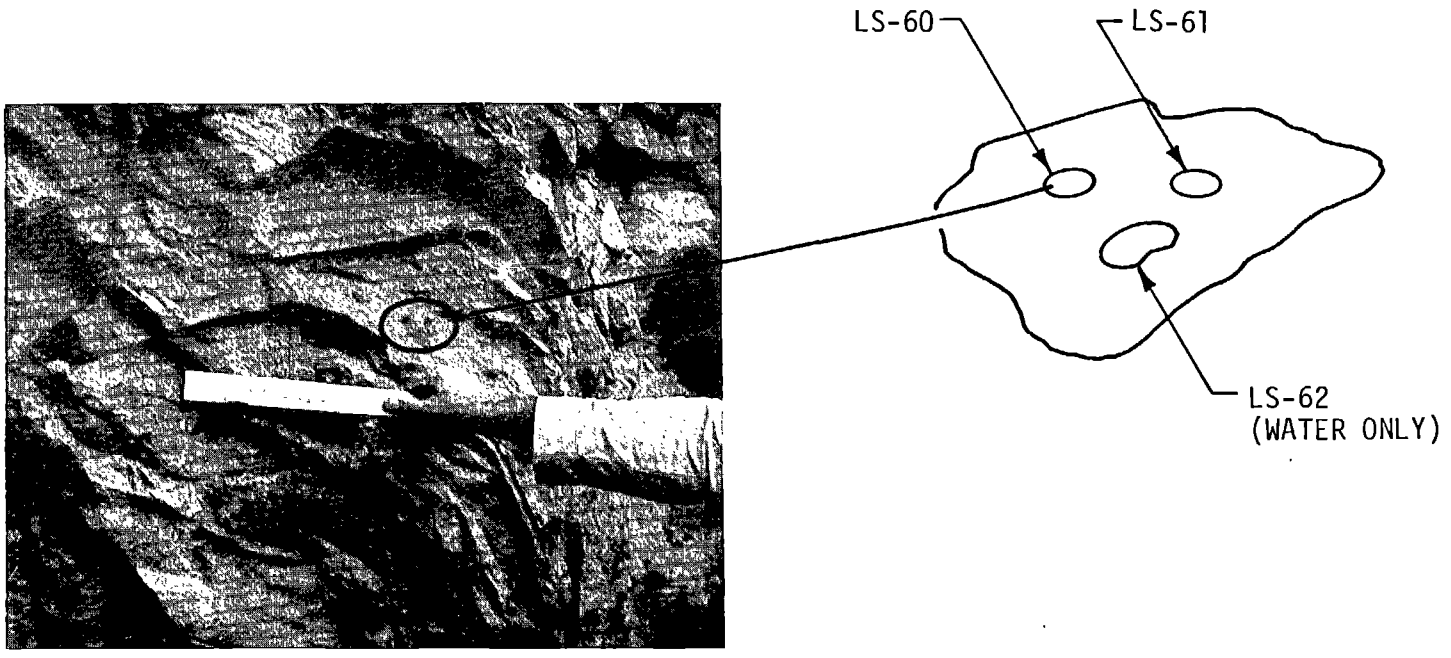

AFTER TEST LS-65

FIGURE 6-5. PHOTOGRAPH OF LIMESTONE TARGET AFTER TEST LS-65

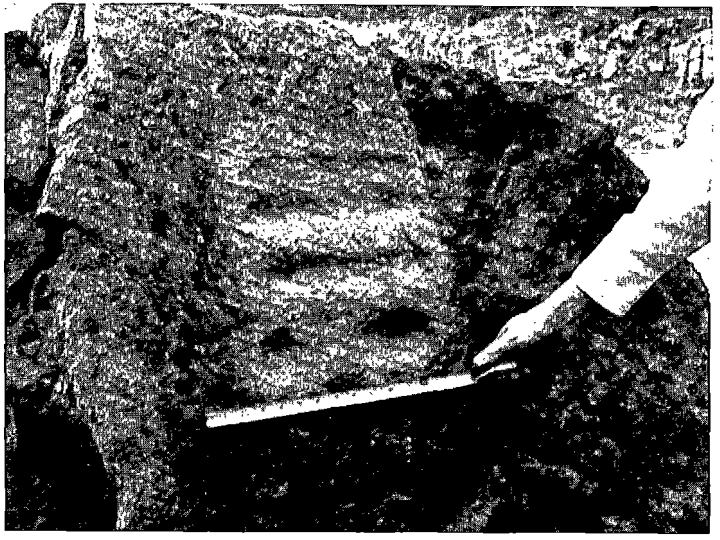

AFTER LS-51

FIGURE 6-6. PHOTOGRAPH OF TARGET AFTER TESTS LS-94 THROUGH LS-103

kerfs were produced as a result of Tests LS-94 through LS-99 using limestone particles entrained in the jet. The second kerf was produced by four tests (LS-94 through LS-17) and the third kerf by two tests (LS-98 and LS-99). The bottom kerf was produced using steel shot injected into the jet.

Testing of Nozzle Configuration No. 6 was started with Test X-104. After the development testing, excavation tests were conducted using limestone boulders obtained from a limestone quarry approximately 5 miles from the previous tests. Brinell hardness tests indicated that the limestone used as target material for all Nozzle No. 6 tests (i.e., LS-113 and subsequent) was approximately twice as hard as that of previous limestone target material. There is little doubt that the hardness of the target material would decrease the amount of material removed and thereby increase the specific energy.

Figure 6-7a shows the cavity scoured during Test LS-117 using Nozzle Configuration No. 6. As can be seen in the figure, most of the impacts appeared to occur in the outer periphery of the 5-inch-diameter cavity. Figure 6-7b shows a large fragment cracked from the target during Test LS-119. It was anticipated that because of the change in the water nozzle design a significant increase in cutting ability would be gained using Nozzle No. 6 as compared to Nozzle Configuration No. 5. Although it is unclear how the hardness of the target material would quantitatively affect the excavation capabilities of the jet, no significant increase in jet cutting was indicated by the testing of Nozzle Configuration No. 6.

Figure 6-8 shows the specific energy originally predicted for a rock-rock impingement (sandstone). The predicted performance did not include the water in the jet. As can be seen in the figure, the predicted specific energy for a velocity of 600 to 700 ft/sec was 300 to 400 joules/cm^3. Using steel shot, Safhl obtained specific energies on the order of 25 joules/cm^3. Using steel shot in the rock nozzle and neglecting the mass of the water gives a specific energy of approximately 300

FIGURE 6-7a. CRATER SCORED WITH NOZZLE NO. 6 USING STEEL SHOT, TEST LS-117

FIGURE 6-7b. FRAGMENT CRACKED FROM TARGET USING NOZZLE NO. 6, TEST LS-119

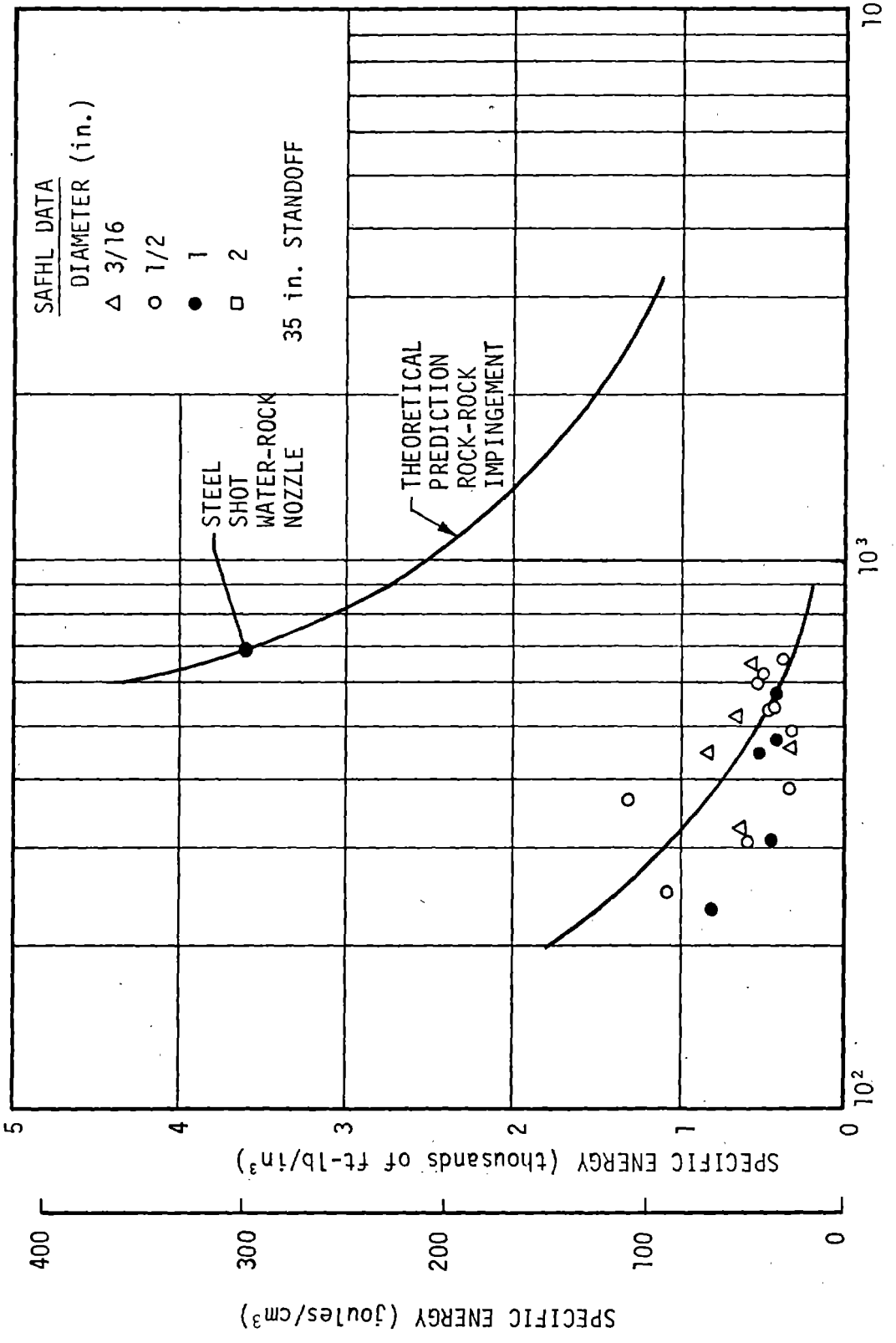

FIGURE 6-8. COMPARISON OF SPECIFIC ENERGY OF ROCK EXCAVATION (from Ref. 6-3)

joules/cm^3. Likewise, limestone particles produced a specific energy of approximately 1,000 joules/cm^3, ignoring the mass of the water.

Figure 6-9 shows a comparison of the specific energy versus pressure from different test results. The specific energies obtained for the water-rock nozzle using various particulate materials are also shown in Figure 6-9. The results reported in Reference 6-1 show a decrease in specific energy with pressure, whereas the specific energies reported in Reference 6-2 show the opposite trend. Generally, the specific energy obtained from the rock nozzle was comparable to that reported by other investigators.

Figure 6-10 shows the specific energy obtained for individual tests. The open symbols shown in Figure 6-10 denote tests where "scouring" only was observed and the solid symbols denote tests where fragmentation resulted. As can be seen in the figure, including fragmentation reduces the specific energy by as much as three orders of magnitude below that of "scouring" only. Also included in the figure are the specific energies obtained ("scouring" only), with a traverse mode of operation. As can also be seen in the figure, traversing the nozzle appears to reduce the specific energy by approximately one to two orders of magnitude below that obtained during the static mode operation.

Figure 6-11 shows the specific energy obtained from the rock nozzle tests during the traverse mode of operation. The solid symbols denote the cumulative specific energy obtained by including fragmentation. The open symbols denote tests where "scouring" only was observed. The cumulative specific energy was obtained by adding the volume of material removed from the same target area over a series of tests. The amount of material removed was determined by collecting fragments from a drop cloth placed in front of the limestone face. It has been estimated that approximately one-third to one-half of the fragments cut from the target landed beyond the drop cloth. As a result, the cumulative specific energy could be as much as two-thirds to one-half of that shown in the figure. Characteristically, the cumulative specific energy appeared to

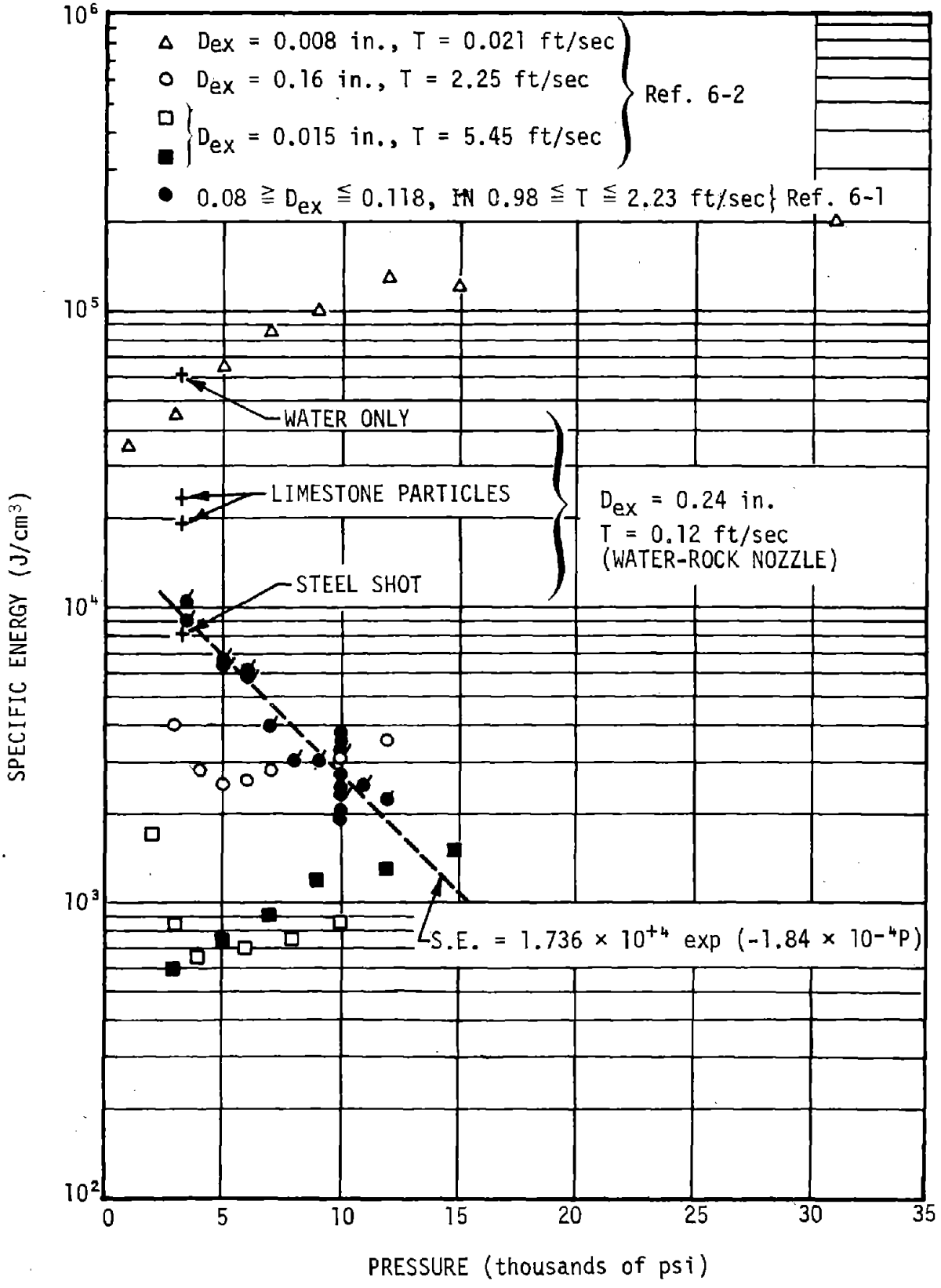

FIGURE 6-9. COMPARISON OF SPECIFIC ENERGY VERSUS PRESSURE FROM DIFFERENT TESTS

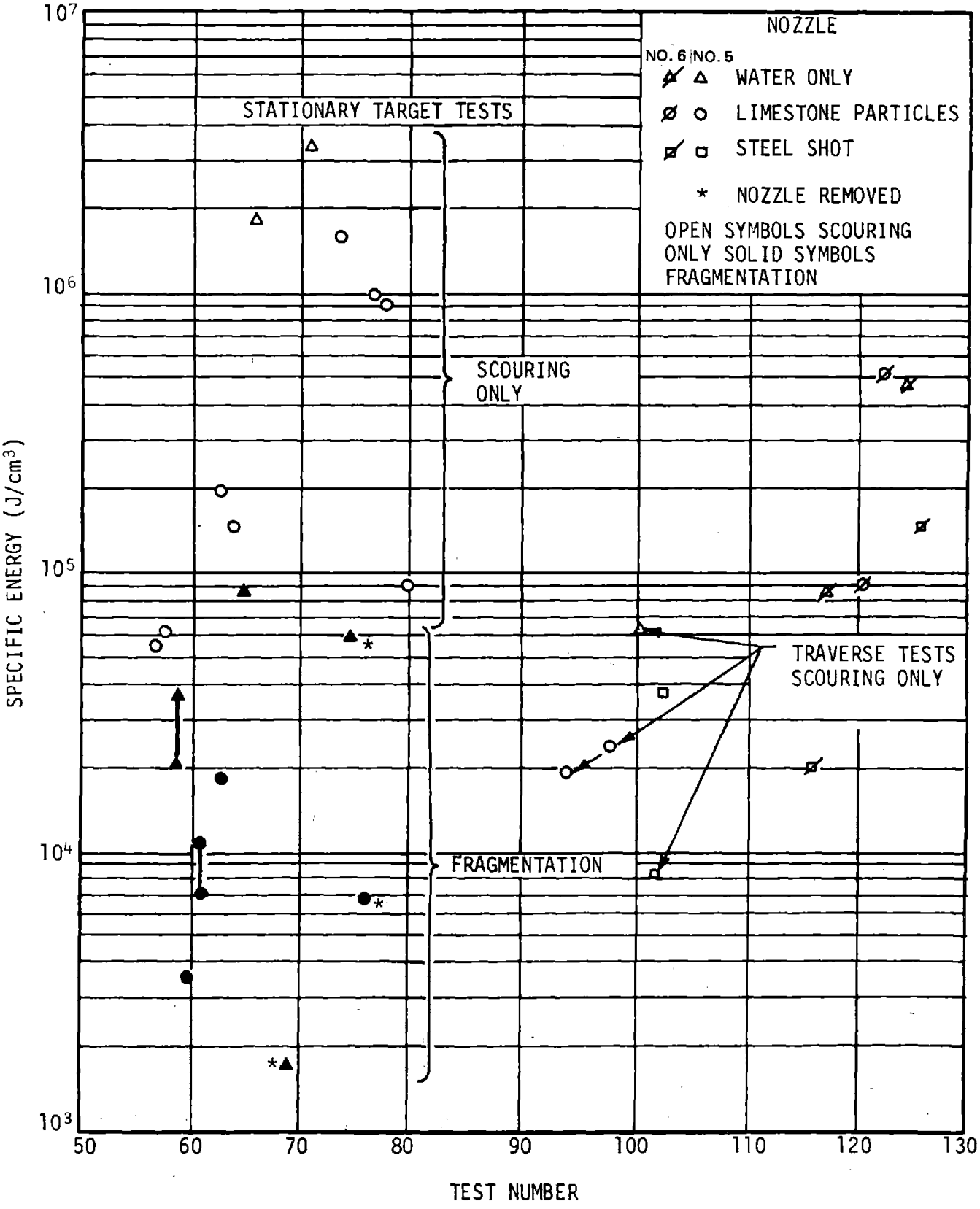

FIGURE 6-10. SPECIFIC ENERGY OBTAINED DURING STATIC TESTS FOR WATER-ROCK NOZZLE

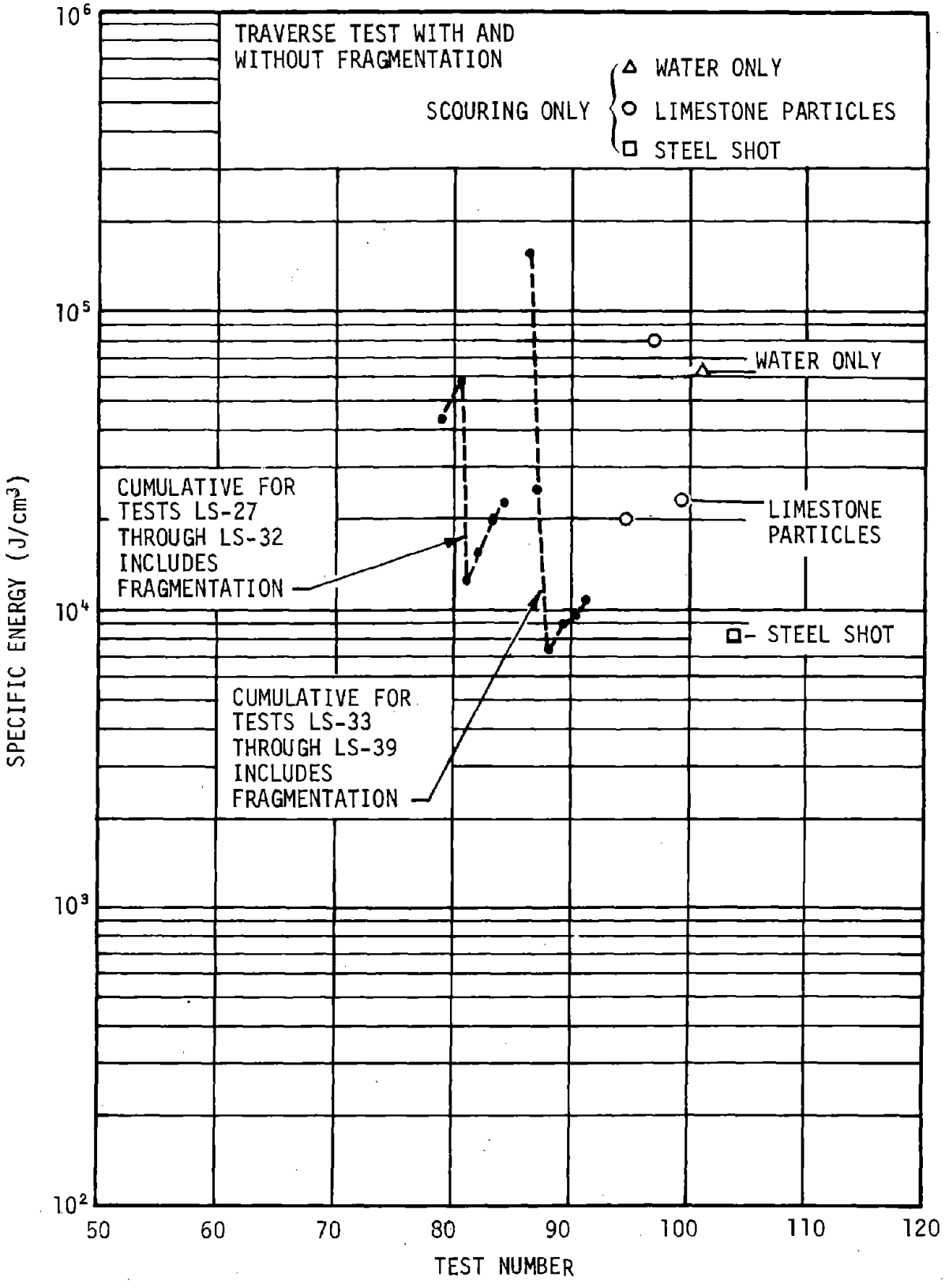

FIGURE 6-11. SPECIFIC ENERGY OBTAINED DURING TRAVERSE TESTS OF WATER-ROCK NOZZLE

show a significant drop after the second or third test. This has been attributed to the development of large cracks in the target during the first tests. Subsequent tests resulted in breaking large fragments from the target area, thus reducing the specific energy.

Tests where "scouring" only was observed are also shown in Figure 6-11. A photograph showing the target area after this test series was shown in Figure 6-6. The traverse rate for these tests was equivalent to approximately 1.5 in/sec. Figure 6-12 shows the specific energy as a function of standoff distance. These results tend to indicate a reduction in specific energy as the standoff distance is increased. Considering the axial decrease in average kinetic energy over the impact area, implied by the spreading jet, this is not what one would anticipate. However, if the indicated trend in specific energy is correct, then one plausible explanation may be the following. As cutting proceeds and a paraboloid shaped cavity develops, the impacting fluid may have greater difficulty in leaving the cavity. As the cavity deepens, the problem worsens because more of the fluid must turn through ever-increasing angles to flow out of the cavity. The flow of fluid leaving the cavity being impeded may produce a very deleterious effect on the cutting ability of the entering fluid. Such an effect was observed by Brook and Summers, as reported in Reference 6-2. This effect may be reduced by increasing the standoff distance. However, beyond some optimum standoff distance, the reduction in average kinetic energy would have to result in an increase in specific energy.

The latter effect may be the reason that traversing and pulsating a water jet appears to decrease the specific energy. The specific energy obtained from this unit during traverse operation is also shown in Figure 6-12.

REFERENCES - SECTION 6

6-1. McClain, W. C. and G. A. Cristy, "Examination of High Pressure Water Jets for Use in Rock Tunnel Excavation", Report ORNL-HUD-1, Oak Ridge National Laboratory, January 1970

6-2. Harris, H. D., "Rock Cutting with Water Jets", National Research Council of Canada, Ottawa, Presentation at 75th Annual General Meeting of the Canadian Institute of Mining and Metallurgy, April 15 - 18, 1973

6-3. Denardo, B. P., "Projectile Shape Effects on Hypervelocity Impact Craters in Aluminum", NASA TND-4953, December 1968

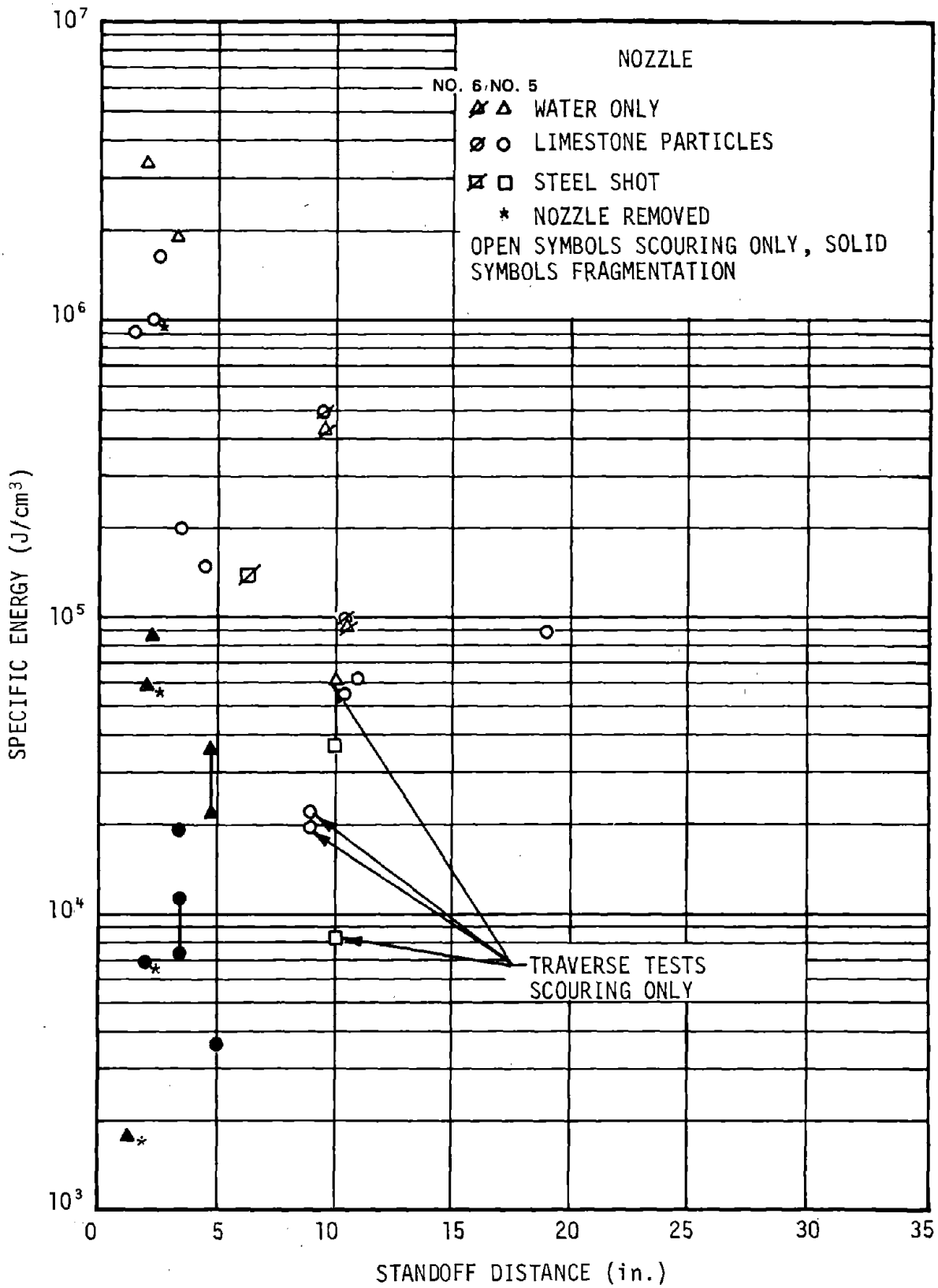

FIGURE 6-12. SPECIFIC ENERGY OF WATER-ROCK NOZZLE VERSUS STANDOFF DISTANCE

7. RESULTS AND CONCLUSIONS

As a result of the in situ test series, the following has been concluded:

- When concrete was the target material, the jet tended to excavate a clean paraboloid-shaped crater.

- Excavation tests with concrete tended to indicate an order of magnitude decrease in specific energy with limestone particle injection as compared to using water without particles.

- Further reductions in specific energy accompanied the use of harder and/or more dense particles.

- When limestone was used as the target material, significant chipping and fragmentation of the target was observed. Including fragments in computing the specific energy appeared to reduce the specific energy by a factor of two to ten below that observed for "scouring" only.

- Excavation tests with limestone as the target material indicated that the addition of limestone particles appeared to reduce the specific energy produced by the jet by a factor of three below that produced by water only. The use of steel shot appeared to reduce the specific energy produced by the jet by a factor of three below that produced by particles.

- Tests with Nozzle Configuration No. 5 (i.e., axial-fed peripheral jet) indicated that internal turbulence reduced the effective velocity of the rock nozzle jet to a level which was only slightly above the minimum velocity required for effective limestone cutting.

- Even though Nozzle Configuration No. 6 discharged a lower water mass flow rate it appeared to reduce jet spread and improve the velocity significantly as compared to Nozzle Configuration No. 5.

- Tests with Nozzle Configuration No. 6 (i.e., peripheral-fed axial jet) with the velocity estimated to be approximately twice that of Configuration No. 5 did not indicate a significant increase in excavation ability.

- Velocity comparisons between two jets were made using high-speed photography of the jets and inferentially through the time/volume of water relationship. Based on excavation capability, the two jets did not appear to have as large a velocity difference as that indicated above.

- The excavation ability of the jet appeared to increase as the mass of the individual particles increased.

8. RECOMMENDATION FOR FUTURE WORK

Over the pressure range tested, it would appear that the addition of particles can increase the cutting ability of hydraulic rock excavation machines. Furthermore, particles can be injected at reasonable feed rates without great difficulty and do not appear to seriously increase the downstream spread of the jet. For these reasons, it is recommended that future work be carried out in the following areas.

The downstream momentum loss as indicated by the jet spread appears to be a problem in that it requires operation with close stand-off distances. The present equipment is unsuited for use at very close working distances, so that this conclusion is surmised from results of previous investigations compared to this one. Furthermore, very little information was found in the literature concerning jet spread and energy exchange pertaining to high-velocity incompressible fluid jets. Recent work in this area appears to be fruitful for continuation to allow basic experimental studies to be performed using more applicable models than originally used here. Work should be done on containing jet spread at greater distances from the nozzle.

The addition of particles to higher velocity hydraulic jets and to lower velocity jets excavating softer and/or more friable materials would appear to be another fruitful area for future work.

APPENDIX A. TEST DATA

DATE	TEST NUMBER	PRESSURE P_o (psi)	PRESSURE P_f (psi)	PARTICULATE MATERIAL	NOZZLE	FILM	ADDITIONAL COMMENTS
5/10/74	X-1	14,000	11,000	None	No. 1 With insert	Hi Speed	With cylindrical extension
5/10/74	X-2	14,000	11,000	None	No. 1 With insert	Hi Speed	Without cylindrical extension
5/16/74	X-3	14,200			No. 1		X ≈ 0.006 inch D_{ex} ≈ 0.1562 inch Significant backflow
5/16/74	X-4				No. 1		Back pressure ≈ 2,000 psi
5/16/74	X-5				No. 2		Back pressure ≈ 0 Significant jet spreading
6/16/74	X-6				No. 2		Same as Test D-3
5/21/74	X-7				No. 2	Hi Speed	Same as Test D-3
5/21/74	X-8	14,200			No. 1	Hi Speed	X ≈ 0.0058 inch D_{ex} ≈ 0.200 inch Back pressure ≈ 2,000 psi
5/21/74	X-9	14,200			No. 1		X ≈ 0.0058 inch D_{ex} ≈ 0.250 inch Back pressure ≈ 0
5/21/74	X-10				No. 1		Same as Test D-7 Back pressure ≈ 0
5/25/74	X-11	13,000			No. 3		X ≈ 0.0058 inch D_{ex} ≈ 0.1562 inch Back pressure ≈ 5,000 psi
5/25/74	X-12	14,000			No. 3		Same as Test D-9

X - Designates System Development Test
R - Designates Excavation Testing

P_o - Initial Tank Pressure
P_f - Final Tank Pressure

DATE	TEST NUMBER	PRESSURE P_o (psi)	PRESSURE P_f (psi)	PARTICULATE MATERIAL	NOZZLE	FILM	ADDITIONAL COMMENTS
5/25/74	X-13	15,400			No. 3		X ≃ 0.0058 inch D_{ex} ≃ 0.180 inch Back pressure ≃ 4,000 psi
	14						
6/3/74	X-15	14,500		Rock Hopper Installed	No. 4		X ≃ 0.0058 inch D_{ex} ≃ 0.230 inch Slight backflow at start of test
6/3/74	R-16	14,000		Coal < 0.125 inch dia.	No. 4		First test with coal particles in stream. Significant pitting of concrete block. Pit depth less than 0.125 inch
6/3/74	R-17	14,200		Coal < 0.125 inch dia.	No. 4		Same results as Test R-16. Significant pitting. Pit depth less than 0.125 inch
6/3/74	R-18			Shop polishing balls 0.125 inch < dia. < 0.175 inch	No. 4	Still Shots (results photographed)	Cut significant crater in concrete 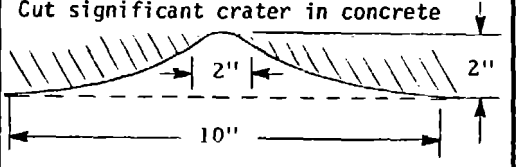
6/3/74	R-19			Shop polishing balls 0.125 inch < dia. < 0.175 inch	No. 4	Still Shots (results photographed)	Same as Test R-18. Concrete removed; 3.8 < W_c < 4.5 lb
6/4/74	R-20	14,200	10,500	Shop polishing balls 0.125 inch < dia. < 0.175 inch	No. 4	Still Shots (results photographed)	Traverse drive operational. Traverse length 36 inches; distance from nozzle to concrete 49 inches minimum to 66 inches maximum. Depth of cut: 1 inch at closest distance to 0.25 inch at farthest distance. 7.3 seconds run time. Approximately 12,500 balls injected at rate of 1,700 balls/second. Feed rate setting 53%.

X - Designates System Development Test
R - Designates Excavation Testing

P_o - Initial Tank Pressure
P_f - Final Tank Pressure

DATE	TEST NUMBER	PRESSURE P_o (psi)	PRESSURE P_f (psi)	PARTICULATE MATERIAL	NOZZLE	FILM	ADDITIONAL COMMENTS
6/4/74	R-21	14,200	10,400	Shop polishing balls	No. 4	Still Shots (results photographed)	Nozzle Configuration No. 4, test time 7.3 sec. Particle feed rate ≈ 1,700/second. Feed rate setting 30%. Increased cavity from 1 inch deep to 3.25 inches deep. 5-inch-diameter concentration. Slight nozzle erosion noted.
6/4/74	R-22	14,400	10,400	Shop polishing balls	No. 4	Still Shots (results photographed)	Same as Test R-21. Cavity depth increased to 4 inches with 7-inch-diameter concentration. Significant pitting and erosion of nozzle extension.
6/4/74	R-23	14,400	10,400	Shop polishing balls	No. 4	Still Shots (results photographed)	Same as Test R-21 except feed rate set at 90%. Cavity depth increased to 4.75 inches. Nozzle plugged during test. Feed rate setting 90%.
6/4/74	R-24	13,100	11,000	Shop polishing balls	No. 4	Still Shots (results photographed)	Severe erosion of nozzle deflected jet. Very little cutting of concrete. Inspection of nozzle showed damage beyond repair.
6/7/74	X-25	14,400	10,600		No. 5		D_{ex} = 0.200 inch backflow experienced. X = 0.0058
6/7/74	X-26	14,400	11,000		No. 5		D_{ex} = 0.200 inch backflow experienced. X ≈ 0.003 inch
6/7/74	X-27	13,000	11,000		No. 5		D_{ex} = 0.210 inch backflow experienced. Less than Test R-26. X ≈ 0.003 inch
6/7/74	X-28	12,600	11,200		No. 5		D_{ex} = 0.220 inch backflow at initiation, aspiration starts half-way through test run. X = 0.003
6/10/74	X-29	14,400	11,200		No. 5		D_{ex} = 0.225 inch backflow experienced. X = 0.003 inch

X - Designates System Development Test
R - Designates Excavation Testing

P_o - Initial Tank Pressure
P_f - Final Tank Pressure

DATE	TEST NUMBER	PRESSURE P_o (psi)	PRESSURE P_f (psi)	PARTICULATE MATERIAL	NOZZLE	FILM	ADDITIONAL COMMENTS
6/10/74	X-30	13,000	10,600		No. 5		D_{ex} = 0.230 inch backflow experienced. X = 0.003 inch
6/11/74	X-31	14,400	10,000		No. 5		D_{ex} = 0.234 inch aspiration flow achieved.
6/11/74	R-32	14,400	10,800	Crushed limestone 1/16 in. < size < 1/8 in.	No. 5		D_{ex} = 0.234 inch cut significant crater in concrete. Distance from nozzle to concrete approximately 33 inches. 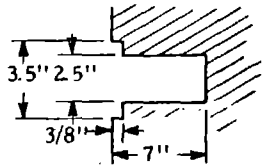 9.8 second run time, approximately 69,000 particles injected. Minimum feed rate = 7,000 particles/sec or 0.31 lb/sec. Feed rate setting 30%.
6/11/74	R-33	14,300	10,800	Crushed limestone 1/16 in. < size < 1/8 in.	No. 5	Hi-Speed	D_{ex} = 0.234 inch. Significant crater 1/4 to 1/2 inch deep. Distance from nozzle to concrete, 8 to 10 feet. 9.8 second run. Approximately 91,400 particles injected. Minimum feed rate 9,326 particles/sec or 0.410 lb/sec.
6/11/74	R-34	14,300	11,100	Crushed limestone 1/16 in. < size < 1/8 in.	No. 5		Same as Test R-33 except water pumped into rock hopper before start of test. Significant backflow experienced and more jet expansion.
6/11/74	R-35	14,300	11,000	Crushed limestone	No. 5		Same as Test R-34 except water pump started after nozzle flow established. Aspiration experienced. Signification cutting. No discernible cutting improvement over particle injected without water. 9.8 second run. Approximately 69,000 particles injected.

X - Designates System Development Test
R - Designates Excavation Testing

P_o - Initial Tank Pressure
P_f - Final Tank Pressure

DATE	TEST NUMBER	PRESSURE P_o (psi)	PRESSURE P_f (psi)	PARTICULATE MATERIAL	NOZZLE	FILM	ADDITIONAL COMMENTS
6/11/74	R-36	14,100	11,000	Crushed limestone 1/16 < size <.1/8	No. 5		Same as Test R-35 except with traverse operating at 6 deg/sec and no water into hopper. Backflow experienced probably caused by partially plugged nozzle. Feed rate setting 30%.
6/11/74	X-37	14,400	11,000	Crushed limestone 1/16 < size < 1/8	No. 5		Same configuration as Test R-35 except with sheet rock placed at target. Test initiated accidentally; otherwise operated as expected. Results indicated that whole particles arrive at the target. Target area of sheet rock destroyed and some cutting of concrete. Feed rate greater than 9,500 particles/sec.
6/13/74	R-38 (BM-1)	14,200	10,100	Crushed limestone 1/16 < size < 1/8	No. 5		D_{ex} = 0.234 inch X = 0.0038 inch First Bureau of Mines demonstration test. Distance to concrete target ≈ 23.5 inch. Feed rate set at 30%. Feed rate greater than 9,500 particles/sec. Cut significant greater in concrete target. 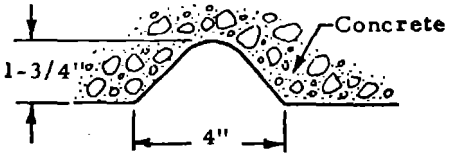
6/13/74	R-39 (BM-2)	14,200	10,400		No. 5		Second Bureau of Mines demonstration test. Same configuration as Test R-38 except added cover to rock hopper. Water only test. Cut smaller crater than Test R-38. 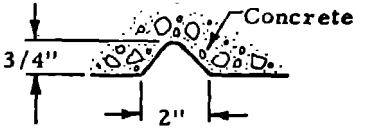

X - Designates System Development Test
R - Designates Excavation Testing

P_o - Initial Tank Pressure
P_f - Final Tank Pressure

DATE	TEST NUMBER	PRESSURE P_o (psi)	PRESSURE P_f (psi)	PARTICULATE MATERIAL	NOZZLE	FILM	ADDITIONAL COMMENTS
6/13/74	R-40 (BM-3)	14,400	11,200	Crushed limestone 1/16 < size < 1/8	No. 5		Third Bureau of Mines demonstration test. Same configuration as R-38 except cover closed on rock hopper and feed rate set at 55%. Very low particle feed rate (582 to 1,200 particles/sec). Probably caused by cover. Traverse test of 6 deg/sec. Very little cutting 1/4 inch to 3/8 inch deep.
6/13/74	R-41 (BM-4)	14,400	11,000	Crushed limestone 1/16 < size < 1/8	No. 5		Fourth Bureau of Mines demonstration test. Same configuration as R-40 except particle feed rate set at 100%. Traverse test at 6 deg/sec. Poor test run. Nozzle may have plugged.
6/13/74	R-42 (BM-5)	14,400	11,000	Crushed limestone 1/16 < size < 1/8	No. 5		Fifth Bureau of Mines demonstration test. Same configuration as R-40 except no traverse rate. Feed rate set at 100%. Feed rate greater than 9,500 particles/sec. Cut significant crater in concrete target. 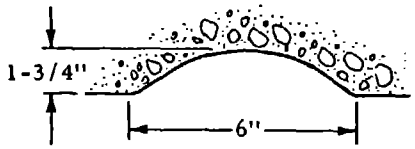
6/13/74	R-43 (BM-6)	14,600	11,000	Shop polishing balls 0.155 < size < 0.175	No. 5	Results photographed	Sixth Bureau of Mines demonstration test. Same configuration as Test R-43 except using shop polishing balls and cover removed. Feed rate set at 30%. Feed rate ≈ 1,500 particles/sec. Cut significant hole in concrete at 25-inch distance. 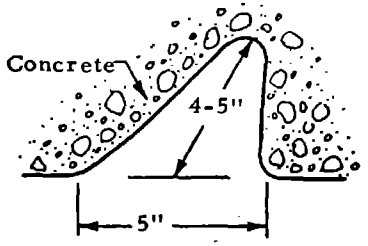

X - Designates System Development Test
R - Designates Excavation Testing

P_o - Initial Tank Pressure
P_f - Final Tank Pressure

DATE	TEST NUMBER	PRESSURE P_o (psi)	PRESSURE P_f (psi)	PARTICULATE MATERIAL	NOZZLE	FILM	ADDITIONAL COMMENTS
6/13/74	R-44 (BM-7)	14,400	11,200	Shop polishing balls 0.155 < size < 0.175	No. 5	Results photographed	Seventh Bureau of Mines demonstration test. Same configuration as Test R-43 except traverse test at 6 deg/sec. Rock hopper lid open. Feed rate ≈ 1,700 particles/sec. Significant cutting of concrete target 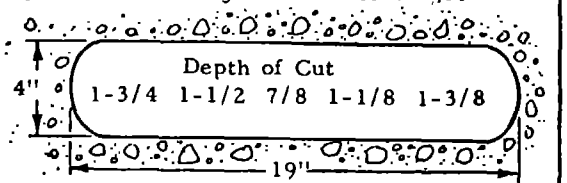
6/14/74	R-45 (BM-8)	14,400	10,000	Crushed limestone 1/16 < size < 1/8	No. 5		Eighth Bureau of Mines demonstration test. New nozzle installed. D_{ex} = 0.234 inch. Traverse test. Distance to target 16.5 inches. Backflow experienced.
6/14/74	R-46 (BM-9)	14,300	10,500	Crushed limestone 1/16 < size < 1/8	No. 5		Ninth Bureau of Mines demonstration test. Repeat of test R-46. Traverse rate at 6 deg/sec. Distance to target 16.5 inches. Feed rate greater than 9,500 particles/sec. Moderate cutting. 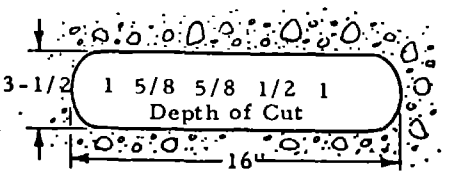
6/14/74	R-47 (BM-10)	14,400	10,500	Crushed limestone 1/16 < size < 1/8	No. 5		Tenth Bureau of Mines demonstration test. Repeat of test R-46 with average distance to target 108 inches. Feed rate approximately 11,700 particles/sec. Very little cutting. 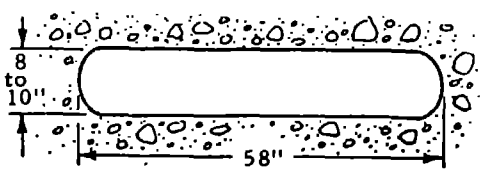

X - Designates System Development Test
R - Designates Excavation Testing

P_o - Initial Tank Pressure
P_f - Final Tank Pressure

DATE	TEST NUMBER	PRESSURE P_o (psi)	PRESSURE P_f (psi)	PARTICULATE MATERIAL	NOZZLE	FILM	ADDITIONAL COMMENTS
6/15/74	R-48 (BM-11)	14,400	10,500	Crushed limestone 1/16 < size < 1/8	No. 5		Eleventh Bureau of Mines demonstration test except feed rate set at 70% and rock hopper lid closed. Significant backflow experienced.
6/14/74	R-49 (BM-12)	14,400	11,000	Shop polishing balls 0.155 < size < 0.175			Twelfth Bureau of Mines demonstration test. Repeat of Test R-43 with nozzle 15 inches from target. Feed rate greater than 1,300 particles/sec. Significant cutting. Particle supply depleted 3 to 4 seconds prior to conclusion of test. 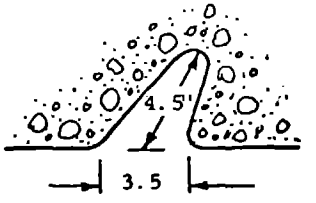

X - Designates System Development Test
R - Designates Excavation Testing

P_o - Initial Tank Pressure
P_f - Final Tank Pressure

DATE	TEST NUMBER	PRESSURE (kpsi) P_o	PRESSURE (kpsi) P_f	FEED MATERIAL TYPE/SIZE (in.)/RATE* (part./sec)	FEED RATE SETTING (%)	NOZZLE NUMBER	TARGET**	DIST. NOZZLE TO TARGET (in.)	FILM***	CAVITY SIZE BASE DIA. (in.)	CAVITY SIZE DEPTH (in.)	CAVITY VOLUME (in^3)	SPECIFIC ENERGY ($J/cm^3 \times 10^{-3}$)	ADDITIONAL COMMENTS
8/29/74	LS-50	14.0	10.6	LSP 1/16 - 1/8	0	5	QF	8 - 9	P, B, A	--	--	--	--	Feed screw switch off; very little feed; significant cracking; some material removed. Not measured.
8/29/74	LS-51	14.3	10.6	LSP 1/16 - 1/8	0	5	QF Same as LS-50	9	--	--	--	--	--	Feed screw switch off; backflow; chipped large piece from target.
8/29/74	LS-52	14.2	10.4	LSP 1/8 - 3/16	0	5	QF Same as LS-50	9	--	--	--	--	--	Feed screw switch off; very little particle feed; very litte cutting.
8/29/74	LS-53	14.2	10.4	LSP 1/8 - 3/16 2,700	30	5	QF Same as LS-52	9	--	--	--	--	--	Significant cracking of target area.
8/29/74	LS-54	14.2	10.7	LSP 1/8 - 3/16 2,700	30	5	QF	10.5	P, B, A	2.45	0.85	2.0	54.6	Scoured clean crater
8/29/74	LS-55	14.4	10.8	LSP 1/16 - 1/8 9,000	30	5	QF Same as LS-54	10.5	--	2.8	1.22	3.15	94.9	Dimensions of cavity and volume are increase in LS-54 cavity.
8/30/74	LS-56	14.0	9.4	W	--	5	QF	4.5	P, B, A	1.4 - 3.7	2.7	--	--	Cracked large triangular - shaped cavity. 1.4 in. base × 2.7 in. depth. Probably loose rock.
8/30/74	LS-57	14.0	9.4	LSP 1/16 - 1/8 11,000	60	5	QF Same as LS-56	4.5	P, B, A	--	--	9 - 10	11.5	Significant fragmentation; removed large fragment approximately 3.5 in. × 1.25 in. Volume removed; 9 to 10 in^3 is rough estimate.
8/30/74	LS-58	14.0	10.2	LSP 1/8 - 3/16 3,000	60	5	QF	3.5	P, B, A	2 - 5	2.8	--	--	Chipped large fragment. Probably loose rock; volume not measured.
8/30/74	LS-59	14.0	10.4	LSP 1/16 - 1/8 11,500	80	5	QF	6 - 10	--	--	--	--	--	Traverse rate of approximately 7 in./sec eroded oblong cavity 2.5 to 3.0 in. wide × 7.0 in. long, 1.3 to 1.4 in. deep. Very little actual cutting.

*LSP - Limestone Particles, SS - Steel Shot, W - Water Only
**QF - Vertical Face of Quarry Wall, LSB - Large Limestone Boulder
***P - Photograph, B - Before Test, A - After Test

P_o - Initial Tank Pressure
P_f - Final Tank Pressure

DATE	TEST NUMBER	PRESSURE (kpsi) P_o	PRESSURE (kpsi) P_f	FEED MATERIAL TYPE/SIZE (in.)/RATE* (part./sec)	FEED RATE SETTING (%)	NOZZLE NUMBER	TARGET**	DIST. NOZZLE TO TARGET (in.)	FILM***	CAVITY SIZE BASE DIA. (in.)	CAVITY SIZE DEPTH (in.)	CAVITY VOLUME (in^3)	SPECIFIC ENERGY ($J/cm^3 \times 10^{-3}$)	ADDITIONAL COMMENTS
9/4/74	LS-60	13.8	10.0	LSP 1/8 - 3/16 2,700	40	5 See comment	QF	3.5	--	1.3	0.9	0.551	198	Nozzle No. 5 with extension removed. Volume removed does not include large fragment chipped from target.
9/4/74	LS-61	13.9	10.2	LSP 1/8 - 3/16 3,000	40	5	QF	4.5	--	1.4	0.9	0.736	148	Scoured clean crater with cracks
9/5/74	LS-62	13.6	10.0	W	0	5	QF	2.3	P, B, A	2.3	0.75	1.26	86.4	Scoured clean crater with cracks
9/5/74	LS-63	13.9	9.3	W	0	5	QF	3.3	--	0.7	0.3	0.06	1,843	Scoured clean crater
9/5/74	LS-64	13.8	9.4	LSP 1/8 - 3/16 0	40	5	QF	3.3	--	--	--	--	--	Feed system malfunction
9/5/74	LS-65	13.8	9.4	LSP 1/8 - 3/16 2,700	80	5	QF	0.5	P, B, A	0.5	4 - 6	--	--	Significant cracking of target in all directions. One hole 4 to 6 in. deep.
9/11/74	X-66	14.4	11.0	W	0	5	--	--	High-Speed Camera	--	--	--	--	Velocity and jet expansion test. Ink injected during test.
9/11/74	X-67	14.4	11.1	W	--	5 See comment	--	--	High-Speed Camera	--	--	--	--	Same as X-66 except with nozzle extension removed.
9/11/74	X-68	14.4	11.0	W	--	5 See Comment	--	--	High-Speed Camera	--	--	--	--	Same as X-67
9/12/74	LS-69	14.4	10.9	W	0	5 See Comment	LSB	2.5	P, A	--	--	.43	2.5	Nozzle No. 5 with extension removed. Cracked large pyramid-shaped fragment from target dimension 4 in. × 5 in. base × 6.5 in. height.
9/12/74	LS-70	14.3	10.4	W	0	5 See Comment	LSB	2.5	P, B, A	--	--	2,770	0.039	Nozzle No. 5 with extension removed. Cracked very large fragment from boulder, rough estimate of volume 2770 in^3.

*LSP - Limestone Particles, SS - Steel Shot, W - Water Only
**QF - Vertical Face of Quarry Wall, LSB - Large Limestone Boulder
***P - Photograph, B - Before Test, A - After Test

P_o - Initial Tank Pressure
P_f - Final Tank Pressure

DATE	TEST NUMBER	PRESSURE (kpsi) P_o	PRESSURE (kpsi) P_f	FEED MATERIAL TYPE/SIZE (in.)/RATE* (part./sec)	FEED RATE SETTING (%)	NOZZLE NUMBER	TARGET**	DIST. NOZZLE TO TARGET (in.)	FILM***	CAVITY SIZE BASE DIA. (in.)	CAVITY SIZE DEPTH (in.)	CAVITY VOLUME (in^3)	SPECIFIC ENERGY ($J/cm^3 \times 10^{-3}$)	ADDITIONAL COMMENTS
9/12/74	LS-71	14.0	10.2	W	0	5	LSB	2.0	P, B, A	0.5	0.15	0.032	3,370	Repeat of LS-69 and LS-70 with extension in place. Only slight scouring.
9/12/74	LS-72	11.6	10.4	LSP 1/8 - 3/16 3,400	40	5	LSB	2.0	P, B, A	0.75	0.25	0.060	1,976	Short duration test approximately 5 sec compared to usual 10-sec test. Repeat of LS-71 with particles feed.
9/16/74	LS-73	14.2	10.4	LSP 1/8 - 3/16 3,000	40	5	LSB	3.5	P, B, A	--	--	--	--	Scoured crater
9/16/74	LS-74	14.3	10.6	LSP 1/8 - 3/16 2,700	40	5	LSB	2.5	P, B, A	--	0.5	0.067	1,624	Scoured crater with crack
9/16/74	LS-75	14.1	10.5	W	40	5	LSB	2.0	P, B, A	--	--	1.87	58.4	Fragmentation
9/16/74	LS-76	14.2	10.5	LSP 1/8 - 3/16 2,700	60	5	LSB	2.0	P, B, A	5.75	1.5	16.0	6.82	Large irregular-shaped fragment chipped from target
9/16/74	LS-77	14.2	10.5	LSP 1/8 - 3/16 2,000	60	5	LSB	2.3	P, B, A	0.75	0.5	--	--	Scoured clean crater
9/16/74	LS-78	14.5	10.5	LSP 1/8 - 3/16 2,700	40	5	LSB	1.5	P, B, A	--	--	0.12	909.3	Scoured clean crater
9/18/74	LS-79	13.6	9.4	LSP 1/8 - 3/16	40	5	QF	19.0	P, B, A	--	--	2.5 (2.5)	44.1 (44.1)	Particle feed malfunction
9/18/74	LS-80	14.2	10.2	LSP 1/8 - 3/16 2,700	60	5	QF	19	--	2.25	0.75	1.2 (3.7)	90.0 (59.2)	Test LS-70 through LS-84 were series tests using the same target except for LS-80 (which was static). All tests had traverse rates of approximately 1.5 in/sec. Numbers in brackets are cumulative volume removed and specific energy.
9/18/74	LS-81	14.3	10.5	LSP 1/8 - 3/16 3,000	60	5	QF	19	P, A	--	--	23.17 (26.9)	4.71 (12.2)	
9/18/74	LS-82	14.3	9.7	LSP 1/8 - 3/16 3,000	60	5	QF	19	--	--	--	0 (26.9)	(16.2)	

*LSP - Limestone Particles, SS - Steel Shot, W - Water Only
**QF - Vertical Face of Quarry Wall, LSB - Large Limestone Boulder
***P - Photograph, B - Before Test, A - After Test

P_o - Initial Tank Pressure
P_f - Final Tank Pressure

DATE	TEST NUMBER	PRESSURE (kpsi) P_o	PRESSURE (kpsi) P_f	FEED MATERIAL TYPE/SIZE (in.)/RATE* (part./sec)	FEED RATE SETTING (%)	NOZZLE NUMBER	TARGET**	DIST. NOZZLE TO TARGET (in.)	FILM***	CAVITY SIZE BASE DIA. (in.)	CAVITY SIZE DEPTH (in.)	CAVITY VOLUME (in^3)	SPECIFIC ENERGY ($J/cm^3 \times 10^{-3}$)	ADDITIONAL COMMENTS
9/18/74	LS-83	14.5	10.6	LSP 1/8 - 3/16 2,000	60	5	QF	19	--	--	--	0 (26.9)	(20.31)	
9/18/74	LS-84	14.7	10.6	LSP 1/8 - 3/16 2,700	60	5	QF	19	P, A	--	--	0 (26.9)	(24.4)	
9/18/74	LS-85	14.7	10.6	LSP 1/8 - 3/16 3,400	60	5	QF	19	P, B	--	--	0	--	Tests LS-85 through LS-91 were series tests using the same target. All tests had traverse rates of approximately 1.2 to 1.5 in/sec. Numbers in brackets are cumulative values of volume removed and specific energy.
9/18/74	LS-86	14.7	10.6	LSP 1/8 - 3/16 2,000	60	5	QF	19	--	--	--	1.39 (1.39)	78.7 (157.3)	
9/18/74	LS-87	14.8	9.9	LSP 1/8 - 3/16 3,400	60	5	QF	19	P, A	--	--	11.89 (13.3)	9.18 (24.6)	
9/19/74	LS-88	14.3	9.7	LSP 1/8 - 3/16 3,400	60	5	QF	14 - 16	--	--	--	55.04 (68.3)	7.98 (6.39)	
9/19/74	LS-89	14.4	9.8	LSP 1/8 - 3/16 1,700	60	5	QF	14 - 16	--	--	--	0.53 (68.85)	204.3 (7.92)	
9/19/74	LS-90	13.9	10.0	LSP 1/8 - 3/16 2,700	60	5	QF	14 - 16	--	--	--	0.3 (69.2)	320.9 (9.5)	
9/19/74	LS-91	14.5	9.8	LSP 1/8 - 3/16 2,000	60	5	QF	14 - 16	P, A	--	--	0 (69.2)	(11.04)	
9/19/74	LS-92	14.6	10.0	LSP 1/8 - 3/16 2,700	60	5	QF	14 - 16	--	--	--	0	--	Traverse rate approximately 1.2 in/sec. Very little cutting.
9/19/74	LS-93	14.6	10.4	LSP 1/8 - 3/16 2,700	60	5	QF	14 - 16	P, A	2.25	0.9	1.1	99.2	Scoured clean cavity
9/20/74	LS-94	14.7	10.4	W	--	5	LSB	9	--	--	--	--	--	Tests LS-94 and LS-95 were series tests.

*LSP - Limestone Particles, SS - Steel Shot, W - Water Only
**QF - Vertical Face of Quarry Wall, LSB - Large Limestone Boulder
***P - Photograph, B - Before Test, A - After Test

P_o - Initial Tank Pressure
P_f - Final Tank Pressure

DATE	TEST NUMBER	PRESSURE (kpsi) P_o	PRESSURE (kpsi) P_f	FEED MATERIAL TYPE/SIZE (in.)/RATE* (part./sec)	FEED RATE SETTING (%)	NOZZLE NUMBER	TARGET**	DIST. NOZZLE TO TARGET (in.)	FILM***	CAVITY SIZE BASE DIA. (in.)	CAVITY SIZE DEPTH (in.)	CAVITY VOLUME (in^3)	SPECIFIC ENERGY ($J/cm^3 \times 10^{-3}$)	ADDITIONAL COMMENTS
9/20/74	LS-95	14.7	10.4	W	--	5	LSB	9	--	--	--	11.13 (LS-94 and LS-95)	19.6 (LS-94 and LS-95	Traverse rate 1.4 in/sec. Scoured oblong cavity 2.5 in. wide × 10.5 in. long × 0.6 in. deep.
9/20/74	LS-96	14.8	10.4	LSP 1/8 - 3/16 2,700	70	5	LSB	9	--	--	--	--	--	Tests LS-96 and LS-97 were series tests. Traverse rate 1.4 in/sec. Scoured oblong cavity. Increased LS-95 and LS-96 cavity to 0.8 in. deep.
9/20/74	LS-97	14.8	10.0	LSP 1/8 - 3/16 3,000	70	5	LSB	9	P, A	--	--	2.85 (LS-96 and LS-97)	76.5 (LS-96 and LS-97)	
9/20/74	LS-98	14.9	10.0	LSP 1/8 - 3/16 3,300	70	5	LSB	9	--	--	--	--	--	Tests LS-98 and LS-99 were series tests. Traverse rate 1.4 in/sec. Scoured oblong cavity 2.5 in. wide × 10.5 long × 0.8 in. deep.
9/20/74	LS-99	15.0	11.0	LSP 1/8 - 3/16 3,300	70	5	LSB	9	P, A	--	--	9.22 (LS-98 and LS-99)	23.7 (LS-98 and LS-99)	
9/27/74	LS-100	13.9	9.8	W	--	5	LSB	10	--	--	--	--	--	Tests LS-100 and LS-101 were series tests. Traverse rate 1.4 in/sec. Scoured oblong cavity.
9/27/74	LS-101	13.8	9.4	W	--	5	LSB	10	P, A	--	--	3.55 (LS-100 and LS-101)	61.6 (LS-100 and LS-101)	
9/27/74	LS-102 LS-103	13.6	10.2	SS 0.125 450	40	5	LSB	10	P, A	--	--	13.33	8.19	Most of steel shot and cavity scoured during LS-102 test. Remaining (approximately 10%) fired in second test. Volume removed LS-102 = 10.4 in^3, LS-103 = 2.93 in^3. Traverse rate 1.4 in/sec.
2/4/75	X-104	9.1	6.5	W	--	6	--	--	--	--	--	--	--	Development Test Nozzle 6. Pressure measure in particle chamber indicated 2 to 2.5 psi vac. Test time = 15 sec.
2/4/75	X-105	9.1	6.8	W	--	6	--	--	--	--	--	--	--	
2/4/75	X-106	9.1	6.4	W	--	6	--	--	--	--	--	--	--	
2/5/75	X-107	9.1	6.4	W	--	--	--	--	--	--	--	--	--	

*LSP - Limestone Particles, SS - Steel Shot, W - Water Only
**QF - Vertical Face of Quarry Wall, LSB - Large Limestone Boulder
***P - Photograph, B - Before Test, A - After Test

P_o - Initial Tank Pressure

P_f - Final Tank Pressure

DATE	TEST NUMBER	PRESSURE (kpsi) P_o	PRESSURE (kpsi) P_f	FEED MATERIAL TYPE/SIZE (in.)/RATE* (part./sec)	FEED RATE SETTING (%)	NOZZLE NUMBER	TARGET**	DIST. NOZZLE TO TARGET (in.)	FILM***	CAVITY SIZE BASE DIA. (in.)	CAVITY SIZE DEPTH (in.)	CAVITY VOLUME (in^3)	SPECIFIC ENERGY ($J/cm^3 \times 10^{-3}$)	ADDITIONAL COMMENTS
2/5/75	X-108	9.4	6.6	LSP 1/16 - 1/8 8,000 (dry)	--	--	--	--	--	--	--	--	--	Development test to check particle feed rate.
2/5/75	X-109	9.5	6.7	LSP 1/16 - 1/8	--	6	--	--	--	--	--	--	--	Very little particle feed.
2/5/75	X-110	9.5	7.0	LSP 1/16 - 1/8 7,000	--	6	--	--	--	--	--	--	--	Added water to particles.
2/9/75	X-111	9.5	7.1	LSP 1/16 - 1/8 3,500 - 4,500	--	6	--	--	--	--	--	--	--	Test with hopper sealed.
2/9/75	X-112	9.5	6.7	LSP 1/16 - 1/8 6,850	--	6	--	--	--	--	--	--	--	Development test Nozzle No. 6.
2/18/75	LS-113	9.8	7.4	LSP 1/16 - 1/8 8,000	--	6	LSB	--	--	--	--	--	--	First limestone test for Nozzle No. 6. Slight chipping of surface.
2/18/75	LS-114	9.8	7.4	LSP 1/16 - 1/8 9,150	--	6	LSB	--	--	--	--	--	--	Slight cutting
2/18/75	LS-115	9.7	7.4	LSP 1/8 - 3/16 1,340	--	--	LSB	--	--	--	--	--	--	Slight cutting
2/18/75	LS-116	9.8	7.4	LSP 1/8 - 3/16 1,340	--	--	LSB	--	--	--	--	--	--	Slight cutting
2/18/75	SL-117	9.8	7.4	SS 0.125 200	--	6	LSB	42	--	5	0.7	11.1	20.3	Cut significant crater. 5 in. diameter × 0.7 in. deep. Most impacts appear in outer 1.0 to 1.5 in.
2/21/75	LS-118	14.5	10.7	W	--	6	LSB	10.5	--	--	0.75	3.7	87.6	Increased tank pressure, test time 12.5 seconds. Chipped semi-circular fragment from surface 5 to 6 in. long × 0.75 in. deep.

*LSP - Limestone Particles, SS - Steel Shot, W - Water Only
**QF - Vertical Face of Quarry Wall, LSB - Large Limestone Boulder
***P - Photograph, B - Before Test, A - After Test

P_o - Initial Tank Pressure
P_f - Final Tank Pressure

DATE	TEST NUMBER	PRESSURE (kpsi) P_o	PRESSURE (kpsi) P_f	FEED MATERIAL TYPE/SIZE (in.)/RATE* (part./sec)	FEED RATE SETTING (%)	NOZZLE NUMBER	TARGET**	DIST. NOZZLE TO TARGET (in.)	FILM***	CAVITY SIZE BASE DIA. (in.)	CAVITY SIZE DEPTH (in.)	CAVITY VOLUME (in^3)	SPECIFIC ENERGY ($J/cm^3 \times 10^{-3}$)	ADDITIONAL COMMENTS
2/21/75	LS-119	14.0	10.7	LSP 1/8 - 3/16 1,350	--	6	LSB	10.5	--	--	--	972	0.33	Chipped very large piece from boulder; triangular segment 36-in. base × 18-in. height × 6-in. thick
2/21/75	LS-120	14.6	10.3	LSP 1/8 - 3/16 2,000	--	6	LSB	10.5	--	--	--	--	--	Very little cutting
2/21/75	LS-121	14.6	10.3	LSP 1/8 - 3/16 2,000	--	6	LSB	10.5	--	3.0	1.0	3.53	91.8	Scoured clean crater
2/24/75	X-122	14.2	9.4	LSP 1/8 - 3/16 1,350	--	6	Plywood	70	--	--	--	--	--	Check to examine particle break-up. Particles embedded in target. Main pattern 7 to 8 in. wide.
2/24/75	LS-123	14.1	9.7	LSP 1/8 - 3/16 2,000	--	6	LSB	9	--	--	--	0.64	507	Scoured clean cavity
2/24/75	LS-124	13.9	9.8	W	--	6	LSB	9	--	--	--	0.692	468.6	Scoured clean cavity
2/24/75	LS-125	13.9	9.6	SS 0.125 360	--	6	LSB	7	--	--	--	2.26	143.7	

*LSP - Limestone Particles, SS - Steel Shot, W - Water Only
**QF - Vertical Face of Quarry Wall, LSB - Large Limestone Boulder
***P - Photograph, B - Before Test, A - After Test

P_o - Initial Tank Pressure
P_f - Final Tank Pressure

APPENDIX B.
OPERATING AND SAFETY PROCEDURES

B.1 SCOPE

This document establishes the procedures required for preparation and operation of the Hydraulic Excavation System.

B.2 REQUIREMENTS

B.2.1 Safety

During and after pressurization of the GN_2 high-pressure subsystem, the immediate test area should be cleared of all nonessential personnel. Access to areas forward of the nozzle should be prohibited to all personnel during any time that the accumulator (TB-1) is charged and the GN_2 subsystem pressurized. Access to the nozzle forward area should be limited to one person at a time and then only when the accumulator is fully discharged and the main power switch open. All flex lines shall be fully depressurized prior to disconnection. Other safety requirements are:

- Sound Level: The sound level produced by operation of this device cannot be predicted. If noise protection is warranted, it should be provided.
- Eye and Face Protection: Hard hats and safety glasses are required in operation of this system.
- Feet: Safety shoes are required for personnel operating this equipment.
- Medical and First Aid: Provisions for first aid and medical services should be provided.
- Fire Protection: Fire extinguishers, Class B, Light Hazard, rated 4B, should be provided at the system.

B.2.2 Personnel

All operating stations and personnel required will be specified in this procedure.

B.3 HANDLING INSTRUCTIONS

To prepare the system for transportation, the pipe support between HV-5 and the accumulator TB-1 must be loosened. Locking pins must be installed in nozzle bracket to prevent rotation. After system is located for test, remove locking pins from nozzle bracket and readjust pipe support.

B.4 HYDRAULIC EXCAVATION SYSTEM (PREPARATION FOR OPERATION)

The Hydraulic Excavation System is prepared for operation as five subsystems (see Figure 3-1):

- Electrical Subsystem
- Control Valve Pressure Subsystem
- High-Pressure GN_2 Subsystem
- Hopper Fill
- Water Subsystem.

B.4.1 Electrical Subsystem

The Electrical Subsystem consists of the following:

- Power cable
- Power panel
- Circuit breaker (CB) panel
- Control Box Assembly
- Remote Control Panel
- Solenoid valve SV-1
- Feed drive motor
- ad/dc converter
- Indicator light
- Nozzle motor
- Two pump motors.

To prepare the Electrical Subsystem for operation:

1. Verify main switch in "off" position.
2. Verify all CBs in "off" position.
3. Connect power cable to power source (120/208 Vac, 3ϕ, 60 Hz).
4. Apply power to system.

5. Verify proper voltage on all phases.

6. Position main switch to "on" position.

7. Actuate triplex pump "start" button.

8. Check for proper rotation of triplex hydraulic pump (PM-1). (Proper rotation is clockwise as indicated on end of pump motor.)

9. Actuate triplex pump "stop" button.

10. Place main CB in CB panel to "on" position.

11. Place CB-1 to "on" position. Verify that centrifugal pump (PM-2) operates.

12. Place CB-1 to "off" position. (Note that PM-2 is operated by CB-1.)

13. Verify other circuits through CB-2, CB-3, and CB-6.

14. Remove remote control box from enclosure assembly.

15. Verify position of switches:

    a. S1: "nozzle motor"--"off" position
    b. S2: "feed motor"--"stop" position
    c. S3: "solenoid valve"--"close" position.

16. Verify solenoid valve operation:

    a. Verify CB-2 and CB-3 are in "on" position.

    b. Place switch S-3 on remote control panel to "open" position.

    c. Solenoid valve should open (notable sound).

    d. Place switch S-3 to "close" position.

    e. Solenoid valve should close (notable sound).

17. Verify feed motor circuits:

    a. Verify "on-off" switch on the ac/dc converter speed control is in the "on" position.

NOTE

The "start-stop" switch on the ac/dc converter has been electrically bypassed and is not used in this operation.

b. Adjust timing relay (K-4), located in the control box assembly, for 5 sec (initially). [Indicator light (L-1) will be on during the time the feed drive motor is energized and may be used as a guide to set the timing.]

c. The feed drive motor is a dc variable-speed motor which may be adjusted from the ac/dc converter speed control located in the enclosure box. Set the speed of the feed drive motor to the desired rpm using the dial on the ac/dc converter speed control.

18. Verify nozzle motor circuit. This circuit operates the rotation (left-right) of the nozzle assembly. The motor will rotate in either the clockwise or counterclockwise direction. Limit switches (LS-1 and LS-2) located on the frame assembly control the limits of rotation.

NOTE

Before operating the nozzle motor switch (S1) on the remote control assembly, be prepared to physically operate the limit switches to verify proper limit switch operation.

a. Place nozzle motor switch (S-1) to forward "FOR" position. Motor should turn nozzle toward right limit switch.

b. Physically activate right limit switch. Motor should stop rotation of nozzle.

c. Deactivate right limit switch. Motor should continue rotating nozzle toward right until right limit switch is activated by cam on nozzle frame. Motor stops.

d. Place nozzle motor switch to reverse "REV" position. Motor should rotate nozzle toward left limit switch.

e. Activate left limit switch. Motor should stop rotation of nozzle.

f. Deactivate left limit switch. Motor should continue rotation of nozzle toward left until left limit switch is activated by cam on nozzle frame. Motor stops.

g. Place nozzle motor switch in "OFF" position.

19. Electrical subsystem is prepared for operation.

B.4.2 Control Valve Pressure Subsystem

The Control Value Pressure Subsystem consists of the following:

- One "K" bottle of GN_2 (PV-2) (3000 psig max. bottle pressure)
- Standard regulation unit [pressure gages (PG-4 and PG-5) and pressure regulator (PRV-1)]
- Vent valve (HV-21)
- Hand valve (HV-20)
- Relief valve (RV-1)
- GN_2 receiver (PV-3)
- Control solenoid valve (SV-1)

To prepare the Control Value Pressure Subsystem for operation:

1. Close hand valves HV-20 and HV-21 and regulator PRV-1.
2. Open hand valve HV-22. (If pressure on PG-4 is equal to or greater than 200 psig, proceed to step 8. If less than 200 psig, replace bottle PV-2 according to steps 3 through 7.)
3. Close hand valve HV-22.
4. Open hand valve HV-21.
5. Open regulator PRV-1.
6. Verify that gages PG-4 and PG-5 indicate 0 psig.
7. Replace pressure bottle PV-2 and refer to step 1.
8. Adjust regulator PRV-1 until gage PG-5 indicates 200 psig.
9. Open hand valve HV-20 (GN_2 receiver PV-3 will be charged).
10. Verify pressure gage PG-5 indicates 200 psig and no leaks occur in system up to control solenoid SV-1.

11. Cycle control solenoid valve SV-1 "open". Leak check valve SV-1 and line to pneumatically operated valve RCV-1.

12. De-energize solenoid valve SV-1. (Gas should flow from vent port until stable.)

13. The control valve pressure subsystem is now prepared for operation.

B.4.3 High Pressure GN_2 Subsystem

The HP GN_2 Subsystem consists of the following:

- High pressure gas booster (PI-1)
- Air compressor with hand valve (HV-31) (not supplied with system)
- GN_2 fill panel [Check valve (CV-2); hand valves (HV-1, HV-2, HV-3, and HV-4); pressure gage (PG-1), and gage surge suppressor (GP-1)]
- Hand valves (HV-5, HV-6, and HV-7)
- GN_2 pressure bottle (PV-1)
- Pressure gage (PG-2)
- Accumulator (TB-1 is considered part of this subsystem and the water subsystem.)

To prepare the High Pressure GN_2 Subsystem for operation:

1. Open hand valves HV-1, HV-5, and HV-7. Open hand valve HV-10 on water fill panel.

2. Close hand valves HV-2, HV-3, HV-4, and HV-6. (Pressure gages PG-1 and PG-2 indicate 0 psig.)

3. Connect GN_2 supply to high pressure gas booster PI-1 supply. (Normal GN_2 supply is from rack of GN_2 "K" bottles at 2100 psig.)

4. Open "K" bottle outlet valve.

5. Cycle hand valve HV-3 open and closed. (Line blow-down.)

6. Open hand valve HV-2. After system pressure stabilizes, close hand valve HV-10 and leak check system from GN_2 supply to high pressure gas booster PI-1, including leak check at vent port of hand valve HV-6.

7. Verify air compressor is activated. (Max. compressor output pressure not to exceed 150 psig.)

8. When pressure gage PG-1 indicates pressure approximately equal to "K" bottle supply pressure, open hand valves HV-31 and HV-32. (Begins high pressure charging of GN_2 system using gas booster PI-1.)

9. Repeat leak checks as in step 6 when pressure gage PG-1 indicates 3,000, 6,000, and 10,000 psig.

10. Continue pressurizing the system from "K" bottles using gas booster PI-1 until pressure gage PG-1 indicates 12,000 psig.

11. Close hand valve HV-2.

12. Close "K" bottle outlet valve.

13. Close valves HV-31 and HV-32 and deactivate compressor.

14. Open vent valve HV-3 (vents "K" bottle supply and GN_2 fill panel).

15. Remove GN_2 supply from gas booster PI-1 inlet.

16. Verify that compressor supply line is vented and disconnect.

17. The high pressure GN_2 subsystem is now prepared for operation.

B.4.4 Hopper Fill

To prepare Hopper Fill for operation, fill hopper with applicable quality and quantity of particles specified for test.

B.4.5 Water Subsystem

The Water Subsystem consists of the following:

- Water reservoir (R-1)
- Check valve (CV-4)

- Centrifugal feed pump (PM-2)
- Pressure gage (PG-7)
- Check valve (CV-3)
- Filter (F-1)
- Triplex Hydraulic Pump (PM-1)
- Pressure gage (PG-6) located on PM-1.
- Water fill panel [hand valves (HV-10, HV-11, and HV-12), pressure gage (PG-3), gage surge suppressor (GP-2), and check valve (CV-1)].
- Main control valve (RCV-1) and nozzle.

To prepare Water Subsystem for operation:

1. Fill the water reservoir R-1 with 50 gal of water mixed with approximately 1.5 gal of water-soluble lubricant.
2. Close hand valves HV-11 and HV-10.
3. Open hand valve HV-12.
4. Start centrifugal feed pump PM-2 and circulate water for approximately 3 min (mixes water and lubricant).
5. Open hand valve HV-11 and control valve RCV-1.
6. Close hand valve HV-12. (Water should exit through nozzle.)
7. Close control valve RCV-1. Leak check system from reservoir to control valve RCV-1.
8. Open hand valve HV-12. Start triplex hydraulic pump PM-1. Close hand valve HV-12.
9. When pressure gage PG-6 indicates 15,000 psig or begins to rise rapidly, stop pump PM-1 (approximately 8 minutes are required to fill TB-1).
10. Stop pump PM-2.
11. Close hand valve HV-11.

12. Open hand valve HV-12 (relieves pressure between PM-1 outlet and water fill panel).

13. The water system is now charged and ready for firing (provided the high pressure GN_2 subsystem has been pressurized per Section B.4.3 herein).

B.5 HYDRAULIC EXCAVATION SYSTEM (OPERATION)

The operation of the Hydraulic Excavation System is accomplished with the remote control panel (attached to cable located in control box). The specific time of flow (controlled by opening valve RCV-1 from remote control panel), sweep rate (determined by gearing combination used), and particle feed rate for each test will be at the direction of the test conductor.

After each test flow is completed, the system must be recharged for the next test by performing/verifying the following steps:

1. Verify that pressure gage PG-5 indicates 200 psig

2. Verify that PG-2 indicates approximately 12,000 psig

3. Fill hopper with applicable quality and quantity of particles specified for test

4. Open hand valve HV-11. Start centrifugal feed pump PM-2.

5. Start triplex hydraulic pump PM-1. Close hand valve HV-12.

6. When pressure gage PG-6 indicates 15,000 psig or begins to rise rapidly, stop pump PM-1. (Approximately 8 minutes are required to fill TB-1.)

7. Stop pump PM-2.

8. Close hand valve HV-11.

9. Open hand valve HV-12 (relieves pressure between PM-1 outlet and water fill panel).

10. The hydraulic system is now ready for operation.

APPENDIX C. REPORT OF INVENTIONS

Brown Engineering Company, Inc., certifies that there were no inventions conceived or first actually reduced to practice in its work called for under Contract No. H0232062.

E. R. Andrzejewski
Manager, Contract Administration